WADC TECHNICAL REPORT 55-156
PART 2
ASTIA DOCUMENT No. 118104

INSTALLATION OF AN AUTOMATIC CONTROL SYSTEM IN A T-33 AIRPLANE FOR VARIABLE STABILITY FLIGHT RESEARCH

PART 2. DETAIL DESIGN, FABRICATION AND INSTALLATION

FLIGHT RESEARCH DEPARTMENT

CORNELL AERONAUTICAL LABORATORY, INC.

DECEMBER 1956

AERONAUTICAL RESEARCH LABORATORY
CONTRACT No. AF 33(616)-2578
PROJECT No. 1364

WRIGHT AIR DEVELOPMENT CENTER
AIR RESEARCH AND DEVELOPMENT COMMAND
UNITED STATES AIR FORCE
WRIGHT-PATTERSON AIR FORCE BASE, OHIO

Carpenter Litho & Prtg. Co., Springfield, O.
200 - April 1957

FOREWORD

The work covered by this report has been carried out by the Flight Research Department of the Cornell Aeronautical Laboratory, Inc., Buffalo, New York. The project is being sponsored by the Aeronautical Research Laboratory of the Wright Air Development Center. The phases of the project covered by this report have been done under Air Force Contract AF33(616)-2578, Project No. 1364, Task Nos. 70525 and 70501. For the first half of the work reported herein, the project was administered by Mr. P.P. Cerussi of the Aeronautical Research Laboratory, and for the second half by Mr. R.W. Rautio of the same Laboratory. Mr. J.N. Ball has been the project engineer at the Cornell Aeronautical Laboratory in charge of the work. The engineers who have directed and carried out the principal portions of the work include C.L. Muzzey, W.J. Hirtreiter, J.L. Beilman, W. Close, C.H. Hutchinson, W.J. Thayer, and H.S. Radt, Jr.

Part 1 of this report covered the Preliminary Design phase of the project. The present report covers the Detailed Design, Fabrication and Installation phases, which were accomplished in the period from April 1955 to June 1956. Cornell Aeronautical Laboratory report number TB-936-F-2 has been assigned to the present Part 2 report.

ABSTRACT

The Cornell Aeronautical Laboratory has recently completed the detail design, fabrication, and installation of an artificial stability system in a T-33 airplane. Irreversible hydraulic servos are used to vary the stability around all three axes. Variable artificial feel and several special provisions for research on cockpit controls are included, making the system highly versatile. In some instances the basic design was altered slightly, and decisions on the alternate proposed design solutions were made; but most of the detailed work proceeded directly from the preliminary design as reported in WADC TR 55-156, Part 1. Photos of the completed installations are included.

PUBLICATION REVIEW

This report has been reviewed and is approved.

FOR THE COMMANDER:

Nathan L. Krisberg

NATHAN L. KRISBERG, Colonel, ~~USAF~~
Chief, Aeronautical Research Laboratory
Directorate of Research, WADC

TABLE OF CONTENTS

LIST OF TABLES

LIST OF ILLUSTRATIONS

LIST OF ILLUSTRATIONS (CONT'D)

SECTION I
INTRODUCTION

by J.N. Ball

The development of military aircraft to reach higher and higher speeds and altitudes requires continual progress in the design of high-performance aerodynamic configurations. The use of new and different configurations designed for maximum performance invariably raises problems in the fields of flight control and aerodynamic stability. The Cornell Aeronautical Laboratory has been engaged for some years in flight research in these fields, and in the course of this work has demonstrated the value of the variable stability airplane as a research vehicle of considerable versatility. The special advantage of the variable stability airplane is that it permits systematic variation of the test configuration. The effect of changing the size of a vertical tail, for example, can be investigated in the course of a single flight by simply altering potentiometer settings. It is also possible to try out the characteristics of airplanes which have not yet reached the flight test stage. Problems of matching the design of flight control systems to the basic aerodynamics of various airplane configurations can be investigated on such a test airplane.

In order to increase the effectiveness of the Laboratory's flight research work on the problems that are continually arising in the field of airplane stability and control, a T-33 airplane is being equipped as a new variable stability test vehicle. The stability and control characteristics of this airplane will be variable about all three axes. The automatic control equipment being installed has the capability of altering the test airplane's characteristics over wide ranges. This makes it possible to set up any of a large variety of stability and control problems for flight research work. Thus it is believed that this new T-33 variable stability airplane will be a versatile and highly useful research tool.

The project has been divided into several phases. Phase I covered Preliminary Design, and work done under this phase has been reported in Reference 1. This reference discusses in more detail the nature and scope of the project and the capabilities that the test airplane will have. It also discusses the

This manuscript was released by the author for publication 1 June 1956

engineering principles used in the design of the special control system, and the results of preliminary design studies. The present report covers work done under the next three phases: Phase II, Detail Design; Phase III, Fabrication, and Phase IV, Installation. Some extensions of the Phase I analysis work and several design changes and engineering decisions made since Reference 1 was written are also reported herein. At the end of Phase IV, all the mechanical, hydraulic, and electronic equipment was installed in the airplane, and the system was ready for ground check-outs. Work on ground check-out and flight check-out of the test airplane will be reported subsequently.

SECTION II

CONTRACT STATUS AND PROGRAM OUTLINE

The program is being carried out under Air Force Contract No. AF33(616)-2578. The work is being sponsored by the Aeronautical Research Laboratory of the Wright Air Development Center. The contract initially covered Phase I only, which commenced on 1 July 1954. This phase was completed in April 1955. Phases II and III were covered by Supplemental Agreement No. S1 (55-1179), dated 1 April 1955, and Phase IV was covered by Supplemental Agreement No. S3(56-442), dated 28 September 1955. In large part, Phases II, III and IV ran concurrently. The work done under these phases was essentially complete at the end of June 1956.

The T-33A airplane to be used for the project, Serial No. 51-4120, was delivered to Cornell on 14 October 1954. It has been bailed to the Laboratory under Bailment Agreement No. AF33(600)-2214.

Phase I covered the preliminary design studies. This phase commenced with an analysis of methods of using variable stability equipment to reproduce desired flight characteristics. From this study, a system block diagram was worked out and design requirements were developed for the various mechanical, hydraulic and electronic installations. Preliminary studies were then made to establish methods and principles to be used in the design of the equipment to be installed. In several instances, these studies were supplemented with bench tests. This work has been reported in Reference 1.

Several important design decisions have been made since Reference 1 was written. The decision was made to locate all three control surface servos in the plenum chamber. Additional analysis and test work led to a firm decision to continue as planned with the pressure-control type of feel servo. To gain the room needed for the electronic equipment, it was found to be feasible to replace the normal T-33A nose section with an F-94A nose section. This change has been made. An improved analysis has been made of the theory and method of producing desired lateral dynamic characteristics. These matters are discussed in more detail in subsequent sections.

Phase II consisted of the detail design work. All the necessary drawings and wiring diagrams were prepared. A stress analysis was carried out for the servo installations and the control system modifications. This is reported in Reference 2. The results of servo performance analyses were used to develop detail design requirements for the servos. Specifications were developed for all purchased components. A review was made of the flight loads to be expected with the artificial stability system in operation, and these were checked against the airplane's structural flight restrictions. Special attention was also given to safety devices and emergency procedures.

Phase III included fabrication of parts and components, and the procurement of purchased parts. The major parts and components were subjected to qualification bench tests and were made ready for installation in the test airplane.

Phase IV consisted of installing all the equipment and preparing the test airplane for ground tests.

The program proceeded in early July 1956, into the Ground Check-Out phase, Phase V. This will be followed by Phase VI, the Flight Check-Out phase. It is expected that the airplane will be ready in early 1957 to undertake research flight test programs.

SECTION III

METHODS FOR PRODUCING DESIRED STABILITY AND CONTROL CHARACTERISTICS

by J.N. Ball

A general, descriptive outline of the concepts which have governed the design of the variable stability system is given in Section III of Reference 1. This description is still applicable to the system as it is now installed in the airplane.

Section V of Reference 1 discusses the design of several special provisions in the control system which have been included for research work on the design and function of cockpit controls. This discussion also is still applicable to the present system.

Some further considerations need to be presented, however, to supplement the material presented in Section IV of Reference 1, which was concerned with the analysis of methods for producing desired dynamic stability and control characteristics. The analyses of the simulation of longitudinal short-period and phugoid characteristics are still applicable. Some additional work has been done, however, to develop in detail the method to be used in setting up the T-33 to simulate the longitudinal characteristics of another airplane. This is discussed in Reference 3, which includes also an example of simulating the F-100A airplane in one representative flight condition. The results obtained substantiate the original analysis presented in Reference 1.

The original analysis of simulation of the lateral modes of motion started out on the basis of attempting to match the equations of motion term by term. It was found that this could be done for the rolling moment and yawing moment equations, but that the side force equation would not generally be matched exactly. The important terms of the side force equation are matched, however, when the test airplane's true speed can be chosen to match the true speed of the airplane being simulated, and the test airplane's altitude can be chosen to match the stability derivative Y_β. This is not always possible, in which case some compromise is necessary. Reference 1 proposed matching Y_β in any case, and pointed out that the characteristic time of the spiral mode would come out low if the test airplane's true speed was low.

Further consideration has led to two changes in the method to be used for the lateral case. It is recognized that it is desirable to simulate the side load factor acting on the airplane. To achieve this as closely as is practical calls for obtaining the correct relation between side load factor and sideslip angle, and this in turn means matching $Y_\beta (V/g)$ rather than Y_β. This conclusion corresponds to the choice of $L_{\dot\alpha} (V/g)$ as the parameter to be matched by choice of flight condition in the longitudinal case. Reference 4 contains a more detailed discussion of the choice of $Y_\beta (V/g)$ as the parameter to be matched.

The second change provides an improved method of matching the fixed control characteristic quartic equation in case the side force equation is not matched exactly. The quartic equation is

$$d^4 + B d^3 + C d^2 + D d + E = 0$$

If level flight is assumed so that Y_ψ is zero, and if Y_p and Y_r are neglected, the coefficients of the quartic are

$$B = \underline{\underline{- Y_\beta - L_p - N_r}}$$

$$C = \underline{\underline{N_\beta}} + \underline{L_p (Y_\beta + N_r)} + (Y_\beta N_r - L_r N_p)$$

$$D = - \underline{\underline{L_p N_\beta}} + \underline{L_\beta (N_p - Y_\phi)} + Y_\beta (L_r N_p - L_p N_r)$$

$$E = \underline{\underline{Y_\phi (L_\beta N_r - L_r N_\beta)}}$$

(The notation here is the same as in Reference 1. The quartic is derived from equations (63), (64) and (65) of Reference 1, with the right-hand sides set equal to zero.) In the expressions for the coefficients, the most important terms are indicated by a double underline, and the secondary terms by a single underline. The remaining terms are generally unimportant. N_β, L_p and L_β are usually the three most important lateral stability derivatives, and so we choose the artificial stability settings to match them exactly.

This results in matching of the primary terms in the coefficients C and D. Experience has also shown that the ratio of L_β to N_β should be matched to obtain the correct roll/yaw ratio in the Dutch roll mode. We next match B by choosing N_r for the test airplane to compensate for any mismatch of Y_β ; i.e., we match the sum ($Y_\beta + N_r$). With this we also match the secondary term in C. We match the secondary term in D by choosing N_p for the test airplane to compensate for any mismatch of Y_ϕ ; i.e., we match the term ($N_p - Y_\phi$). Finally we choose L_r for the test airplane as necessary to match E. The third terms in C and D may be somewhat mismatched, but since they are of small importance, this mismatching is usually of not much consequence. By using this procedure to match all the coefficients of the quartic, we obtain the correct time constant for the spiral mode as well as the correct time constant for the roll mode and the correct Dutch roll frequency and damping. A more detailed discussion is given in Reference 4.

Some additional examples of simulation of lateral dynamic stability characteristics have been worked out, using the improved methods just described. Reference 5 shows calculations and also analog computer results for a case of simulation of the F-101A airplane. In general, very good simulation was shown by this example. In the spiral mode, the ratio of rolling velocity to yawing velocity comes out low because the T-33 cannot reach the speed assumed for the F-101A. In the Dutch roll mode, the ratio of rolling to yawing velocities, p/r , is duplicated very well. Another parameter sometimes used in describing the Dutch roll mode is ϕ/v_e, which equals $(1/V_e)(\phi/\beta)$. Our method matches ϕ/β quite well, and so ϕ/v_e will be mismatched to whatever extent the equivalent air speed is not matched. It is believed that it is more important to simulate the parameter p/r , since it represents the motion of the airplane as it is sensed by the pilot in watching the horizon or a target.

Reference 6 is a similar study for simulation of the F-104A airplane in one flight condition. The results obtained were generally satisfactory and were like those obtained for simulation of the F-101A. In this particular case, though, it was not practical to choose the flight condition to match $Y_\beta(V/g)$

very well, as the case assumed for the F-104A was a severe combination of high speed and low altitude. As a result, the side load factors obtained in the T-33 would be only about half those of the F-104A for this low altitude condition. Better results would be obtained for the F-104A at higher altitudes. The period, damping ratio, and ratio of rolling velocity to yawing velocity were simulated almost exactly for the Dutch roll mode. Also the time constants for the roll subsidence and the spiral mode were simulated very well.

Another refinement was made in the method of deriving the angle of attack and sideslip angle signals from the accelerometer readings. The same reasoning applies in each case, so only the computation of angle of attack will be discussed. The refinement is simply to account for lift due to elevator deflection (at constant angle of attack); i.e., the derivative $C_{L_{\delta_e}}$. Starting with the assumption that

$$C_L = C_{L_\alpha} \alpha + C_{L_{\delta_e}} \delta_e ,$$

the following expression can be derived

$$\alpha = \left(\frac{\frac{W}{S}}{C_{L_\alpha}} \right) \frac{n_z}{q} - \left(\frac{C_{L_{\delta_e}}}{C_{L_\alpha}} \right) \delta_e$$

The computing circuit is now arranged so that after the accelerometer signal is divided by q, a constant times the elevator angle signal is subtracted to obtain the angle of attack signal. Not only does this give a more accurate result for α, but also it avoids a possible source of system stability trouble. If n_z/q were to be used directly as a measure of α, the following loop could give trouble. Assume the elevator oscillating with the airplane restrained to be at constant α. The resultant variations in tail load would be felt by the accelerometer. The accelerometer signal goes through the servo system to the elevator, and the loop is closed. This explanation is oversimplified, as angle of attack will in fact respond to the assumed elevator angle variations. At high frequencies, though, the angle of attack response will become small and the situation will approximate the simplified case just described. Some study of this situation had indicated the possibility of system instability. This possibility is now avoided by the revised computing circuit which cancels out accelerometer signals due to $C_{L_{\delta_e}}$. Similarly, the effect of $C_{Y_{\delta_r}}$ is now cancelled out in the circuit for computation of sideslip angle.

It has been found advisable to include somewhat more complete provisions for trimming the system than indicated in Reference 1. The rear pilot has a set of trim controls which he adjusts to trim the system just prior to engaging the servos. The front pilot has another set of trim controls which act like trim tabs and which he may use as he pleases during the test runs. This arrangement keeps the maximum responsibility for correct engagement of the control system in the hands of the rear pilot.

Reference 1 proposed the inclusion in the artificial feel system of channels representing non-linear springs. It has been found difficult, though, to devise good general-purpose provisions for non-linearities. Therefore, it has been decided to defer the installation of non-linear provisions and to develop them in the future according to the requirements of specific research programs.

SECTION IV

SAFETY PROVISIONS AND SYSTEM OPERATION

by C.R. Chalk

A. SAFETY PROVISIONS

A general description of the safety provisions of the special control system is given below.

1. Hydraulic Pressure Dump Controls

The feel servo system has two control valves. One is a solenoid actuated selector valve which either pressurizes or opens to return the feel servo circuits. The control switch for this valve is located on the front cockpit switch console. This is a fail safe type valve, i.e., in the event of electrical failure it assumes the "open to return" configuration.

The second control valve in the feel servo system permits the pressure in one side of the elevator feel servo to be released and the control column to be moved forward. When the wheel configuration is installed it engages a latch which holds it forward. This provides the maximum clearance for the front pilot in the event he must eject. The former front cockpit aileron boost valve is used for this purpose. Operation of this valve also actuates an interlock circuit which shuts off the variable stability system.

The pressure controls for the hydraulic position servos are located in the aft cockpit, and are operated by the safety pilot. The three solenoid actuated selector valves which pressurize the position servo circuits are operated by a single switch on the aft cockpit switch console. Another switch on this console operates the three solenoid valves which bypass the three position servo actuators. These valve installations are also of the fail safe type. As mentioned below, there are also switches on both front and rear sticks and on the front control panel which deactivate the position servos.

In addition to the electrical valve controls, there are two mechanical valve controls in the aft cockpit. One is the normal aileron boost control valve. This valve has an interlock with the electrical system which prevents pressurizing the servos with aileron boost on. The other mechanically operated valve permits releasing the pressure on both sides of the pistons of all three position servos. Thus, in an emergency the position servos can be depressurized and manual control of the airplane regained by operating one mechanically controlled valve.

2. Hinge Moment Limits

Each of the position servos is equipped with a pressure limiting circuit which limits the maximum force or hinge moment output of the servo actuator. The servos were designed to have a higher capacity than required by normal operation to insure that they would have satisfactory dynamic performance. For reasons of safety, it was then necessary to limit the maximum differential hydraulic pressure which could occur across any of the servopistons to a fraction of the supply pressure. An important reason for limiting the maximum hinge moments from the actuators was to prevent excessive horizontal or vertical tail loads which might occur when simulating airplane dynamics different from the normal T-33. In conjunction with the hinge moment limits, the system has a provision for automatically turning itself off if the normal or lateral accelerations exceed pre-set values. The lateral acceleration limit is especially important in preventing excessive vertical tail loads.

3. Servo Valve Trim Controls

The safety pilot in the aft cockpit is provided with trim controls and a trim meter. With these controls he checks and trims the elevator, aileron, and rudder servo valve error signals to zero before the position servo circuits are pressurized, thus preventing large surface motions from occurring when the servo bypass valves are closed. After engaging, the trim meter automatically indicates the magnitude of the elevator hinge moment, and the safety pilot may keep the airplane in trim during steady maneuvers by adjusting the normal T-33 elevator trim tab. This insures that the control system may be disengaged, at any time, without causing a sudden maneuver.

4. Automatic Safety Trip

The automatic safety trip monitors servo valve error signals and the normal and lateral accelerometer output signals. If these signals exceed pre-set values, the system is automatically shut off. Monitoring the servo valve error signals provides protection against a malfunction in the variable stability system or an inadvertent control motion which would produce a dangerous control surface deflection. Monitoring the accelerometer signals prevents maneuvers which would cause the airplane's structural limitations to be exceeded.

5. Design of Control and Interlock Circuitry

The T-33 variable stability installation has been equipped with a system of control and interlock features which are designed to provide a maximum in operational safety.

The system energizing and servo engage process advances in a sequence of steps, which bring into operation first those functions which least affect safety of flight. The power supply equipment and the data recording system are energized first; then, the feel servo and auxiliary surface servo systems are put into operation. Next, the position servo system is trimmed and the servo circuits pressurized and finally, the actuator bypasses are closed thus completing the engagement process.

Extensive use was made of holding circuits in the design of the control and interlock system. Through use of these holding circuits and momentary switches the system will automatically revert to the OFF position in the event of a malfunction or normal servo shut-off without the necessity of repositioning a number of switches. To re-engage the servos it is necessary to repeat the entire engage procedure.

The holding circuits are also well suited to the use of interlock arrangements and indicator lights. Properly designed and arranged interlocks and indicators prevent omitting steps in the operating procedure and also serve as automatic safety guards in the event of malfunction.

Generally the controls for the T-33 variable stability and control system were arranged with the following considerations in mind:

a. Controls that have the same general function (such as gain controls) were grouped together with the most frequently used controls placed most conveniently.

b. Switches, indicators, and trimming devices for engaging the system were, insofar as possible, located together so that the engage procedure can progress smoothly.

c. Safety and emergency devices were placed very conveniently, with duplication as required. For example, switches for shutting off the servos are provided on the cockpit switch consoles and on the front and rear control sticks.

B. NORMAL OPERATION OF THE T-33 VARIABLE STABILITY AND CONTROL SYSTEM

A general description of the normal operating procedure for the T-33 variable stability and control system is given below. Reference is made to the sketch of the T-33 control and interlock circuitry, Figure 5, and to the sketches of the four pilot control displays which are included as Figures 1-4.

1. Set-up of Gain Controls

The gain controls for the artificial stability and control inputs are mounted on a panel which is located on the right-hand side of the rear cockpit. These controls are color coded and arranged in three rows according to their association with either the pitch, roll, or yaw axis (See Figure 1). Bronze indicates pitch axis signals, green indicates roll axis signals, and red indicates yaw axis signals. The individual gain controls in each row have an identifying letter engraved on the control button.

These gain controls are positioned by the rear pilot, either on the ground or before the start of the engagement procedure in the air.

2. Power Controls

The entire electrical system for the variable stability installation is turned ON or OFF by switch Sw 1 located on the switch console in the rear cockpit (see

Figure 2). In series with Sw 1 are the "normally closed" contacts of relay K 25. This relay will be energized and turn the electrical system OFF when the front stick dump valve is opened (prior to ejection). It also prevents engaging the system with the dump valve open. The entire system will revert to the OFF position when power is removed.

A test power selector switch Sw 3 (located in the power distribution unit in the nose section) may turn on either or both the control and recording systems for ground operation. With Sw 3 in the center or normal flight position both recording and control systems will be turned on.

Following a warm-up interval, relay K 21 is energized. A READY indication will appear (L 1 and L 2 will light on the front and aft cockpit switch consoles) if all three static converters are operating and if the servo shut-off switches (Sw 5 through Sw 7) are closed. The ground return for the READY lights is made through the normally closed contacts of K 38 which bypasses the safety trip contacts while the surface servos are disengaged.

Following the READY indication, the front pilot may start the engage procedure for the feel servos.

3. Engagement of Feel Servos

The feel servos are always mechanically connected to the front cockpit controls. The engagement process consists of trimming the servo valves and pressurizing the servo circuits.

Prior to engaging the feel servos, the front pilot sets his servo trim controls to previously determined positions which should be the ones required to center the stick and pedals. These trim controls are arranged on a panel as shown in Figure 4 and mounted on the left-hand side of the front cockpit. The front pilot engages the feel servos by momentarily depressing switch Sw 9. Indicator lights L 6 and L 7 come on, and the wheel latching mechanism on the front stick is disarmed by the column latch solenoid while the feel servos are engaged. This is to prevent the wheel from becoming locked forward during a test.

The front pilot then positions the stick in the X-Z plane and centers the rudder pedals by further adjusting the rudder and aileron trim controls. Both the elevator trim control and the elevator stick trim control are used for longitudinal stick trimming. The purpose of the elevator stick trim control is to cancel the stick force due to the normal accelerometer signal at $n_z = 1$ if necessary and the stick force due to drift of the feel servo valve. The elevator stick trim is adjusted with front cockpit elevator trim and all artificial feel gain controls except stick position set on zero, until the stick moves as easily forward as it does backward. In other words, all stick forces are cancelled out. Then the gain controls are placed at their proper settings and the stick positioned for simulation by use of the front cockpit elevator trim control. The feel servos are then checked by the front pilot when he moves the stick and pedals and notices the resulting forces. The aft pilot knows that he may proceed with engaging the surface servos after he is told by interphone that the feel servos are working properly.

4. Engagement of the Auxiliary Surface Servo

The rear pilot checks the T-33 flight condition, especially airspeed, and then turns on the auxiliary surface servo by the momentary toggle switch, Sw 10. This also clutches the Δq measuring device in the Kollsman dynamic pressure instrument. Δq is then measured from a reference value equal to q at the time of turning on Sw 10. Indicator light L 8 lights to indicate the auxiliary surface servo is ON. The auxiliary surface may be turned off by momentarily depressing Sw 10 to the OFF position.

5. Engagement of the Position Servos

The position servos are always mechanically connected to the airplane's control system. The engagement process consists of trimming the servo valves and pressurizing the servo circuits. The position-servo engage process is performed by the rear pilot in the following manner:

a. The normal aileron boost is shut off; this closes microswitch Sw 11 and lights indicators L 10 and L 11.

b. Indicator L 11 informs the front pilot that the engage process has started and that he must not move the stick or rudder pedals until it is completed, at which time L 10 and L 11 will go out.

c. The trim meter located on the rear cockpit switch console now indicates the error in the position servos as selected by Sw 12. At the switch position shown in Figure 5, the trim meter indicates the elevator servo valve error which can be nulled by the rear cockpit elevator trim knob. In a similar manner, switch Sw 12 is turned to indicate the aileron servo valve error, then the rudder servo valve errors which are nulled by the aileron and rudder trim knobs, respectively. The fourth position of the selector switch energizes relay K 35 which applies the sum of the three error indications to the trim meter.

d. If the total servo valve error appears satisfactory to the rear pilot, he may pressurize the surface servos by momentarily pressing the toggle switch Sw 13 to ON. The servopistons remain bypassed but some indication of the servo position errors will be felt in the rear cockpit controls due to pressure drops in the servopiston bypass circuits. Pressure to the servos may be immediately shut off by pressing Sw 13 to OFF. The engage process may be completed by momentarily depressing Sw 14 which removes the servopiston bypass.

e. When the engage process is complete, the front cockpit indication (L 11) goes off and the engage indicators (L 12) and (L 13) come on. The trim meter connection reverts to the elevator hinge moment signal so that the aft pilot can keep the airplane in trim during steady maneuvers through the normal T-33 elevator trim control. This insures that the control system may be disengaged at any time, without causing a sudden maneuver.

f. The front pilot then checks the response to his control motions and, if all right, performs the first flight test.

6. Recording System Operation

The recording system is turned on and off by the aft pilot. If a recording is in progress when Sw 1 is turned off, the record will automatically be extended for a pre-set interval (up to 90 seconds) by a time delay. This permits taking records of emergency situations. Indicator light (L 4) flashes while recording is going on.

7. Disengagement of System

After completion of the first set of test maneuvers, the rear pilot may change the artificial stability and/or control gains in one of three ways:

a. By disengaging the position and feel servos by pressing Sw 5, (elevator trim should be checked first) and resetting the gain controls on the aft cockpit right-hand console, and then re-engage by repeating the procedure from step 3.

b. By disengaging the position servos by pressing Sw 13.

c. By changing the controls without disengaging the position servos.

The choice among (a), (b), and (c) depends on the magnitude of the change required and whether there is a question of obtaining an undesirable intermediate condition by changing one control at a time.

When the tests are completed, the system is disengaged as follows: The rear pilot checks the elevator trim by seeing that the trim meter reads zero and then disengages by pressing Sw 5. Finally he restores normal aileron boost by turning the manual hydraulic valve to the "aileron boost" position.

C. ABNORMAL OR EMERGENCY OPERATION

1. Disengage Procedure for Abnormal Operation

Should the operation of the system or a part of it appear abnormal at any time, the entire system or a portion of it can be disengaged by one or more of the switches and/or valves listed in Table I.

Failure of one of the static converters or of a component in the computing equipment which would cause a larger position servo valve signal, will automatically disengage all of the servos.

Protection against severe maneuvers is also provided by the automatic safety trip. All the servos are automatically disengaged if either the lateral or normal acceleration exceeds pre-set limits.

2. Emergency Disengage Procedure

In the event of an emergency, the artificial stability and control system can be completely disengaged by the rear pilot by placing the main power switch (Sw 1) in the OFF position. If the emergency should be due to a malfunction of the electrical control and interlock circuitry which would make switch (Sw 1) ineffective, the rear pilot can actuate the position servo "Emergency Dump Valve" to disengage the position servos and regain control of the airplane. Also, switches Sw 2, Sw 5, Sw 6, Sw 7, Sw 11, and Sw 13 can be used to disengage the system.

If an emergency should make it necessary to abandon the airplane when the wheel and column configuration is installed in the front cockpit, the front pilot should open the "Front Stick Dump Valve" and push the control column forward to engage the safety latch before actuating the seat ejection mechanism. This procedure is necessary to provide clearance for the front pilot's feet and knees.

D. OTHER CONSIDERATIONS AFFECTING SAFETY OF FLIGHT

1. Stress Analysis

An analysis was made to substantiate the strength of the servo control systems and associated structures installed in the T-33 airplane. The modifications to the airframe and control system of the normal T-33 were also investigated. The results of this stress analysis are reported in Reference 2.

2. Vibration Survey

A series of vibration tests are to be conducted to demonstrate that the conversion of the T-33 to a variable stability airplane has not caused any significant adverse effects on flutter. The results of these tests and associated analysis will be reported in detail when completed.

3. Weight and Balance

The various modifications and installations required to convert the T-33 to a variable stability airplane have had significant effects on the weight, balance, and allowable center of gravity travel.

Installation of the F-94 nose section and the variable stability and control equipment had a direct effect on the weight and weight distribution of the T-33 airplane. Also, the F-94 nose section and the auxiliary surfaces caused the aerodynamic center to move forward approximately 1.4%.

With the elevator spring tab locked it was recommended that the center of gravity be maintained as far aft as practical to keep the stick forces down to reasonable values during take-offs. Therefore, a take-off center of gravity location 3.7% forward of the new aft limit was chosen for normal operations.

The net result of these center of gravity considerations was the addition of approximately 125 lb. of ballast in the tail cone.

4. Runway Requirements

A study of the take-off and landing requirements of the T-33 compared to the available runway length at the Buffalo Airport has been made. This study indicated that the T-33 could be safely operated from the Buffalo Airport in the planned test configurations.

5. Horizontal and Vertical Tail Load Studies

The effect of the automatic control system on horizontal and vertical tail loads has been given careful study. The results of the studies were reported in References 7 and 8.

Based on these investigations the control surface hinge moment limits and the normal and lateral acceleration limits for the automatic safety trip were established.

SECTION V
INSTRUMENTATION

by J.L. Beilman

In the fifteen-month period that has elapsed since reporting the preliminary instrumentation design activities in Reference 1, there has been designed, constructed, and installed in the T-33 airplane a substantial amount of electronic equipment which comprises the data handling portion of the Variable Stability and Control System. Three views of the nose of the airplane, where the major portion of the electronic instrumentation has been installed are given in Figure 6. These views provide some idea of the complexity of the system and also show that the increased internal volume, made available by installation of an F-94 nose section, was actually required and quite fully utilized. Other electrical units of the system are located in the cockpits, plenum chamber, dorsal fin, and in the wings and horizontal stabilizer.

Obviously, a system of this kind required a large amount of detail design and construction work. It is not the purpose of this report to become involved with these details but rather to provide a kind of general progress report on the instrumentation work of the past fifteen months with emphasis on special features of the system and any unusual problems solved in its design and construction.

It should be noted here that, since this project was quite a large undertaking relative to the amount of electronic engineering and technician manpower available, it was decided at the outset to make judicious use of those facilities which could be found in sub-contracting companies to best complement our own efforts. Only thus could we hope to apply to the program, in a relatively short time, the required total of design and production effort.

CHRONOLOGICAL DEVELOPMENT OF MAJOR ACTIVITIES OF ELECTRONIC DESIGN

The starting point for instrumentation work in Phase II of this project might well be taken to be the electrical block diagram of the gain computing elements of the system, which evolved from the Phase I work and was given as Figure 12 in Reference 1. This was an over-all system block diagram of the signal generating devices and circuits as well as the elements required for automatic programming of system gains. This diagram was consistent with the functional requirements of the system (as shown in Figures 5, 6, and 7 of Reference 1) and except for a number of detail changes, is fundamentally correct for the completed system. The only signal handling portions of the system not included in Figure 12 of Reference 1 are the closed loops of the elevator, rudder, aileron, and auxiliary surface servos.

With the electrical block diagram as a guide, and equipped with a knowledge of (1) the mechanical and electrical characteristics of the various instruments and pickoffs and (2) the maximum gains required of the variable stability system, the next step was a systematic survey of all signal channels to determine the amplification requirements. (The instruments and pickoffs had been selected or developed as part of the Phase I work and were ordered at the beginning of Phase II.) This survey showed that in addition to six servo amplifiers there would be required ten summing amplifiers and thirty other amplifiers for either signal voltage gain, signal power gain, or both.

As might be expected, the actual voltage gain and output power requirements, at each point in the system where an amplifier was required, varied over a considerable range - from a few milliwatts to a full watt.

These varied requirements were studied for the purpose of arriving at specifications for a few basic types of amplifiers which together would satisfy all of the requirements. Although initially it appeared that more than one type of signal amplifier would be required, because of the range of output power requirements, circuit arrangements were sought and found which reduced the maximum output power requirements for several of the amplifiers to a point where a single basic type would suffice for the entire system. The advantages of having only one type of signal amplifier, as against several types, are obvious.

There thus evolved three sets of amplifier specifications - one each for the servo amplifier, summing amplifier and the voltage or isolation amplifier.

Here there was a problem not only of designing stable feedback amplifiers, but of employing sub-miniaturization techniques in their construction and of producing them in quantity. Consequently, these specifications were submitted to the Rheem Manufacturing Company of Downey, California, who are specialists in the field of subminiature vacuum tube amplifier design and production. They agreed to undertake the development of the required amplifiers and purchase orders were placed for seven servo amplifiers (Rheem Model REL-20), eleven summing amplifiers (Rheem Model REL-19) and thirty-two isolation amplifiers (Rheem Model REL-18). It was determined very early in the amplifier development program that all three amplifier types could be put in identical cases, which permitted additional uniformity in our chassis design and construction. The only physical difference between the various amplifier types is the kind of disconnect on the base or the way the disconnect is keyed with respect to the mounting flange. A quick disconnect feature was incorporated to facilitate installation and removal of the amplifiers from the chassis. The servo amplifier is typical of the design and construction techniques employed in these subminiature tube amplifiers, and three views of it are presented in Figure 7.

Concurrent with the development of the amplifier specifications, detailed specifications were prepared for the four instrument servo systems which were required for programming gains with dynamic pressure and angle of attack and for generating the special function of bank angle needed to automatically maintain altitude in turns. The specifications were detailed and complete in regard to function, electrical characteristics, and dynamic performance, but were quite general with regard to construction details. This was done to provide the subcontractor the greatest possible latitude in employing components and manufacturing techniques which were more or less standard with him. By granting such latitude it was hoped that suitable servo systems could be procured more quickly and at minimum cost.

A satisfactory price and delivery quotation was obtained from the Kollsman Instrument Corporation for the "q Computer" and an order was placed for two systems, providing a spare system. The first delivered system did not meet the specification for resolution of small rates of change of pressure, necessitating some redesign of the rate-generator section. Pictures of the final version of this instrument are given in Figure 8. Not shown is the vacuum tube-magnetic amplifier which drives the servomotor.

Some difficulty was experienced in finding a subcontractor for the three remaining instrument-servo systems. This was due to the combination of their specialized nature and the fact that only unit quantities were involved. After several manufacturers of servomechanisms were approached without success, the Industrial Control Company of Wyandanch, L.I. was contacted and they later submitted acceptable quotations for all three systems. Figure 9 is a view of the "Inverse q Computer", which is typical of the three systems supplied by the Industrial Control Co. The servo amplifiers of these instrument servo systems employ transistors for voltage gain followed by a magnetic amplifier power output stage. For the sake of greater simplicity, it was decided to eliminate the automatic loop gain compensation referred to in Reference 1 on page 130, and Figure 10 shows the measured frequency response of the completed system. While not too sluggish for the intended purpose when the loop gain is low, the system still has an acceptable amount of damping at the highest loop gain. Figure 11 is a calibration of the pressure function generated by this system.

Equipped with a knowledge of the electrical and mechanical characteristics of the building blocks of the system, that is, the amplifiers, the primary sensing instruments and the instrument-servo systems - the next major task was to design the packaging and installation of the complete system in the airplane.

To facilitate the detailed design of the system, the over-all block diagram was divided into several major sections, each one of which was to become a separate chassis or unit of the system. This division was made, as logically as possible, on the basis of distinct functions of the system. There thus evolved a Pedal Force Unit, an Aileron Stick Force Unit and an Elevator Stick Force Unit. Each one of these units includes substantially all of the circuitry necessary to control the corresponding artificial feel hydraulic servo. Likewise, there evolved a Control Surface Servo Unit (containing all the gain controls, summing and servo amplifiers for the aerodynamic surface servos), and an Artificial Stability Master Unit (serving as a central junction box for all the primary sensing instruments and the instrument-servo computers as well as containing all the circuitry for deriving and synthesizing signals). Also, to complete the variable stability system, there was required a Power Control Unit (serving as the main electrical power distribution center of the system), and Auxiliary Surface Servo Control Unit and several cockpit control panels.

In addition to the components of the variable stability system there was required a substantial amount of recording instrumentation for obtaining flight data on the various system parameters. The major CAL built units of the recording system are the Recording Master Unit, the Sampling Switch Unit and the Photo-Observer. The Photo-Observer and a CEC type 114-P3,18-channel oscillograph provide the necessary flight records. The Recording Master Unit contains the amplifiers and phase-sensitive demodulators required for recording the amplitude modulated carrier signal intelligence in the system. The Sampling Switch Unit is a device for making a permanent record of the position of every gain control and switch affecting the configuration of the variable stability system. In the first 10 seconds of every recorded test configuration this switch will sample the pilot's setting of 40 continuously variable gain controls, the position of 6 relays, the voltage output of the Inverse q Computer and finally "home" in a position where it monitors the q Computer operation for the duration of the recording interval. All this information is recorded on one galvanometer.

Once the complete system had been broken down into several units of well defined function, two large and equally important areas of electronic design work were open to simultaneous attack. The first of these was the preparation of detailed schematic diagrams leading to the final wiring and cabling diagrams of the system. (To give some idea of the extent of this type of work, a complete listing of all electrical drawings is given in Table III.) The second area of work was the detailed design of the complete installation.

The first step in the detailed design of the packaging and installation of the system was to make an estimate of the dimensions of all of the units enumerated in the above paragraphs. Next a 1/4-scale mock-up of the F-94 nose was made from cardboard, including 1/4-scale mock-ups of the radio gear and any other equipment normally required. Using the estimated dimensions, 1/4-scale mock-ups were also made of all of the proposed units of the system.

A considerable amount of study was then given to the various possible arrangements for locating all the required equipment in the available nose space. The configuration which finally evolved put the larger and heavier units in the aft section of the nose while the smaller, lighter units are in the forward section under the radome as shown in Figure 6. This results in having most of the control system low-level signal handling units grouped together under the radome, while the inverter, DC power supplies, power control unit, oscillograph and photo-observer are grouped together in the aft nose compartment.

At first, it was contemplated that most of the units under consideration would be of conventional design - namely, a shock-mounted chassis and front panel plus dust cover arrangement. However, detailed design work showed such a plan to be very difficult to accomplish in the limited space available. To continue with this plan would have greatly increased the mechanical design time required because it is basically wasteful of space to have rectangular units inside of the curved surfaces of the nose. In addition, it was felt that cooling the separately packaged units would probably require a blower in each unit.

As a result of these considerations, it was decided to employ an open- type construction in which a thin but rigid shock-mounted aluminum box, located underneath the removable radome, provides two vertical mounting surfaces of considerable area to which most of the major chassis of the system may be attached. Left-hand, right-hand and front views of this shock-mounted box are given in Figure 12.

Components on the individual chassis were then so arranged as to best conform to the airplane contours, as shown in the head-on view of the completed installation in Figure 13. All gain controls, screw-driver adjustments, and plug-in components such as amplifiers, tubes and choppers were then mounted directly on the chassis deck, greatly simplifying the design and construction. Figure 13 also includes left-hand and right-hand views of the shock-mounted nose structure with all electronic chassis installed.

Close-up views of several of the major units of the system are presented in Figures 14 through 21. These were selected as being representative of the type of design and construction employed on electronic units throughout the variable stability and control system. Views of the control panels as installed in the front and rear cockpits are given in Figures 22 through 25.

ELECTRICAL DESIGN FEATURES

In order to maintain some degree of continuity, many details were omitted in the preceding chronological account of the electrical design, construction and installation of the variable stability and control system. It is felt that some of these details are worthy of comment and so they are noted in the following paragraphs.

1. With the intention of securing greater reliability and reducing system maintenance to a minimum, the use of devices in which a contact wipes across a resistance element has been avoided whenever such a device might experience a great number of cycles of operation. Thus the linear-motion position transducer, employed for servopiston feedback on each of the six hydraulic servos, is an inductive-type device developed for this program by Cornell Aeronautical Laboratory and reported in Reference 1. So also, every control surface position is sensed by a synchro, every multiplication and every division is performed by a synchro, and every instrument-servo system employs a synchro for position feedback. Finally, every flight parameter, whether a pressure, an angular velocity or a linear acceleration, is sensed by an instrument employing an inductive pickoff.
2. In order to achieve a high degree of stability of system calibrations, a one-tube, unity-gain feedback amplifier is used instead of a cathode-follower wherever isolation or impedance-transformation is required. This amplifier, with an open-loop voltage gain of 10, is considerably more stable than a cathode-follower and possesses a very low (40 ohms) output impedance. It can also supply a balanced output.

3. A great amount of care was exercised in the design and construction of the system to see that every signal carrying wire was accompanied by and twisted with its ground return, the twisted pair being shielded. This precaution, in combination with low impedance levels and separate systems of power grounds and signal grounds (tied together at just one point in the entire system), has paid real dividends in the low noise levels so far observed.

4. A unique feature of the system is the use of the "chopper differentiator" to obtain, electrically, the angular accelerations and the time derivatives of the angle of attack and angle of sideslip. The operation of this circuit was discussed qualitatively in Reference 1 and a more detailed analysis will be reported subsequently. Briefly, this circuit, employing a synchronous switch or chopper, is capable of producing at its output a carrier signal whose amplitude modulation is, to a close approximation, the first time derivative of the modulation of the input carrier signal. Its advantages are (1) that no output is produced by changes in the carrier frequency as is the case with any frequency selective network which might be used, and (2) the ease of adjustment of the equivalent first-order-system time constant of the circuit. The use of this circuit to differentiate the carrier signal output of the angular velocity gyros obviated the use of angular accelerometers whose output, it was suspected, would require low-pass filtering anyway for reasons of over-all system stability. Any required degree of acceleration signal filtering can now be obtained by increasing the phase lag in the chopper differentiator, which is a simple, calibrated adjustment.

5. At the very beginning, it was obvious that if as many as 30 or 40 gain controls were to be provided for the pilot in an already crowded cockpit, a new device would be required to meet the situation. This device would have to be conservative of panel mounting space, and capable of easy and continuous adjustment

but at the same time not likely to be disturbed inadvertently, or by vibration, or accidental means. It would have to be easy for the pilot to read at a glance and would be highly desirable if the setting selected by the pilot could be automatically monitored. Finally, there would have to be engineered into the device such characteristics as reliability and serviceability, linearity and repeatability - it should be a practical and workable device from the standpoint of assembling and installing it.

A sub-contractor was found who was willing to undertake the development of a device which embodied in a practical manner all of the above characteristics. It was proposed to the sub-contractor that the gain-controlling element be a single turn, dual element, wire-wound potentiometer measuring 7/8 inch in diameter where one winding would operate in the signal circuit and the other winding would serve as a position transmitter or monitor. It was specified that the over-all diameter of the device should not exceed 1-1/8 inches and that a digitized presentation of the setting should be available.

Accordingly, a prototype unit - called a Digitrol - was developed and submitted for approval. It appeared that with minor modifications this device would be acceptable. It had previously been decided that one calibrated master control, to determine the maximum gain available at the pilot's control, should be incorporated in each channel of the system. Detailed design work now showed that panel mounting space for these master controls was at least as limited as the space for the pilot's controls in the cockpit. Therefore, Digitrols were ordered for each place in the system where a calibrated control was required, for no other controls as small and as easy to read were available. Various views of the Digitrols as finally installed are shown in Figures 13, 15 and 23.

The installation of 87 Digitrols in the variable stability and control system, and their use to date has shown them to be highly convenient and satisfactory devices. The combination of Digitrols with standard wire-wound potentiometers, rated nominally at ±2% independent linearity (i.e., best straight line fit does not have to pass through the origin), has resulted in a system of controls with a linearity of about 0.5% and backlash on the order of 0.1 to 0.2%.

6. Approximately 300 circuits are carried through the pressure barrier into the cockpit and many of these are shielded pairs of wires. Initially it was planned to use pressurized electrical connectors, but when the actual installation of cabling in the airplane was under way it turned out that these connectors would have to be in a place with poor accessibility. It was felt undesirable to have so many connections of relatively fragile wire in such a location. Consequently a special potting fixture was designed, machined and installed. All of the wires were then fed through a pair of screen-type separators fixed at opposite ends of the fixture - which kept the wires parallel and uniformly separated as they passed vertically through the cockpit floor. The fixture formed a well into which a thermo-setting compound was poured, thus making a pressure seal. This saved making about 600 soldered connections on the originally comtemplated connectors.

7. All major chassis of the system incorporate a miniature test jack, i.e., a receptacle to which are brought terminals considered important for signal tracing and troubleshooting. A test harness having a plug on one end and a box with test jacks on the other then facilitates getting at these points for measurements.

SECTION VI
MECHANICAL DESIGN

by C.L. Muzzey

Phase I of the T-33 project considered the necessary equipment and control systems for creating a variable stability airplane of great versatility. The final report for Phase I (Reference 1) presented plans for installations of control surface servos, and for the artificial feel system. In some cases, several alternatives were presented, with no final decision. Phase II has now been completed, all of the proposed designs have been carried out and the decisions resolved as will be apparent from the following.

The major designs are described in the installation drawings listed below.

Dwg. No.	Title
FRS-835-015-6	Elevator Position Servo Assembly
FRS-835-015-9	Aileron Position Servo Assembly
FRS-835-015-13	Rudder Feel Servo Installation
FRS-835-015-22	Rear Cockpit Rudder Crossover Installation
FRS-835-015-38	Cockpit Control Installation - Aileron and Elevator
FRS-835-015-62	Auxiliary Surface Installation Assembly
FRS-835-015-68	Rudder Position Servo Installation

These drawings are called out in Figure 26 of this report, which shows pictorially the location of each of the installations in the airplane.

The elevator position servo has been installed on the forward wall of the plenum chamber. This location was indicated as the most desirable choice in Reference 1.

The aileron position servo has been located in the plenum chamber on the rear face of the rear wing spar. This location was given as the probable choice in Reference 1. The questions of cable stretch were satisfactorily answered by dynamic tests on the servo test rig, and by aerodynamic calculations showing that steady state loads and cable stretch still permitted adequate airplane rolling performance. The centerline location also avoids possible questions about effects on flutter characteristics if the servos were to be installed in the wings.

The rudder feel servo is not located in the cockpit as indicated in Reference 1, but is mounted ahead of the fire wall with special cables running through pressure seals into the nose compartment.

The aileron and elevator feel servos and control stick mechanism are designed and installed substantially as shown in Reference 1.

The auxiliary surface installation is generally very similar to that in the F-94 airplane modified under Contract AF33(038)-20659.

The rudder position servo is installed in the engine plenum chamber and drives through the existing cables. The installation differs slightly from the layout suggested in Reference 1 in that a torque tube arrangement replaces a walking beam to connect the left and right hand rudder cables.

Figures 27 through 33 are photographs of these above areas showing the actual installations.

SECTION VII

HYDRAULIC SYSTEM

by C.H. Hutchinson

GENERAL DESCRIPTION

Extensive additions to the normal T-33 hydraulic system were required to accommodate the servo installations of the variable stability system. Two basic hydraulically powered servo systems were incorporated; the position servo system which operates the aircraft control surfaces, and the feel (force) servo system which develops reaction forces at the pilot's cockpit controls. Each of the three position servos constitutes a closed center sub-system which can be isolated from the main hydraulic supply. Each of the three force servos ("feel" system) is a sub-system, and as a group they can be isolated from the main supply. Typical hydraulic circuit schematics of the position and feel servos are presented in Figures 34 and 35.

Other significant additions to, or changes in, the ship's hydraulic system are enumerated below (Also see Figure 36):

1. A self-displacing accumulator was added near the position servos. The original accumulator (a 7-1/2 inch spherical type) was relocated near the feel servos.
2. The forward cockpit aileron boost shut-off valve was deleted from the aileron system. This gives complete control of the aileron boost to the pilot in the rear cockpit. The valve was subsequently utilized as an emergency dump of the elevator feel servo.
3. A micronic filter and a magnetic filter were added to the pressure supply line immediately downstream of the engine-driven hydraulic pump. The filter in the aileron boost circuit became superfluous and was removed.
4. The ability to use the emergency hydraulic pump system as a supply for ground checks was sacrificed by disconnecting the pump suction line from the main hydraulic reservoir. Use of this line for the fluid make-up system of the position servos eliminated any necessity for running an additional line through the rear spar web. It should be

noted that this arrangement in no way impairs the operation of the emergency system during flight.

5. The fluid make-up system was required for two reasons; first, to insure that the pressure limiting circuit was as stiff as possible, i.e., the lines of the circuit contain pressurized fluid at all times which reduces flow due to compressibility below limiting pressure; second, to insure operation of the servopiston solenoid by-pass valve under the adverse condition of pressure on both the pressure and return ports. (The sequence for engaging the position servo may be followed in Figure 34. Initially the pressure shut-off solenoid valve is open, pressure is not admitted, and the by-pass solenoid valve is open from cylinder to return ports. The pressure valve is then closed and the entire limiting circuit is pressurized to approximately 500 psi as determined by the servovalve. The pressure port of the by-pass valve has make-up system pressure on it at this time. Now, the criterion for successful operation of the by-pass valve is that the pressure at the pressure port shall be greater than the pressure at the return port by 150 psi. Closing the by-pass valve connects the cylinder and pressure ports. The relief valve now sees the pressure existing on the high pressure side of the servo actuator. When the relief valve setting is exceeded,flow goes to the low pressure side of the servo actuator tending to raise its pressure until equilibrium is again restored at differential pressures equal to or less than the drop through the relief valve.) The make-up pressure is reduced from system pressure by an integral-reducer-relief valve. Its pressure output may be admitted to the pressure limiting system, or the limiting system may be opened to the system return through a manually operated, three-way, two-position, selector valve. The latter case then provides an emergency dump.

6. A small single-acting, spring-return hydraulic strut was added to introduce aileron friction forces into the aileron feel system. It is controlled by a manually operated three-way, two-position, selector valve.

7. A new engine-driven pump rated at 12.0 in.^{3} /sec at 1500 rpm for 1000 psi supply was installed to replace the original pump (7.6 in.^{3} /sec under the same conditions).

SYSTEM DESIGN

Two aspects of the hydraulic system design will be considered; the total flow requirements, and the pressure limiting circuit of the position servo.

1. Flow Requirements

Individual servo flows are calculated by forming the product of the maximum design servopiston velocity and the piston area $(Q = \dot{\sigma}_p A)$. This information is presented in Table II. Also presented are the maximum design control surface velocities. Studies (see Reference 9) have shown that during strenuous flight maneuvers, control surface rates of less than half of the specified maximums (70 deg/sec) would be required. Thus, a design criterion was established which specified continuous operation at 50% of maximum control surface velocity, or, equivalently, at half of maximum flow plus leakage flow.

$$\left(\frac{45.89}{2} + 4 = 26.95 \text{ in.}^3 \text{/sec}\right).$$

Various combinations of engine-driven pumps and accumulators were evaluated against the design criteria by constructing an alignment chart (Figure 37). The accumulator volume was taken as the fluid available between 1000 psi (system pressure) and 700 psi under adiabatic conditions (accumulator charging pressure, 600 psi). At a system pressure of 700 psi, the load flow output of the position servovalves will be approximately 60 percent of the full rated flow (see Equation (1) under Pressure Limiting Circuit - Theory).

The alignment chart solves the equation

$$t = \frac{V_A}{Q_{servo} - Q_{pump}}$$

where

t = operating time (sec)

Q_{servo} = load flow plus leakage flow (in.^{3}/sec)

Q_{pump} = flow output of the pump and is a function of pump speed (in.^{3}/sec)

V_A = available accumulator volume (in.^{3})

Normal pump speeds vary between 3700 and 3900 rpm (.370 of engine speed). By use of the 12.0 in.^{3}/sec pump (rating at 1500 rpm) combined with an effective accumulator volume of 84 in.^{3} the operating time becomes infinite.

2. Pressure Limiting Circuit

One of the primary factors considered in determining hydraulic servo performance is the relative magnitude of the hydraulic supply pressure to the maximum required load (motor) pressure. The optimum value, which depends on a number of practical as well as theoretical factors, falls in the range P_M / P_S = .5 to .7 (P_S = 1000 psi). Thus, if P_M corresponds to the structural limit load of the system, some means for protecting against loads corresponding to P_S must be incorporated. In the system installed, a pressure limiting circuit (Figure 34) affords this protection by establishing a maximum differential pressure across the servopiston. It also allows the servo to be dumped, i.e., the differential pressure can be maintained at approximately zero.

Questions to be asked about this system are:

(1) How well does it limit pressure?

(2) What are its effects upon over-all servo performance?

To answer these questions the basic theory and the results of a series of tests are presented.

(a) Theory

The load-flow characteristic of a flow control valve can be successfully approximated by using the sharp-edged orifice equation:

$$Q_V = K_V \, x \sqrt{P_S - P_M} \tag{1}$$

where

Q_V = control valve flow

K_V = effective orifice coefficient

x = percent of maximum valve opening

P_S = supply pressure

P_M = motor or load pressure

Now, if a network is added between the valve and the load which passes flow when P_M exceeds some pressure P_L, and if this network can also be considered a sharp-edged orifice, then the flow through the pressure limiting network can be written as

$$Q_L = K_L \sqrt{P_M - P_L} \quad (P_M \geq P_L) \tag{2}$$

where

Q_L = limiting circuit flow

K_L = effective orifice coefficient

P_L = limit pressure

The ratio P_M / P_L can be obtained by equating (1) and (2) giving

$$\frac{P_M}{P_L} = \frac{1 + \left(\frac{P_S}{P_L}\right)\left(\frac{K_V}{K_L}\right)^2 x^2}{1 + \left(\frac{K_V}{K_L}\right)^2 x^2} \tag{3}$$

This value is a measure of the static performance of the limiting system; i.e.,the increase in effective limiting pressure. The ratio is minimized by keeping the parameter K_V / K_L small. (Note that $P_S / P_M \simeq P_S / P_L$ for small flows and that the range of values has previously been set.)

Equation (3) has been plotted (Figure 38) for values representing the aileron servo and the elevator or rudder servo:

Aileron Servo	K_V/K_L	$= .25$
	P_S/P_L*	$= 1.9$
Elevator Servo or Rudder Servo	K_V/K_L	$= .05$
	P_S/P_L*	$= 1.9$

It should be noted that the maximum pressure rise amounts to only 5 percent. Static tests and step input response tests were conducted which confirmed the form of equations (1) and (2), and from which the values of K_V and K_L were derived. Precise quantitative verification of equation (3) was not feasible.

(b) Dynamic Response Tests

Ideally the effects of the limiting circuit upon the dynamic response of the system should be negligible at load pressures less than limit pressure. When limit pressure is reached the load pressure should cut off sharply at this value. An analytical study of the dynamic response of a servo with pressure limiting is beyond the scope of this study; however, tests have been conducted to evaluate the system.

The dynamic tests were conducted using a test setup which represents the aileron position servo. Physical data for the test setup are tabulated below.

Piston Net Area	$= 2.77$ in.^{2}
Piston Lever Arm	$= 3.75$ in.^{2}
Load Spring Rate	= 2690 lb/in. (at the piston)
Load Inertia	$= .276 \dfrac{\text{lb-sec}^2}{\text{in.}}$ (at the piston)
System Pressure	= 1000 psi
Limit Differential Pressure	= 700 psi
Maximum Control Valve Flow	$= 25$ in.^{3}/sec (at zero load)

*At one point in the design, a value of $P_S/P_L = 1.43$ was used which explains the presence of these curves in Figure 38.

Before discussing the test results it must be recognized that there are four regions in the frequency-amplitude domain in which servo frequency response tests may be conducted. One of these domains yields essentially linear results, while the other three are non-linear. As shown in Figure 39, area A_1 corresponds to frequency-amplitudes below both pressure and velocity limiting and is the linear response region; A_2 corresponds to a pressure limiting region determined by the relief valve setting in the limiting circuit (700 psi for these tests, 525 psi for the actual installation); A_3 corresponds to velocity limiting determined by the load-flow characteristics of the control valve (the lower boundary of this region represents frequency-amplitude combinations which just produce velocity limiting during sinusoidal oscillation; the upper boundary represents the maximum frequency-amplitude combinations obtainable for a simple spring load); A_4 corresponds to combined velocity and pressure limiting.

Three tests were conducted to evaluate the limiting ability of the circuit and to determine the effects of the limiting circuit upon servo dynamics. The test points enclosed by triangles in Figures 39 and 40 represent responses to sinusoidal position input commands (e_{in}) which are 1.5 to 2.7 times the command required to just reach the pressure limiting load position. In this test the limiting circuit is connected. Figure 40 shows that the amount of overshoot tends to increase with frequency until the effects of velocity limiting prevail. The plot has been extrapolated to a limit pressure of 525 psi which represents the actual installation of the aileron position servo. The same trend can also be observed in Figure 39 (cf., the points which lie in areas A_2 and A_4). It should also be noted here that the frequencies at which it is possible to reach pressure limiting are in a limited low frequency range.

The other two tests are represented by the points in circles. One test has the limit system connected and the other test has the limit system removed. Test points were identical for both conditions. Input commands ranged between .36 to .80 of the static limit load position command. At frequencies greater than 20 radians per second, all test points became identical (points enclosed by both circles and triangles). All of this data is plotted in the more conventional non-dimensionalized amplitude ratio and phase angle versus frequency planes in Figure 41. Also shown is the response with no-velocity limiting which was obtained previously and reported in Reference 1. The three points which lie in the pressure limiting region become indeterminate in the amplitude ratio-frequency plane and do not appear. The test results substantiate the following conclusions:

1. The limiting circuit functions satisfactorily. It can be expected to allow the pressure to overshoot a maximum of ten percent for the installed aileron position servo and less than this for the rudder and elevator position servos due to the lower flow capacity of their control valves.
2. The limiting circuit does not affect the servo dynamics below limiting pressure.

SECTION VIII
SERVO DESIGN

by W.J. Thayer

INTRODUCTION

A part of the preliminary studies carried out under Phase I of the T-33 program concerned the design and testing of the electrohydraulic servos to position the control surfaces and those to introduce feel into the cockpit controls. These studies were conducted in several steps for both the position and the feel type servos as follows:

(1) The theoretical understanding of each servo system was developed until sound design synthesis of the control systems was feasible.

(2) Experimental test setups of both the position and feel servo systems were designed and constructed so that actual, full-scale measurements and experience could be obtained for each servo system.

(3) The experimental observations and theoretical predictions were correlated to demonstrate the validity of the latter.

(4) Necessary revisions and/or extensions of (1) and (2) were undertaken until a satisfactory correlation was obtained.

Much of this work was reported previously in Reference 1. In general, the experimental results obtained with the test rigs gave good agreement with the theoretical analyses with one important exception, this being the violent instability of the torque servoloop of the pressure-control feel servos, even at very low values of loop gain. This instability was discussed in Reference 1, but no satisfactory explanation of the observed performance was available at that time. Work on this problem continued into Phase II, as the decision to use pressure-control feel servos was contingent upon satisfactory performance with the test rig setups.

This section reports a theory which explains the instability of the feel servos and includes calculations which predict the nature of the instability, together with compensation techniques which yield an acceptable stability margin. Test rig performance with the modified feel servo has demonstrated the suitability of the design for the T-33 control system.

FEEL SERVO SYSTEM

The block diagram of a feel servo with a pressure-control servovalve was given in Reference 1 (Figure 51, page 260) and, for convenience, is repeated here (See Figure 42). The dynamic relationship between the control force and the control position describes the stick "feel", and this expression can be derived for the system of Figure 42 as

$$\left(\frac{F_W}{\delta_W}\right)(s) = m_W s^2 + c_W s + \left\{ \frac{\dfrac{K_5}{K_1} + \dfrac{K_4 K_6 G_6(s)}{OL_P}}{1 + \left(\dfrac{K_5}{K_1}\right)\left(\dfrac{1}{k_c}\right) + \dfrac{1}{OL_P} + \dfrac{K_4 K_6 G_6(s)}{OL_P}\left(\dfrac{1}{k_c}\right)} \right\} \quad (4)$$

Where

OL_P = servo open-loop transfer function (non-dimensional)

$$= K_1 \; K_2 \; G_2(s) K_3 \; G_3(s) K_4 = K_0 \, G_2(s) \, G_3(s) \quad (5)$$

$$K_0 = \text{open loop gain} = K_1 K_2 K_3 K_4 \qquad \text{(non-dimensional)} \quad (6)$$

The first two terms of equation (4) express the normal inertia and damping forces required at the stick, while the large bracketed expression is the apparent spring effect of the servo. If the loop gain is high so that $\frac{1}{OL_P} \ll 1$, and if the column is considerably stiffer than the servo, then the servo contributed term reduces to K_5/K_1 (lb/in.), the equivalent servo spring rate.

A previous investigation, reported in Reference 1, considered the outer feedback loop of Figure 42, representing the inertia reaction of the control wheel. It was shown how this inertia feedback could cause servo instability at high values of servo stiffness; i.e., as the servo stiffness approaches the mechanical stiffness of the control column. This instability was observed in the test rig but was not of major importance as sufficiently high control stiffnesses (on the order of 100 lb/in. at the wheel) could be achieved with satisfactory dynamic performance.

A more disturbing problem which was reported in Reference 1 but which was left unsolved, was the violent instability of the torque feedback loop at extremely low loop gains (in the vicinity of $K_0 = 0.5$). This instability had not been predicted by the servoanalysis, and it was obvious that important dynamic effects were being overlooked or oversimplified. This problem was characterized by several observations:

(1) The instability of the torque servoloop seemed to be independent of the feel stiffness, always occurring near the same value of torque loop gain regardless of the gain of the position input. In fact, the instability was found to exist with the position feedback signal completely disconnected indicating that the difficulty was in the torque servoloop alone. This fact allowed the analysis of the trouble to confine itself to a much simplified system as will be shown below.

(2) The feel servo operated satisfactorily without the torque feedback; but at low stiffnesses, where small forces were encountered at the wheel, the drag of the servopiston contributed objectionable frictional forces.

(3) The torque feedback was effective in reducing this frictional drag, but the frictional effects were still large at gains where the torque servoloop became unstable.

(4) The torque servoloop instability was apparently a loading effect on the servo as the nature of the instability would change with different wheel-column combinations. The relationship between the instability and the servopiston loading indicated that the servovalve had appreciable response to flow which contributed to the deterioration of loop dynamics. A flow dependence of the pressure valve had been recognized, and, in fact, had been included in the original block diagram; however, the effects of this dependence had not been investigated as no information was available on the nature of the dynamic response of the valve with respect to flow.

TORQUE SERVOLOOP ANALYSIS

A linear valve response was assumed so the flow dynamics could be considered superimposed on the normal valve response to control current. This response is expressed as follows:

$$\Delta P(s) = K_3 G_3(s)\, i_\epsilon(s) - K_6 G_6(s)\, Q(s) \tag{7}$$

where: ΔP = differential pressure at the valve control ports (psi)

i_ϵ = valve control current (ma)

Q = hydraulic flow through valve control ports (in^3/sec)

K_3 = valve static response to current (psi/ma)

K_6 = valve static response to flow $\frac{psi}{in^3/sec}$

$G_3(s)$ = valve dynamic response to current

$G_6(s)$ = valve dynamic response to flow

To obtain quantitative information on the nature of the flow dependence of the valve, a series of static and dynamic tests were conducted to obtain flow-pressure data. For these tests a Cadillac Gage Company, type PC2, pressure-control valve was plumbed directly to a piston which was mechanically driven by the ram of a conventional position servo. Flow through the pressure valve was measured from the position of the piston. Both sinusoidal and step position inputs were utilized for dynamic response measurements, while constant velocity inputs yielded valve response to steady flow. A good linear approximation to these data was found to be

$$K_6 G_6(s) = 9.0\,(1 + 0.02\, s) \quad \left(\frac{psi}{in^3/sec}\right) \tag{8}$$

This flow response was then included in the analysis of the torque servoloop by itself. For this analysis the external load on the servopiston was assumed to be a simple spring and mass, representing the column flexibility and wheel inertia, respectively. This dynamic system is sketched on the following page. The transfer function relating servopiston position to servopiston force (which appears in the block diagram of Figure 42) is

$$\left(\frac{\delta_p}{F_p}\right)(s) = \frac{1}{k_c}\left[1 + \left(\frac{\omega_n}{s}\right)^2\right] \tag{9}$$

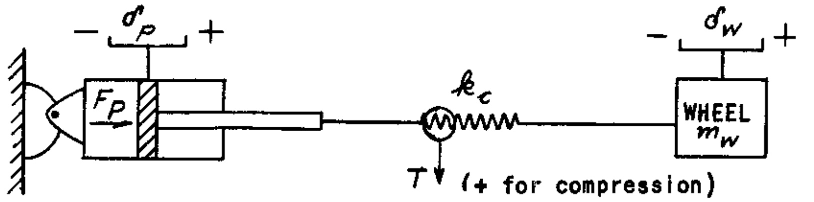

where
δ_p = servopiston position (in.)
δ_w = wheel position (in.)
k_c = column stiffness (lb/ in.)
m_w = wheel inertia effect (lb / in./sec²)
F_p = servopiston force (lb)
T = strain gage signal (lb)

SKETCH A: REPRESENTATION OF SERVOPISTON LOADING IN FEEL SERVO SYSTEM

where $\omega_n = \sqrt{\dfrac{k_c}{m_w}}$ (rad/sec) (10)

and the valve response is

$$\Delta P(s) = K_3 \; G_3 \; i_\epsilon - K_6 \; G_6 \; s \, \delta_p = K_4 \; F_p \; (s) \tag{11}$$

The stability of the torque servoloop may be investigated by redrawing this loop as sketched below.

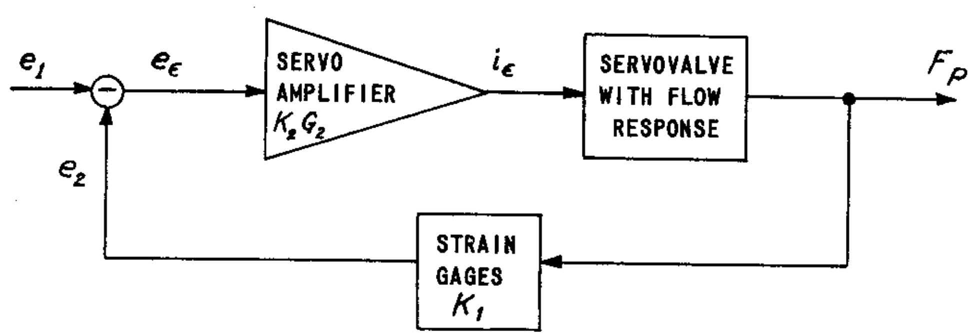

SKETCH B: TORQUE SERVOLOOP BLOCK DIAGRAM

The valve transfer function, F_p/i_ϵ , which includes the response to flow, can be determined from equations 9 and 11 and is

$$\left(\frac{F_p}{i_\epsilon}\right)(s) = \frac{K_3 K_4 G_3}{1 + \frac{K_4 K_6 G_6 s}{k_c}\left[1 + \left(\frac{\omega_n}{s}\right)^2\right]} \tag{12}$$

The stability of this system can be investigated through use of the inverse Nyquist approach utilized in Reference 1. Following this procedure, the equation for the inverse open-loop response is

$$OL_p^{-1} = \frac{1 + \frac{K_4 K_6 G_6 s}{k_c}\left[1 + \left(\frac{\omega_n}{s}\right)^2\right]}{K_0 G_2 G_3} \tag{13}$$

Now, if all dynamic elements are assumed to be first-order effects, as

$$G_2 = \left(\frac{1}{1+\tau_2 s}\right) \quad G_3 = \left(\frac{1}{1+\tau_3 s}\right) \quad G_6 = \left(1 + \tau_6 s\right) \tag{14}$$

then the inverse open-loop expression becomes

$$OL_p^{-1} = \frac{1}{K_0}\left(1+\tau_2 s\right)\left(1+\tau_3 s\right)\left\{1 + \frac{K_4 K_6}{k_c}\left(s + \tau_6 s^2\right)\left[1 + \left(\frac{\omega_n}{s}\right)^2\right]\right\} \tag{15}$$

which may be expanded in the frequency domain to

$$OL_p^{-1} = 1/K_0 \left[1 - \omega^2 \tau_2 \tau_3 + j\omega(\tau_2+\tau_3)\right]\left\{\frac{\left(\frac{K_4 K_6 \omega_n^2}{k_c}\right) - \left(\frac{K_4 K_6}{k_c}\right)\omega^2 + \left[1 + \left(\frac{K_4 K_6 \omega_n^2 \tau_6}{k_c}\right)\right] j\omega - \left(\frac{K_4 K_6 \tau_6}{k_c}\right) j\omega^3}{j\omega}\right\} \tag{16}$$

The constants actually measured for the feel test rig are:

k_c = 3850 lb/in.

m_w = 0.3 lb/in./sec^2

$\omega_n = \sqrt{\frac{k_c}{m_w}}$ = 113 rad/sec = 18 cps

τ_2 = 0.0053 sec

τ_3 = 0.0027 sec

τ_6 = 0.02 sec

K_4 = 0.79 in.

K_6 = 7.1 psi/in./sec

Equation (16) has been evaluated with these constants over the region to 50 cps and the results are plotted as curve "A" in polar form in Figure 43. The scale of this plot is non-dimensional, being equivalent to the torque servoloop gain. It is seen from this plot that the servoloop would be divergently unstable with a loop gain of $K_0 = 0.45$ and the resonant frequency would be near 35 cps.

The intersection of the inverse locus with the negative real axis, which limits the stable torque loop gain, can be effectively "moved out" by the insertion of a low-pass filter in the torque feedback. If the filter has a low corner frequency (e.g., 4 cps), the rapid phase change introduced by the filter through the corner frequency range will not detract from the system stability and the attenuation contributed by the filter near the torque-loop natural frequency will significantly improve the system stability. A filter with a very low corner frequency would cause the torque servoloop to introduce objectionable dynamic feel response. This analysis has been restricted to first-order filters as the practicality of including more complex filters in the AC servoloop is questionable.

The closed-loop response of the torque servo including a feedback filter may be written directly if the feedback block of Sketch B is assumed to have a transfer function $K_1 G_1 (s)$.

$$\left(\frac{F_p}{e_1}\right)(s) = \frac{1}{\dfrac{1 + \dfrac{K_4 K_6 G_6}{k_c}\, s\left[1 + \left(\dfrac{\omega_n}{s}\right)^2\right]}{K_2 K_3 K_4 G_2 G_3} + K_1 G_1} \tag{17}$$

The stability of this loop can be investigated for various settings of loop gain by examining the denominator of equation (17). This is more conveniently accomplished by writing the inverse response as:

$$\left(\frac{F_p}{e_1}\right)^{-1}(s) = K_1 G_1 \left\{ 1 + \frac{1 + \dfrac{K_4 K_6 G_6}{k_c}\, s\left[1 + \left(\dfrac{\omega_n}{s}\right)^2\right]}{K_0\, G_2\, G_3\, G_1} \right\} \tag{18}$$

and then solving for the bracketed term as loop gain varies.

The expression for $G_1 (s)$ will have a first-order time lag, as:

$$G_1 (s) = \left(\frac{1}{1 + \tau_1 s}\right) \tag{19}$$

The OL^{-1} expression associated with the right-hand term inside the brackets of equation (18) was evaluated for the constants of the test rig and with τ_1 = 0.04 seconds. The result appears as Curve B in Figure 43. The increase in available loop gain with the addition of the filter is quite apparent.

A first-order integrating-type filter was introduced into the torque feedback of the test rig feel servo and performance was markedly improved. The primary advantage of external force feedback about the pressure valve is the reduction in the apparent frictional forces felt at the controls. These forces are particularly objectionable at very low control force gradients where they constitute an appreciable portion of the total stick force. But with the additional torque feedback permitted by the feedback compensation network, these frictional forces can be reduced to negligible values.

CONCLUSIONS

It is now known that the flow response of the pressure-control servovalve constitutes the major dynamic element in the torque servoloop of the feel servos, and is the primary factor contributing to the torque servoloop instability. The analysis further demonstrates that a first-order approximation to this flow response is sufficient to predict the torque servoloop performance of the feel servos with gratifying accuracy. By including a first-order time lag in the torque feedback, the stability of the torque servoloop is greatly improved. This time lag can be introduced by a chopper-integration filter in the AC torque circuit, and test rig performance has demonstrated the effectiveness of the compensated torque feedback in reducing objectionable friction feel-forces.

REFERENCES

1. Flight Research Department, Installation of an Automatic Control System in a T-33 Airplane for Variable Stability Flight Research - Part 1 - Preliminary Investigation and Design Studies. Wright Air Development Center Technical Report 55-156, Part 1; Cornell Aeronautical Laboratory Report TB-936-F-1, April 1955.
2. Hutchinson, C. Stress Analysis - Control System Installation Variable Stability T-33. Cornell Aeronautical Laboratory Flight Research Memorandum 252. 2 July 1956.
3. Radt, H.S., (UNCLASSIFIED TITLE) Method of Simulation of the Longitudinal Modes of Motion of Another Airplane by the T-33A Variable Stability Airplane. Cornell Aeronautical Laboratory Flight Research Memorandum 242 17 January 1956 (CONFIDENTIAL report).
4. Radt, H.S., General Method and Procedure for Calculating the Required Artificial Stability for Simulation of the Lateral Modes of Motion of Another Aircraft with the T-33A Variable Stability Aircraft. Cornell Aeronautical Laboratory Flight Research Memorandum 232 9 August 1955.
5. Chalk, C.R., (UNCLASSIFIED TITLE) Simulation of the Lateral Modes of Motion of an F-101A with the Variable Stability T-33. Cornell Aeronautical Laboratory Flight Research Memorandum 237 17 October 1955 (CONFIDENTIAL report).
6. Chalk, C.R., (UNCLASSIFIED TITLE) Simulation of the Lateral Modes of Motion of an F-104A with the Variable Stability T-33. Cornell Aeronautical Laboratory Flight Research Memorandum 238 2 November 1955. (CONFIDENTIAL report).
7. Chalk, C.R., Horizontal Tail Load Study of the T-33 with Artificial Stability. Cornell Aeronautical Laboratory Flight Research Memorandum 243 14 February 1956
8. Chalk, C.R. Vertical Tail Load Study of the T-33 with Artificial Stability. Cornell Aeronautical Laboratory Flight Research Memorandum 247 17 May 1956.
9. Mayer, J.P.; Hamer, H.A., and DeHuff, C.R., A Study of the Use of Control and the Resulting Airplane Response during Service Training Operations of Four Jet Fighter Airplanes. NACA RM L53L28.

TABLE I DISENGAGE CONTROLS

A. MANUALLY OPERATED ELECTRICAL SWITCHES

SWITCH NO.	TYPE SWITCH	LOCATION	ITEMS DISENGAGED
SW 1	TOGGLE	REAR CONTROL PANEL	ENTIRE SYSTEM
SW 2	MICROSWITCH	FRONT AILERON BOOST VALVE	ENTIRE SYSTEM (INTERLOCK)
SW 5	MOMENTARY BUTTON	REAR STICK	ALL SERVOS
SW 6	MOMENTARY BUTTON	FRONT CONTROL PANEL	ALL SERVOS
SW 7	MOMENTARY BUTTON	FRONT STICK	ALL SERVOS
SW 10	MOMENTARY TOGGLE	REAR CONTROL PANEL	AUXILIARY SURFACE SERVO (ONLY)
SW 11	MICROSWITCH	REAR AILERON BOOST VALVE	POSITION SERVOS (INTERLOCK)
SW 13	MOMENTARY TOGGLE	REAR CONTROL PANEL	POSITION SERVOS

B. MANUALLY OPERATED HYDRAULIC VALVES

NAME	TYPE VALVE	LOCATION	FUNCTION	ITEMS DISENGAGED
EMERGENCY DUMP VALVE-POSITION SERVOS	SELECTOR	REAR COCKPIT	DUMPS HYDRAULIC PRESSURE ON POSITION SERVOS AND BYPASSES POSITION SERVO ACTUATORS	POSITION SERVOS
FRONT STICK DUMP VALVE	SHUT OFF	FRONT COCKPIT (FORMER AILERON BOOST VALVE)	DUMPS HYDRAULIC PRESSURE ON ELEVATOR FEEL SERVO. OPERATES INTERLOCK SWITCH SW 2.	ENTIRE SYSTEM
AILERON BOOST	SHUT OFF	REAR COCKPIT	TURNS AILERON BOOST PRESSURE ON OR OFF. OPERATES INTERLOCK SWITCH SW 11.	POSITION SERVOS

C. AUTOMATIC DISENGAGE CONTROLS

NAME	FUNCTION	TYPE CONTROL	ITEMS DISENGAGED
STATIC CONVERTERS	SUPPLY 250 VDC	RELAY	ALL SERVOS
AUTOMATIC SAFETY TRIP	a. PROTECT AGAINST SUDDEN LARGE POSITION SERVO VALVE SIGNALS		ALL SERVOS
	b. LIMIT NORMAL AND LATERAL ACCELERATION		ALL SERVOS

TABLE II (TAKEN FROM REFERENCE I)

HYDRAULIC FLOW CHARACTERISTICS

FEEL SERVOS	PISTON AREA $A(in.^2)$	STICK VELOCITY $\dot{\delta}_c$ (in./sec)	GEAR RATIO δ_c/δ_p (in./in.)	PISTON VELOCITY $\dot{\delta}_p$ (in./sec)	FLOW $Q(in.^3/sec)$
AILERON	.76	16	7.7	2.08	1.58
ELEVATOR	.78	21	3.67	5.72	4.45
RUDDER	1.284	19	4.16	4.55	5.85

POSITION SERVOS	PISTON AREA $A(in.^2)$	SURFACE VELOCITY $\dot{\delta}_s$ (deg/sec)	GEAR RATIO δ_s/δ_p (deg/in.)	PISTON VELOCITY $\dot{\delta}_p$ (in./sec)	FLOW Q $(in.^3/sec)$
AILERON	4.13	70	11.4	6.14	25.35
ELEVATOR	.78	70	12.0	5.83	4.55
RUDDER	1.173	70	20.0	3.5	4.11

MAXIMUM TOTAL FLOW REQUIREMENT $\sum Q = 45.89\ in.^3/sec$

VALVE LEAKAGE FLOW $= 4.0\ in.^3/sec$

TABLE III GENERAL AND DETAIL ELECTRICAL DRAWINGS

DRAWING NUMBER	DRAWING	DATE
835-003 - 1,2,3	LINEAR POSITION TRANSMITTER	11-2-54
835-003 - 12	T-33 VARIABLE STABILITY SYSTEM BLOCK DIAGRAM	10-25-54
835-003 - 13	T-33 VARIABLE STABILITY SYSTEM FUNCTIONAL BLOCK DIAGRAM OF PITCH CONTROL SYSTEM	4-14-55
835-003 - 14	T-33 VARIABLE STABILITY SYSTEM FUNCTIONAL BLOCK DIAGRAM OF YAW AXIS CONTROL SYSTEM	4-27-55
835-003 - 15	T-33 VARIABLE STABILITY SYSTEM FUNCTIONAL BLOCK DIAGRAM OF ROLL AXIS CONTROL SYSTEM	4-27-55
835-003 - 16	T-33 VARIABLE STABILITY SYSTEM ELECTRICAL BLOCK DIAGRAM OF GAIN COMPUTER SECTION	5-5-55
835-020 - 1	T-33 "q" CIRCUITS BLOCK DIAGRAM	9-7-55
835-020 - 2	T-33 ARTIFICIAL STABILITY COMPUTER CIRCUITRY	10-4-55
835-020 - 3 SHEET 1	CHASSIS LAYOUT - ARTIFICIAL STABILITY MASTER UNIT	11-10-55
835-020 - 3 SHEET 2	CHASSIS LAYOUT - ARTIFICIAL STABILITY MASTER UNIT	11-10-55
835-020 - 4	T-33 SYSTEM BUNDLING AND ELECTRICAL BLOCK DIAGRAM	1-3-56
835-020 - 5	CONTROL SURFACE SERVO UNIT BLOCK DIAGRAM	1-5-56
835-020 - 6	CONTROL SURFACE SERVO UNIT SCHEMATIC DIAGRAM	1-5-56
835-020 - 7	CONTROL SURFACE SERVO UNIT WIRING DIAGRAM	1-6-56
835-020 - 8	CONTROL SURFACE SERVO UNIT CHASSIS LAYOUT	1-6-56
835-020 - 9	RATE GYRO CHASSIS	1-6-56
835-020 - 10	RATE GYRO CHASSIS COVER	1-6-56
835-020 - 11	RATE GYRO CHASSIS PLATE	1-6-56
835-020 - 12	CABLE - POWER CONTROL UNIT TO ARTIFICIAL STABILITY MASTER UNIT	2-13-56
835-020 - 13	CABLE - POWER CONTROL UNIT TO MASTER RECORDING UNIT	2-13-56
835-020 - 14	CABLE - POWER CONTROL UNIT TO VARIABLE PHASE POWER SUPPLY	2-13-56
835-020 - 15	CABLE - CONTROL SURFACE SERVO UNIT TO AUXILIARY SURFACE SERVO	2-13-56
835-020 - 16	CABLE - CONTROL SURFACE SERVO UNIT TO CONTROL SURFACE SERVOS	2-13-56
835-020 - 17	CABLE - FORCE UNITS TO FEEL SERVOS	2-13-56

DRAWING NUMBER	DRAWING	DATE
835-020 - 18	CABLE - MASTER RECORDING UNIT AND POWER CONTROL UNIT TO RECORDING POSITION TRANSDUCERS AND TAIL SECTION	2-13-56
835-020 - 19	CABLE - POWER CONTROL TO RUDDER PEDAL FORCE UNIT	2-13-56
835-020 - 20	CABLE - REAR MASTER CONTROL PANEL TO PILOT'S GAIN CONTROL PANEL	2-13-56
835-020 - 21	CABLE - ELEVATOR AND RUDDER FORCE UNITS TO q AND 1/q SERVOS	2-13-56
835-020 - 22	CABLE - CONTROL SURFACE SERVO TO MASTER RECORDING UNIT	2-13-56
835-020 - 23	CABLE - CONTROL SURFACE SERVO TO q SERVO, ϕ SERVO AND α SERVO	2-13-56
835-020 - 24	CABLE - AILERON STICK FORCE UNIT TO MASTER RECORDING UNIT	2-13-56
835-020 - 25	CABLE - ELEVATOR STICK FORCE UNIT TO MASTER RECORDING UNIT	2-13-56
835-020 - 26	CABLE - RUDDER PEDAL FORCE UNIT TO MASTER RECORDING UNIT	2-13-56
835-020 - 27	CABLE - ARTIFICIAL STABILITY MASTER UNIT TO MASTER RECORDING UNIT	2-13-56
835-020 - 28	CABLE - q SERVO CHASSIS TO q PRESSURE SERVO	2-13-56
835-020 - 29	CABLE - ATTITUDE GYRO TO LEAR ATTITUDE GYRO	2-13-56
835-020 - 30	CABLE - ARTIFICIAL STABILITY MASTER UNIT TO NORMAL AND LATERAL ACCELEROMETERS	2-13-56
835-020 - 31	CABLE - ARTIFICIAL STABILITY MASTER UNIT TO RATE GYRO CHASSIS	2-13-56
835-020 - 32	CABLE - ARTIFICIAL STABILITY UNIT TO ATTITUDE GYRO CHASSIS	2-13-56
835-020 - 33	CABLE - ARTIFICIAL STABILITY MASTER UNIT TO α SERVO	2-13-56
835-020 - 34	CABLE - ARTIFICIAL STABILITY MASTER UNIT TO 1/q SERVO	2-13-56
835-020 - 35	CABLE - ARTIFICIAL STABILITY MASTER UNIT TO q SERVO CHASSIS	2-13-56
835-020 - 36	CABLE - ARTIFICIAL STABILITY MASTER UNIT TO ϕ SERVO	2-13-56
835-020 - 37	CABLE - RATE GYRO CHASSIS TO RATE GYRO MOUNT	2-13-56
835-020 - 38	CABLE - POWER CONTROL TO AILERON STICK FORCE UNIT	2-13-56

DRAWING NUMBER	DRAWING	DATE
835-020 - 39	CABLE - POWER CONTROL TO ELEVATOR STICK FORCE UNIT	2-13-56
835-020 - 40	CABLE - POWER CONTROL TO CONTROL SURFACE SERVO UNIT	2-13-56
835-020 - 41	CABLE - POWER CONTROL UNIT TO STATIC CONVERTERS	3-20-56
835-021 - 1	ELEVATOR STICK FORCE UNIT BLOCK DIAGRAM	11-21-55
835-021 - 2	ELEVATOR STICK FORCE UNIT SCHEMATIC DIAGRAM	11-21-55
835-021 - 3	CHASSIS LAYOUT - ELEVATOR STICK FORCE UNIT	11-22-55
835-021 - 4	ELEVATOR STICK FORCE UNIT WIRING DIAGRAM	2-6-56
835-021 - 5	RUDDER PEDAL FORCE UNIT BLOCK DIAGRAM	11-2-55
835-021 - 6	RUDDER PEDAL FORCE UNIT SCHEMATIC DIAGRAM	11-2-55
835-021 - 7	CHASSIS LAYOUT - RUDDER PEDAL FORCE UNIT	11-15-55
835-021 - 8	RUDDER PEDAL FORCE UNIT WIRING DIAGRAM	1-14-56
835-021 - 9	AILERON STICK FORCE UNIT BLOCK DIAGRAM	11-1-55
835-021 - 10	AILERON STICK FORCE UNIT SCHEMATIC DIAGRAM	11-2-55
835-021 - 11	CHASSIS LAYOUT - AILERON STICK FORCE UNIT	11-11-55
835-021 - 12	AILERON STICK FORCE UNIT WIRING DIAGRAM	1-23-56
835-022 - 1	VARIABLE PHASE POWER SUPPLY	10-27-55
835-022 - 2	CHASSIS LAYOUT - VARIABLE PHASE POWER SUPPLY	11-2-55
835-022 - 3	PILOT'S GAIN CONTROL PANEL CABLING AND WIRING DIAGRAM	12-19-55
835-022 - 4	T-33 CONTROL AND INTERLOCK CIRCUITRY	1-4-56
835-022 - 5	PANEL - REAR COCKPIT CONTROL	1-10-56
835-022 - 6	COCKPIT CONTROL PANELS	1-16-56
835-022 - 7	PANEL ENGRAVING - REAR COCKPIT CONTROL	1-20-56
835-022 - 8	POWER CONTROL UNIT	1-27-56
835-022 - 9	POWER CONTROL UNIT FRONT PANEL	1-27-56
835-022 - 10	POWER CONTROL UNIT CHASSIS	1-31-56
835-022 - 11	POWER CONTROL UNIT ENGRAVED PLATES	2-1-56
835-022 - 12	POWER CONTROL UNIT SELECTOR SWITCH PLATE	2-1-56
835-022 - 13	ARTIFICIAL FEEL PANEL SCHEMATIC DIAGRAM	2-1-56
835-022 - 14	ARTIFICIAL FEEL PANEL	2-8-56
835-022-- 15	PANEL - REAR COCKPIT GAIN CONTROL	2-6-56
835-022 - 16	PILOT'S CONTROL BOX - REAR COCKPIT	2-10-56
835-022 - 17	NAME PLATES - PILOT'S GAIN CONTROL PANEL	2-10-56
835-022 - 18	TERMINAL STRIP WIRING FOR PILOT'S CONTROL PANEL	3-16-56

DRAWING NUMBER	DRAWING	DATE
835-023 - 1	MASTER RECORDING UNIT SCHEMATIC DIAGRAM	10-27-55
835-023 - 2	CHASSIS LAYOUT - RECORDING SYSTEM	11-5-55
835-023 - 3	PANEL - RECORDING SYSTEM	11-12-55
835-023 - 4	SUPPORT - RECORDING PANEL	11-16-55
835-023 - 5	NAME PLATES - RECORDING PANEL	11-25-55
835-023 - 6	STIFFNER - RECORDING PANEL	11-26-55
835-023 - 7	SUPPORT POST - RECORDING PANEL	11-26-55
835-023 - 8	PANEL - GALVANOMETER PATCH	11-20-55
835-023 - 9	BOX - TRANSFORMER - RECORDING UNIT	11-29-55
835-023 - 10	NAME PLATES	12-15-56
835-023 - 11	SCALE - TRIMMETER	1-2-56
835-023 - 12	BRACKETS - RELAY SUPPORT PILOT'S CONTROL	2-7-56
835-023 - 13	T-33 SAMPLING UNIT - SCHEMATIC DIAGRAM	1-23-56

FORWARD ←

BA	BB	BC	BD	BE	BF	BG	BH	BJ	BK	BL	BM	BN	BP
GA	GB	GC	GD		GF	GG	GH		GK	GL	GM	GN	RR
RA	RB	RC	RD	RE	RF	RG	RH	RJ	RK	RL	RM	RN	RP

NOTE: THE FIRST LETTER REFERS TO THE COLOR OF THE CONTROL;
THE SECOND IS THE IDENTIFYING LETTER ENGRAVED ON EACH CONTROL.

Figure 1 GENERAL ARRANGEMENT OF GAIN CONTROLS ON RIGHT-HAND CONSOLE IN AFT COCKPIT

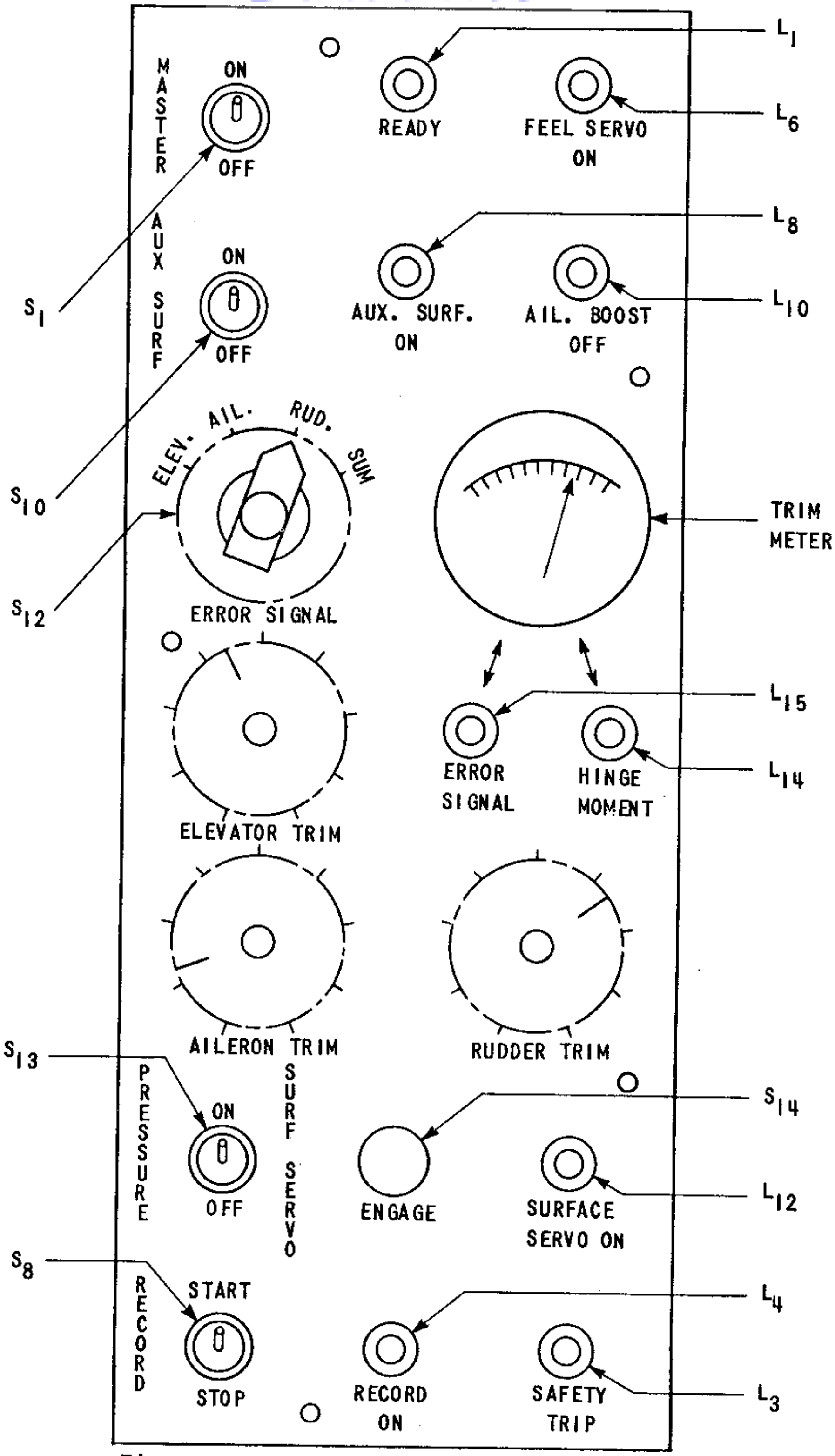

Figure 2 REAR COCKPIT ENGAGE PANEL

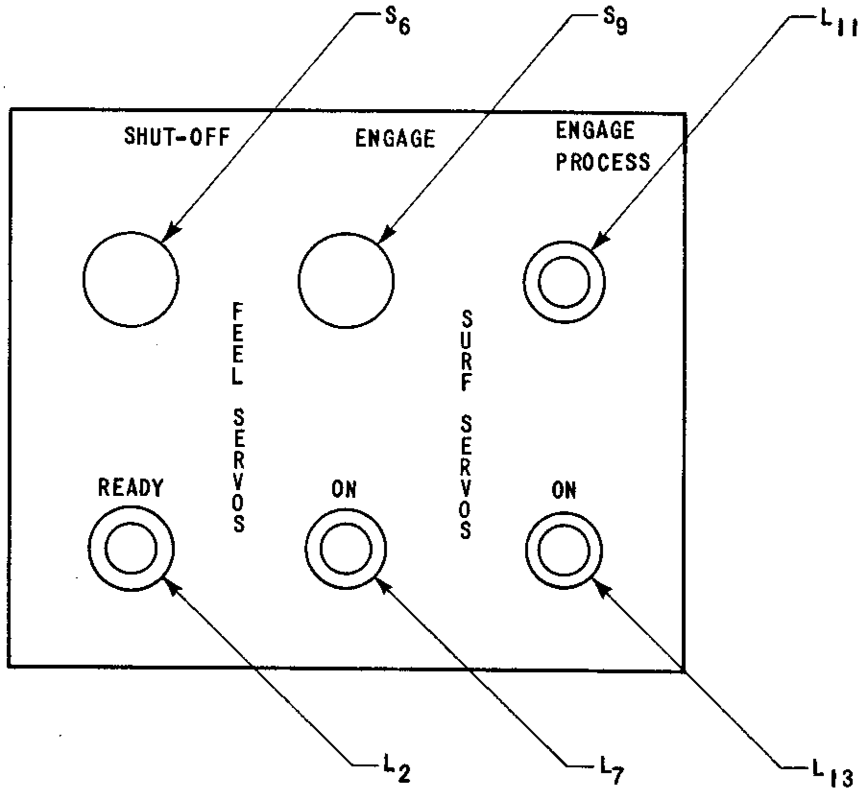

Figure 3 FRONT COCKPIT SWITCH CONSOLE

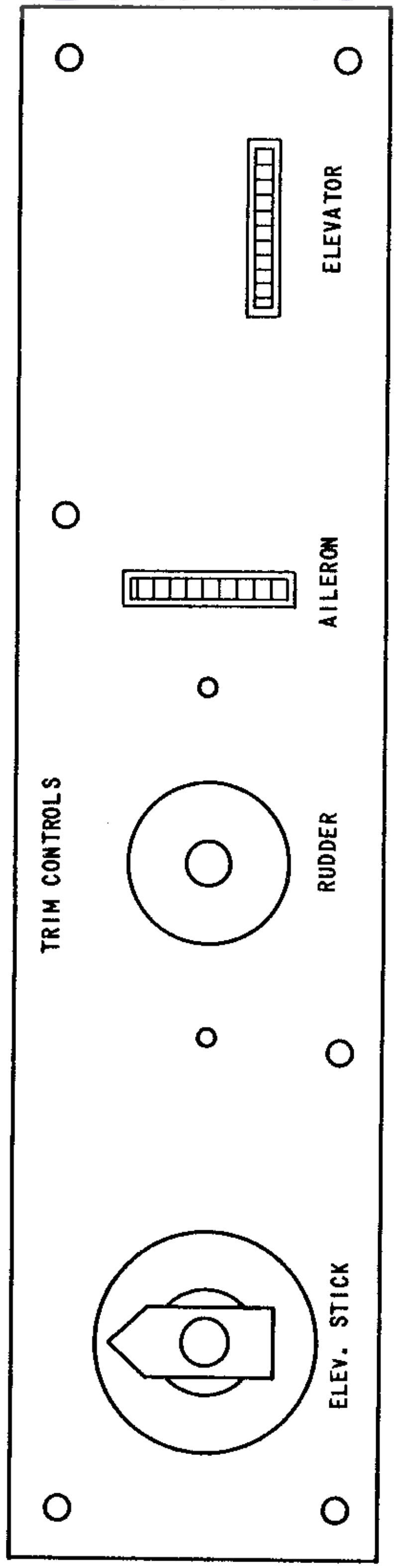

Figure 4 FRONT COCKPIT TRIM CONTROLS

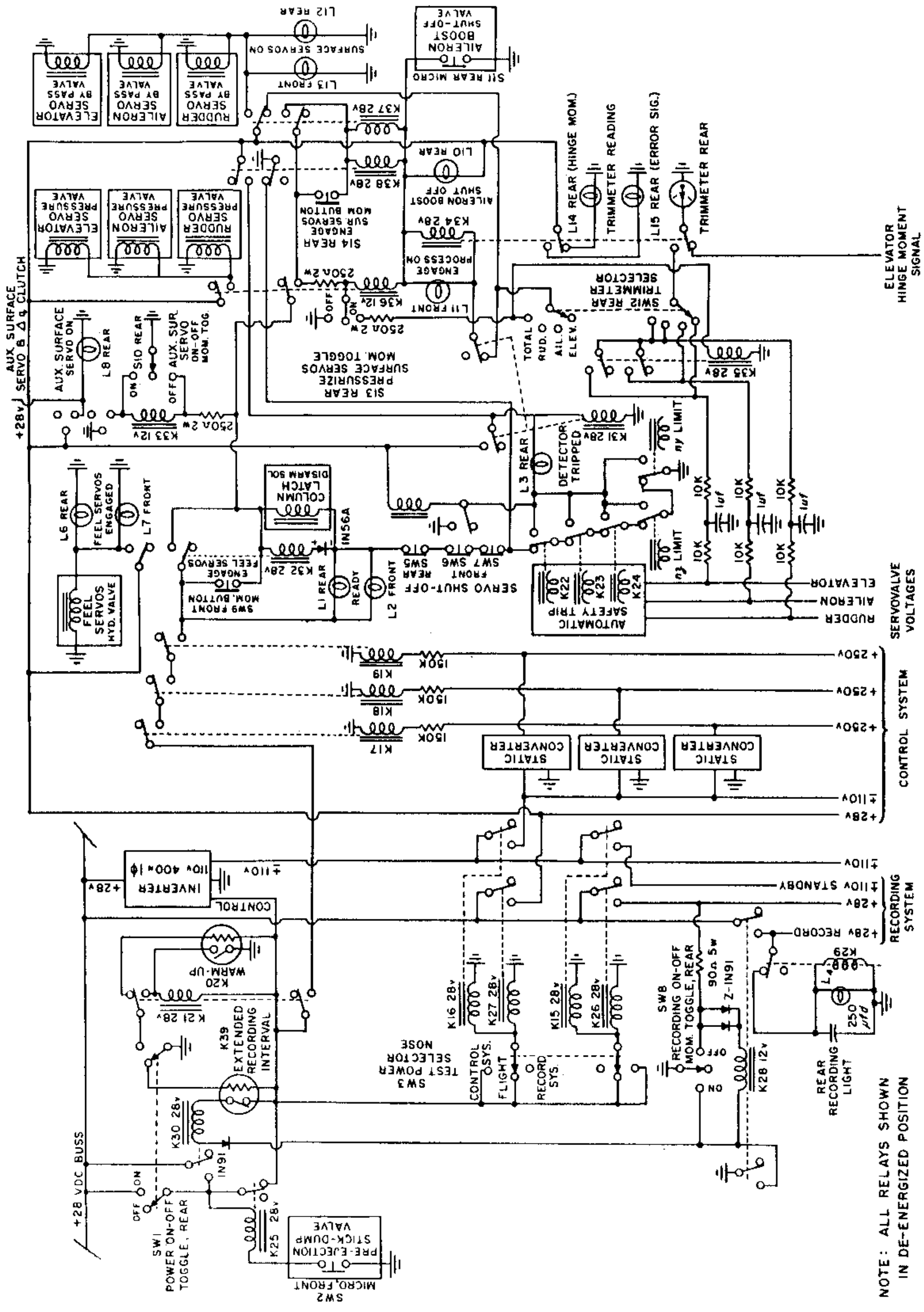

Figure 5 CONTROL AND INTERLOCK CIRCUITRY

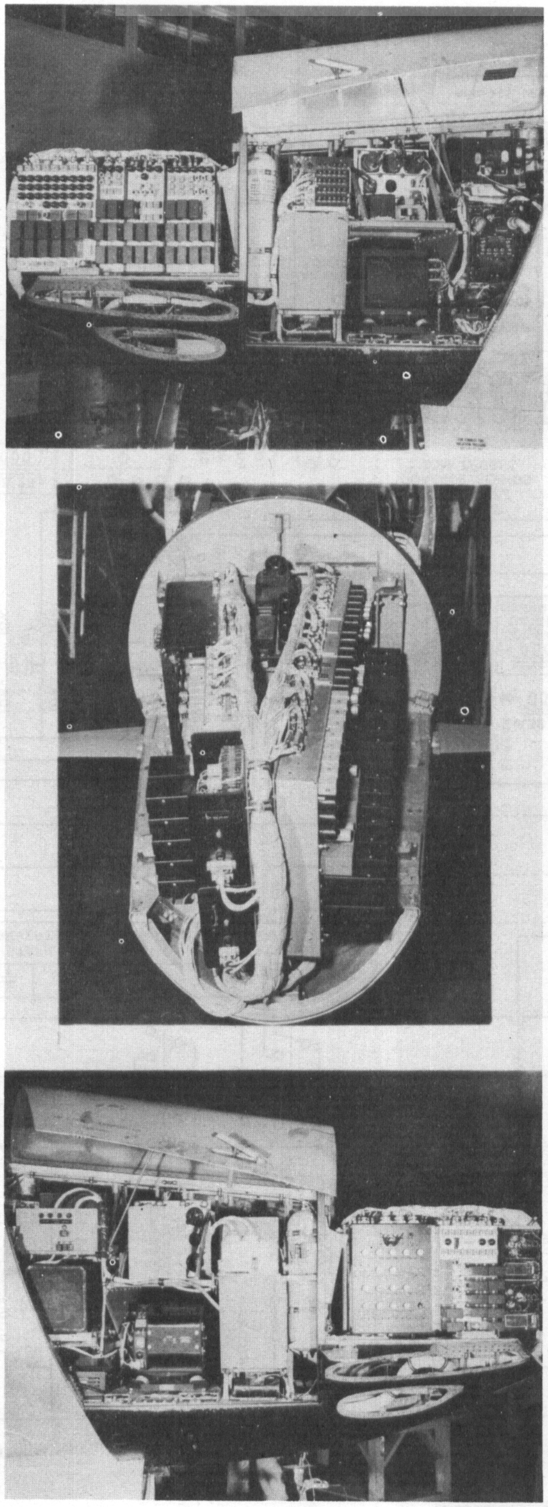

Figure 6   LEFT SIDE, RIGHT SIDE, AND FRONT THREE-QUARTER VIEWS OF VARIABLE STABILITY SYSTEM INSTALLATION IN NOSE SECTION

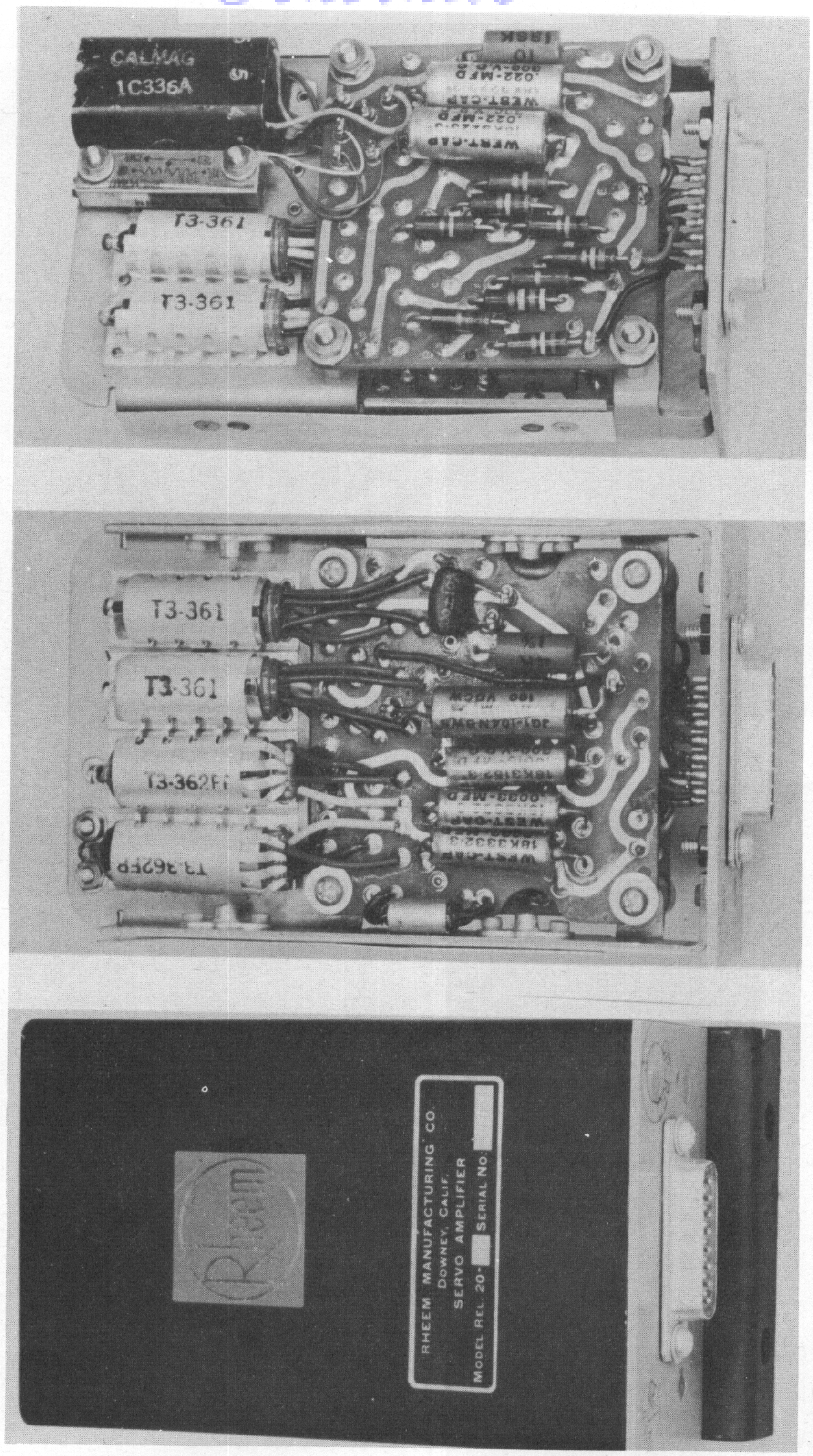

Figure 7 SERVO AMPLIFIER-ONE EXTERNAL AND TWO INTERNAL VIEWS

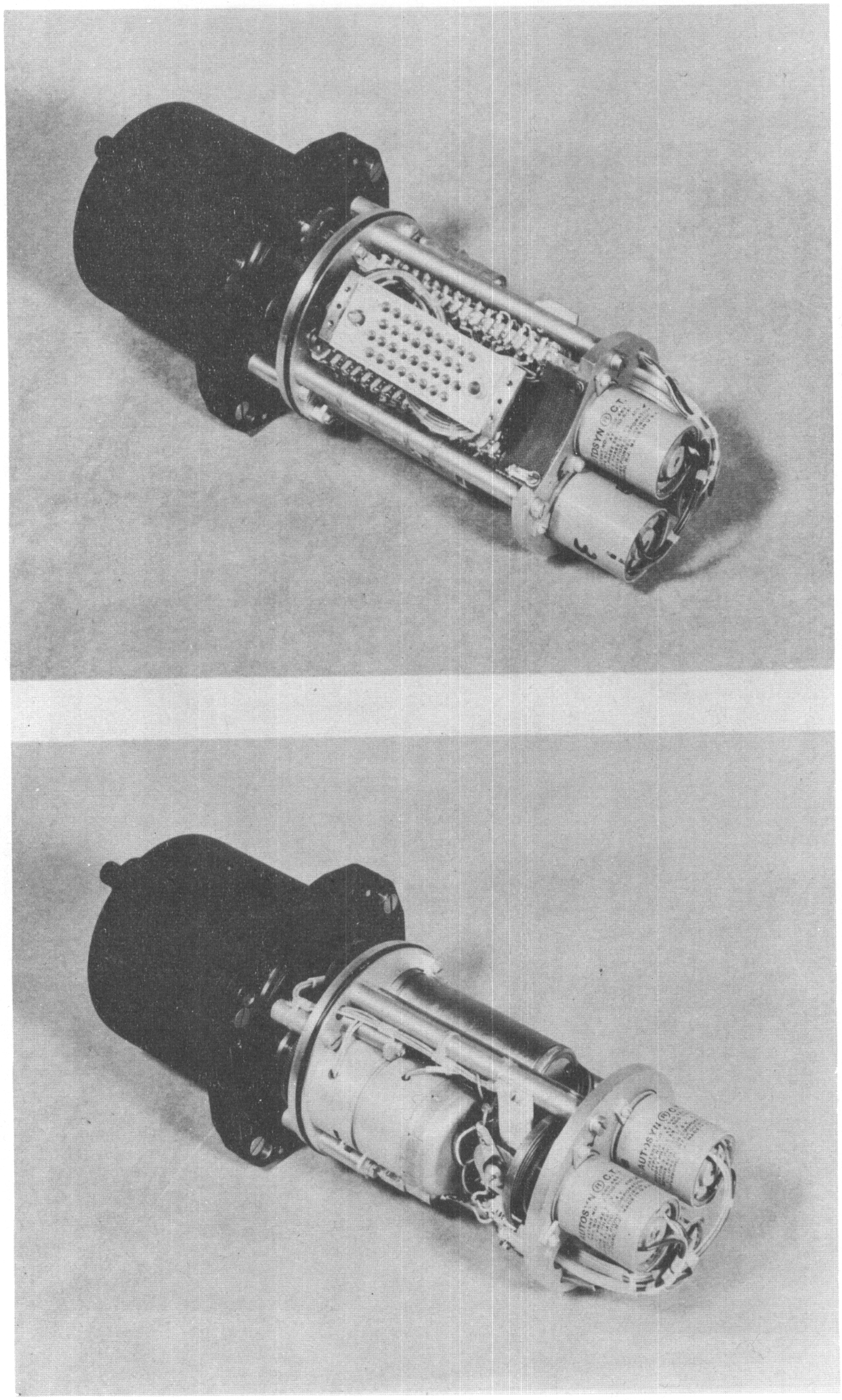

Figure 8 "q" COMPUTER

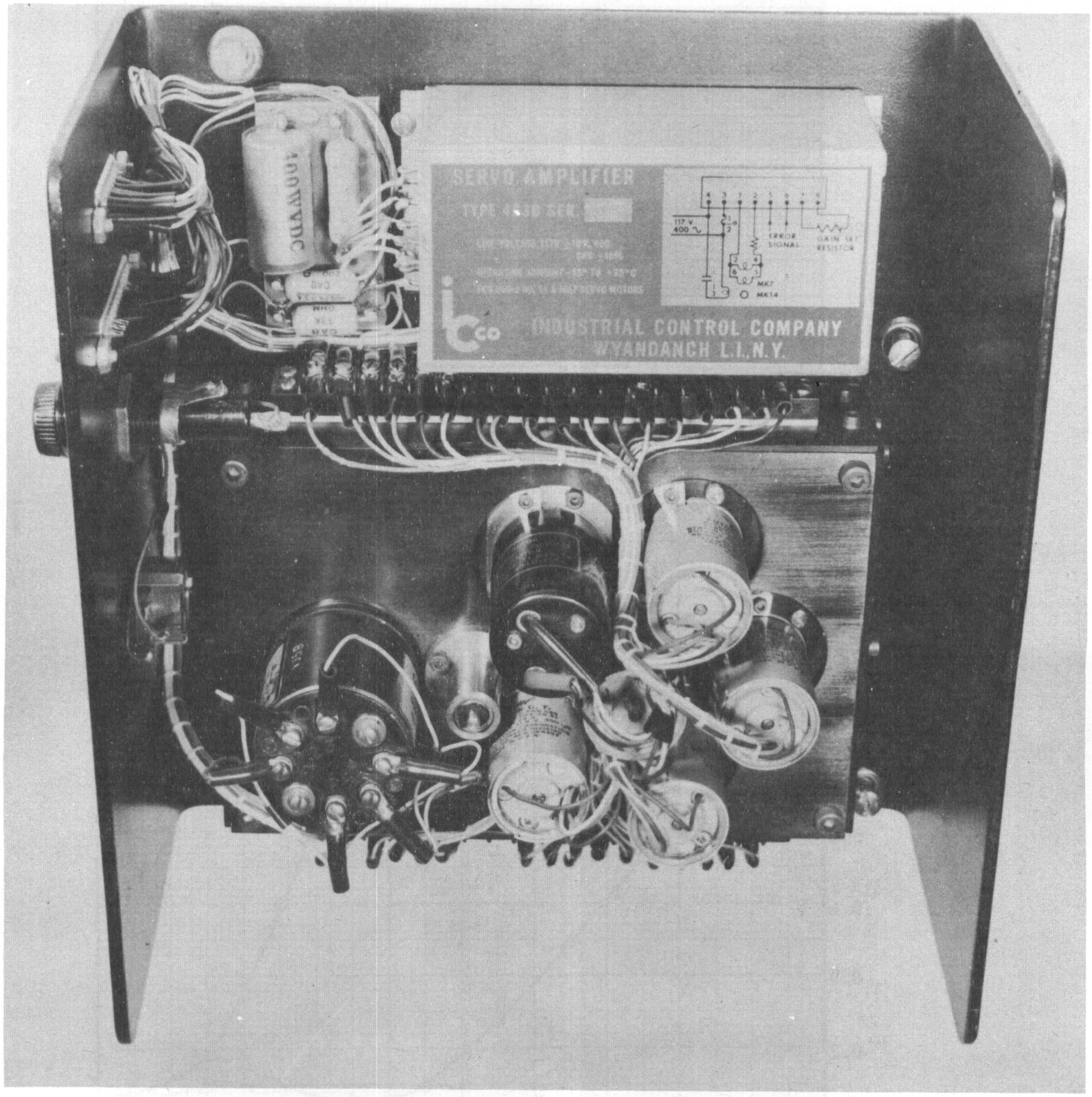

Figure 9 "l/q" COMPUTER

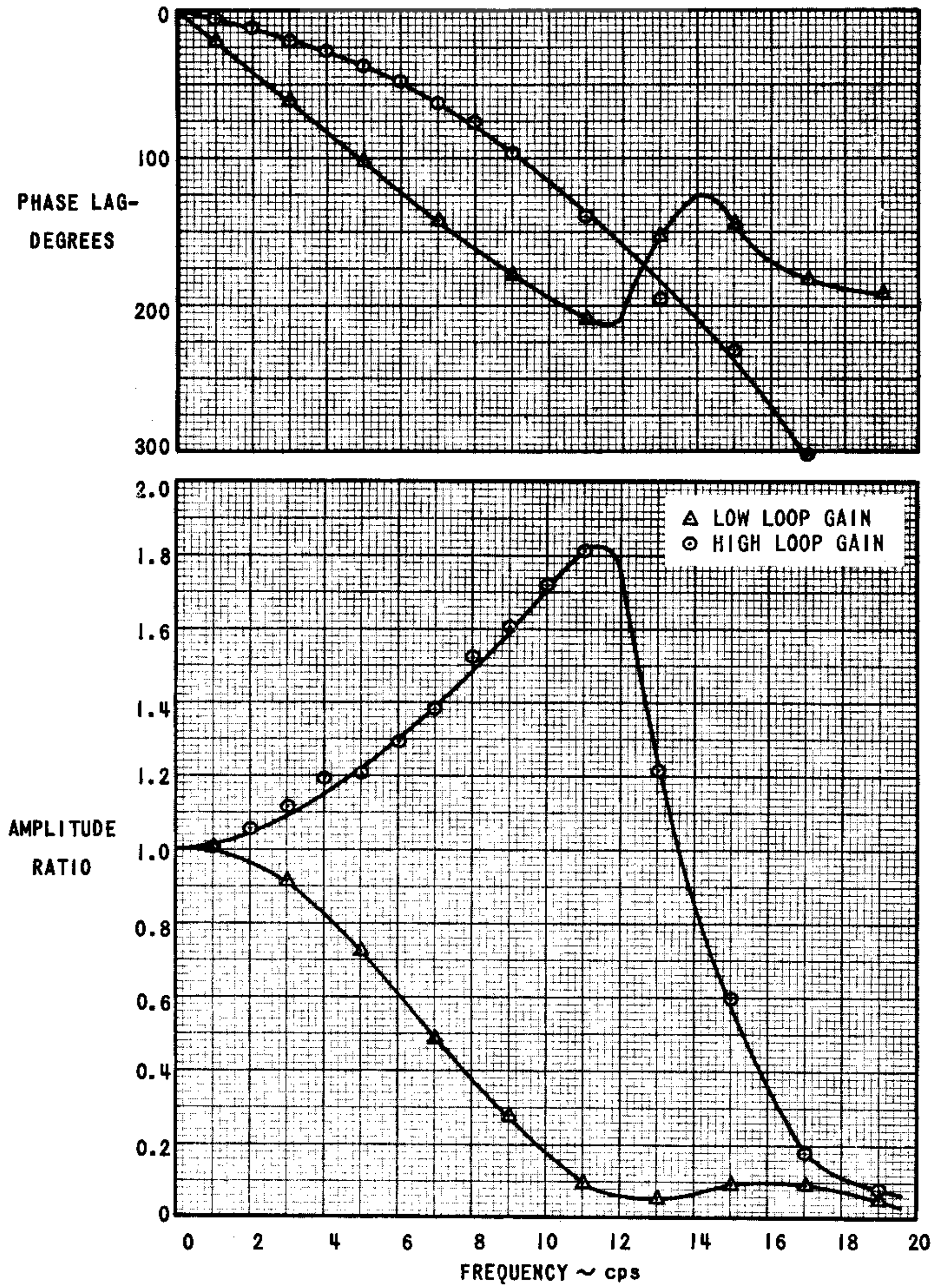

Figure 10 DYNAMIC RESPONSE OF INDUSTRIAL CONTROL CO.
MODEL SL-1013 INVERSE q COMPUTER

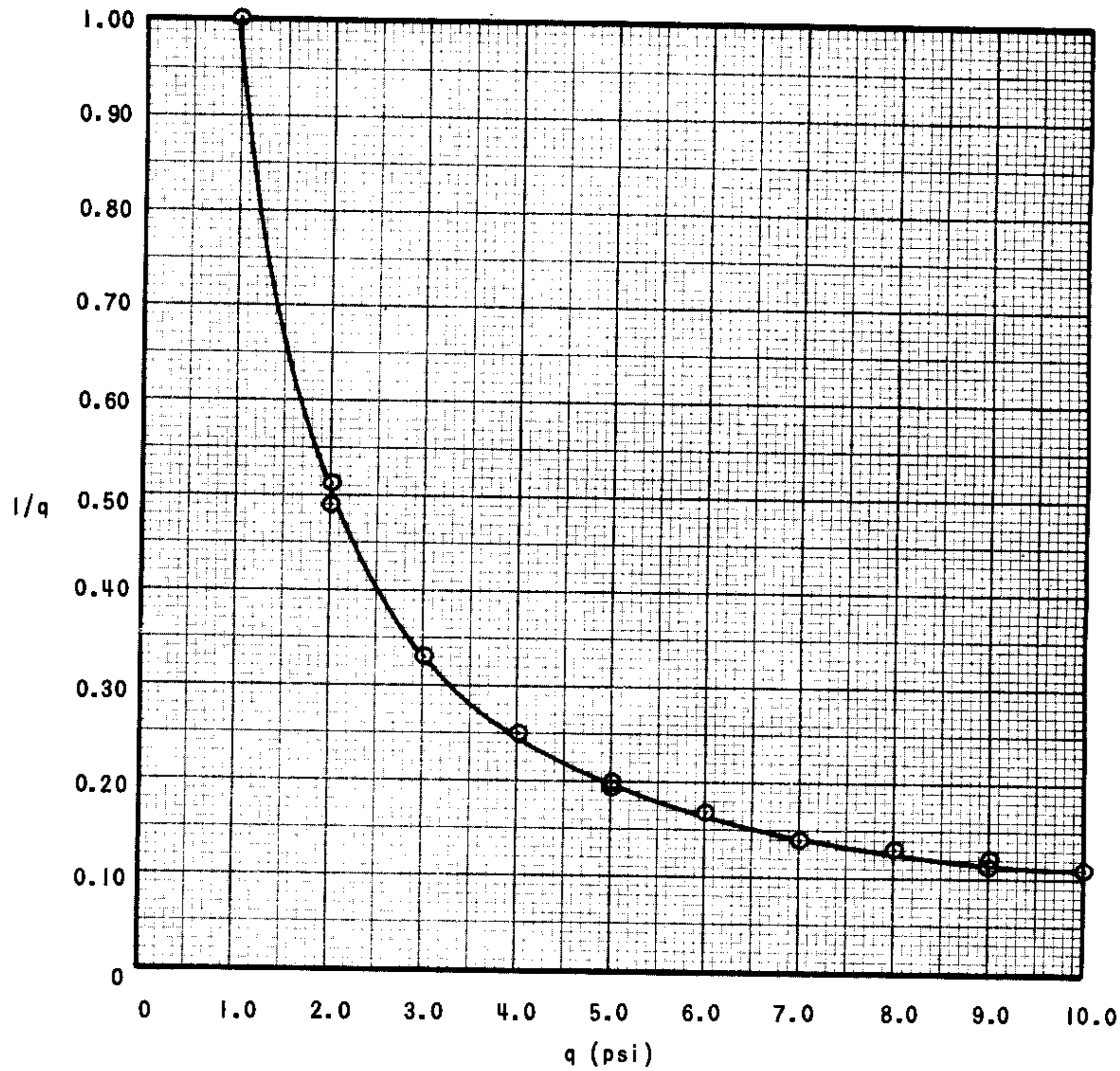

Figure 11 CALIBRATION OF INDUSTRIAL CONTROL CO. MODEL SL-1013 INVERSE q COMPUTER

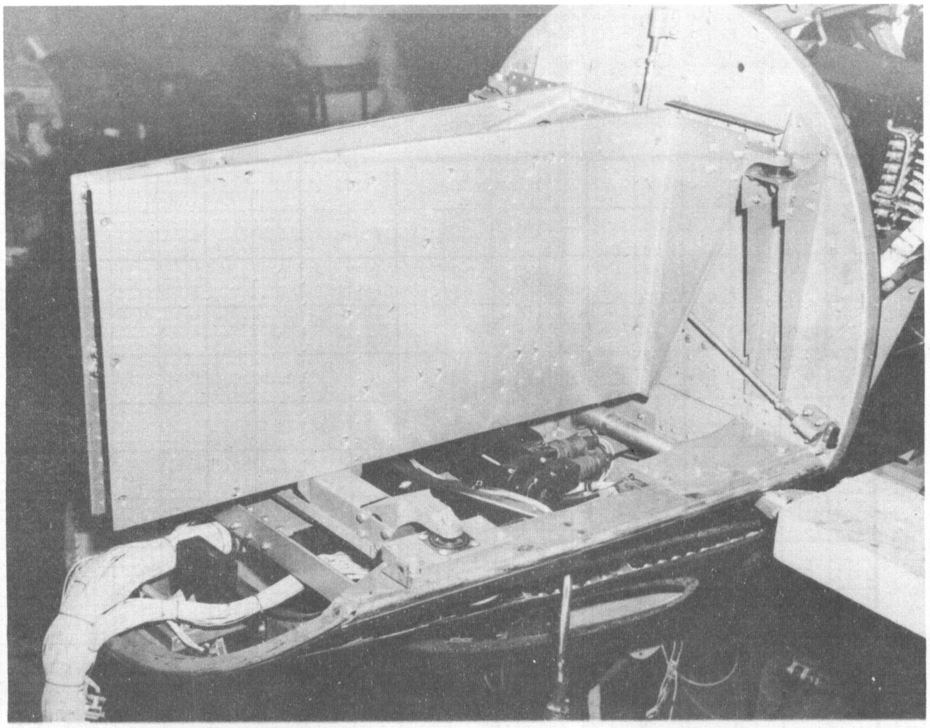

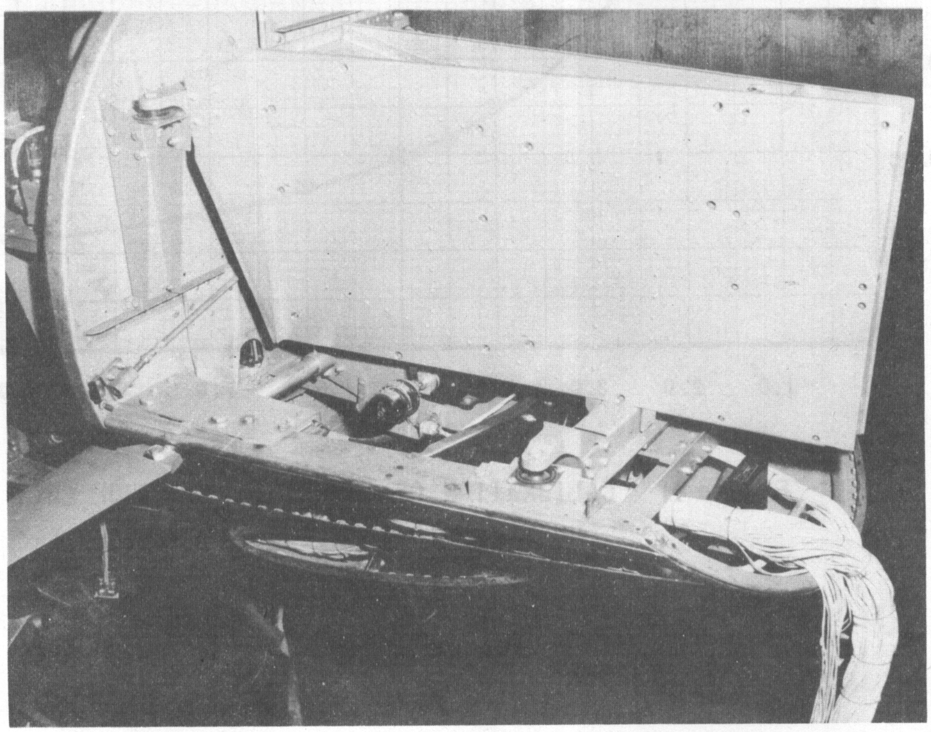

Figure 12 LEFT AND RIGHT SIDE VIEWS OF SHOCK-MOUNTED BOX FOR CHASSIS SUPPORT

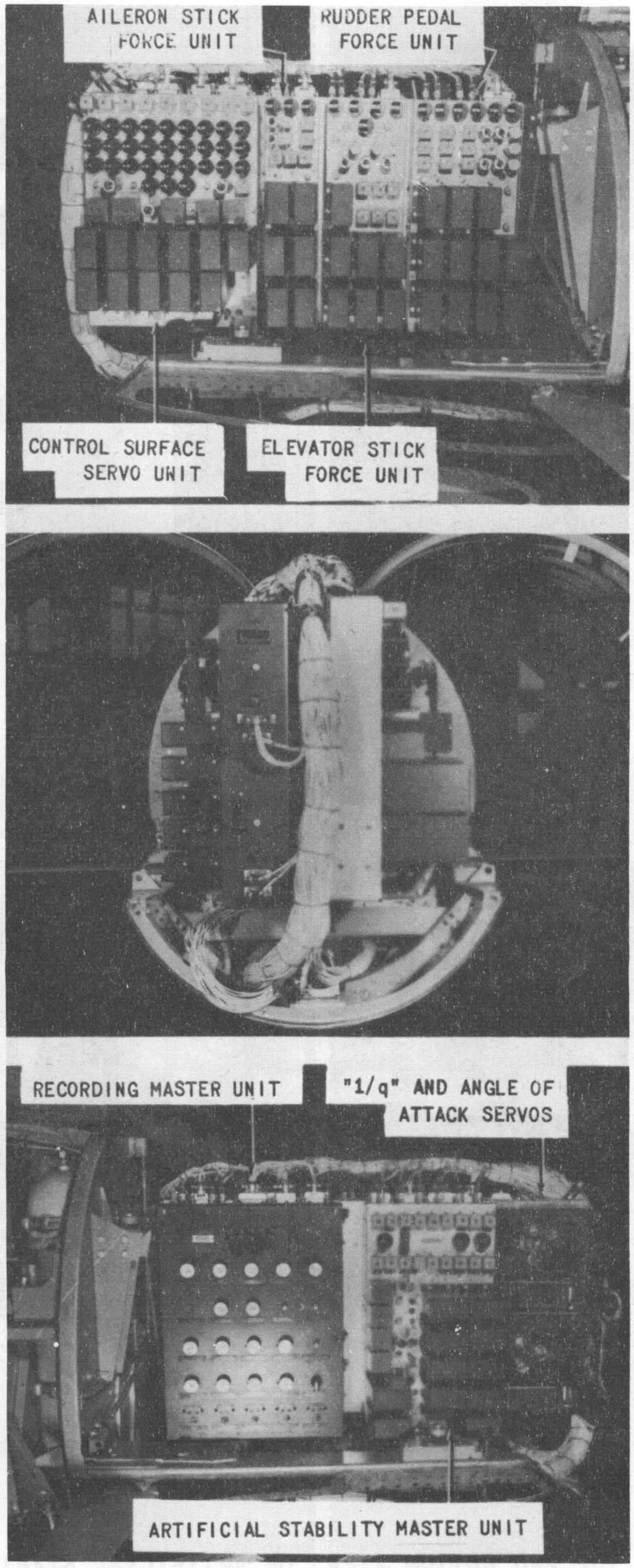

Figure 13 LEFT SIDE, RIGHT SIDE AND FRONT VIEWS OF SHOCK-MOUNTED ELECTRONIC CHASSIS.

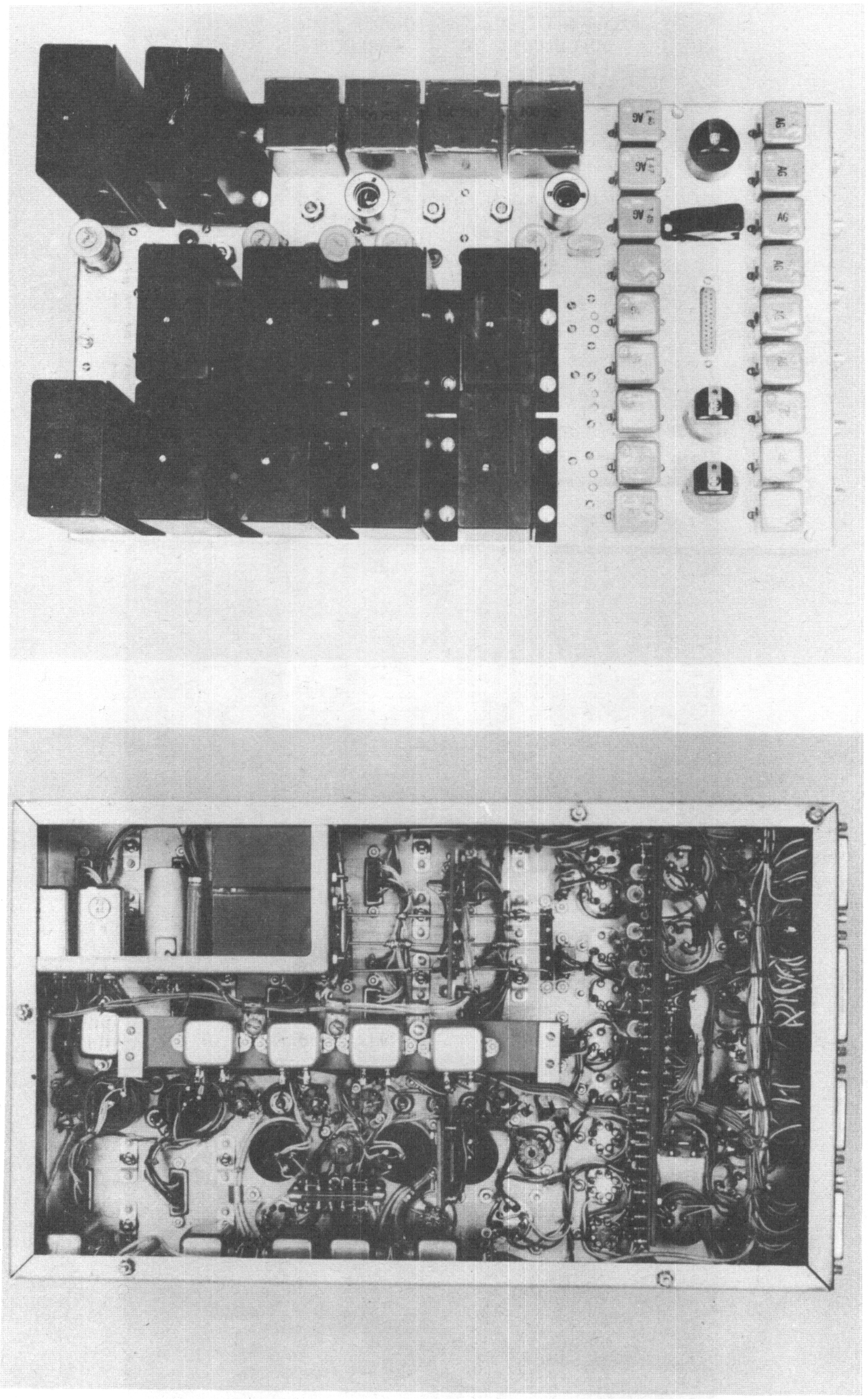

Figure 14 TOP AND BOTTOM VIEWS OF ARTIFICIAL STABILITY MASTER UNIT

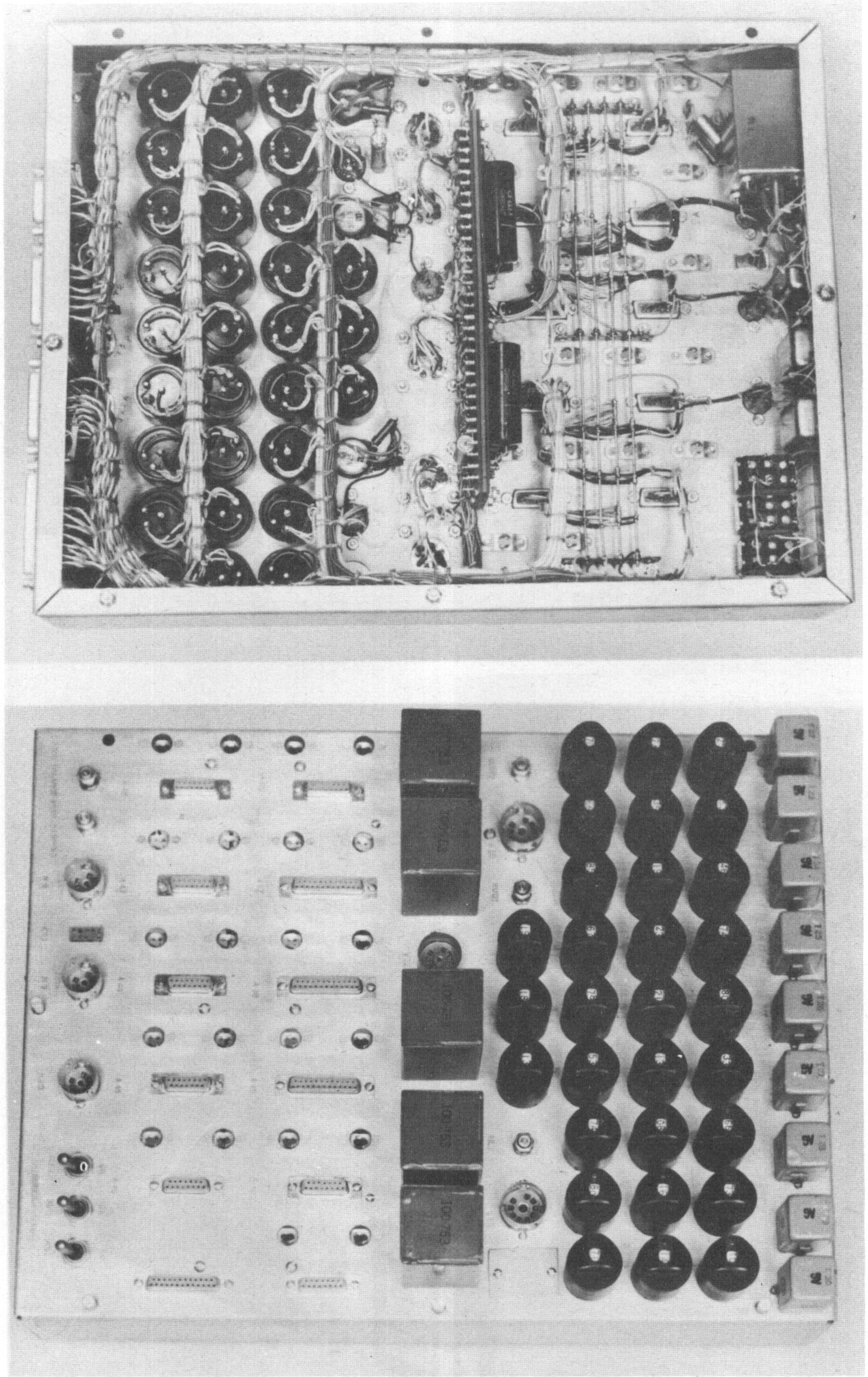

Figure 15 TOP AND BOTTOM VIEWS OF CONTROL SURFACE SERVO UNIT

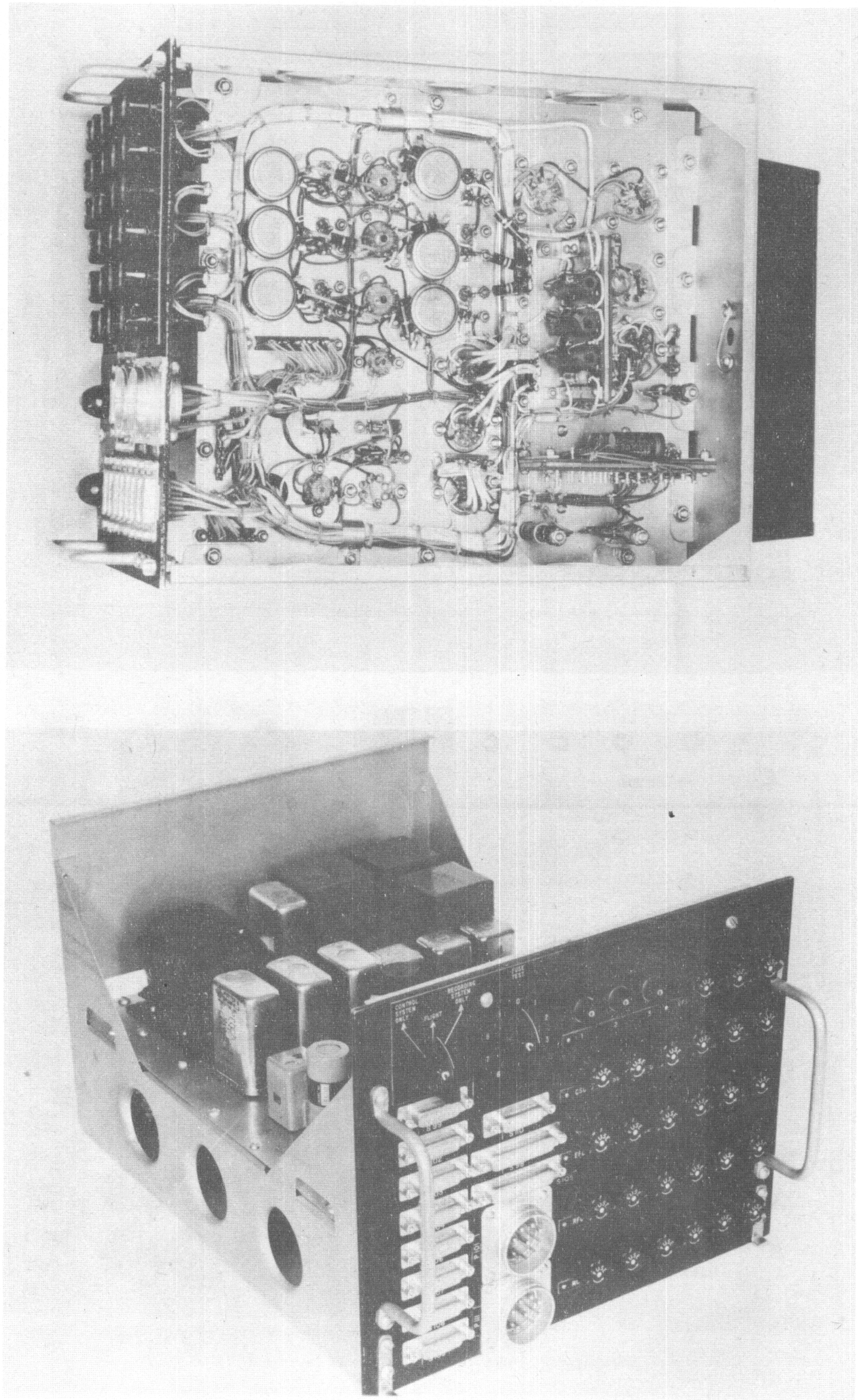

Figure 16 POWER CONTROL UNIT - THREE-QUARTER AND BOTTOM VIEWS

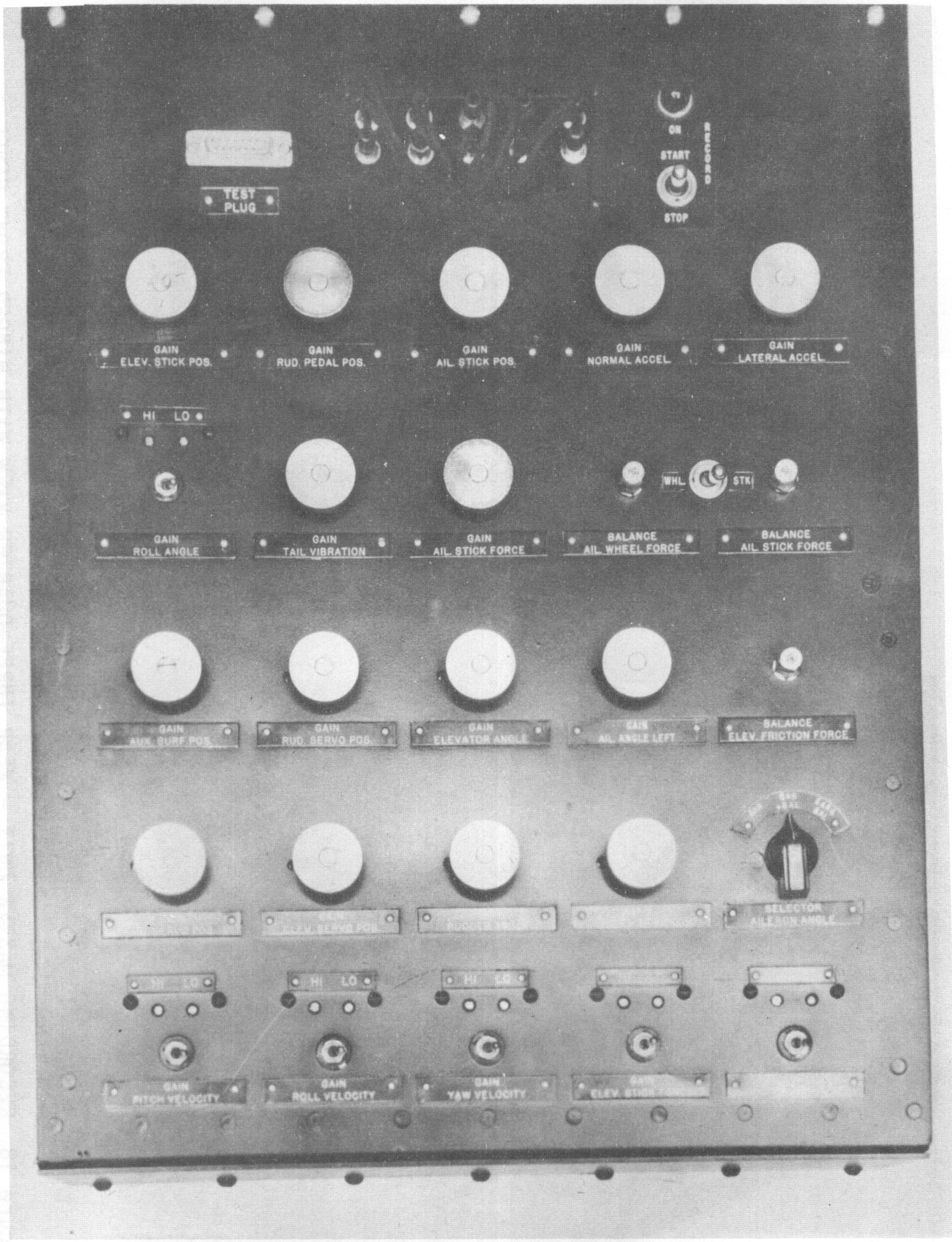

Figure 17 RECORDING MASTER UNIT - FRONT VIEW

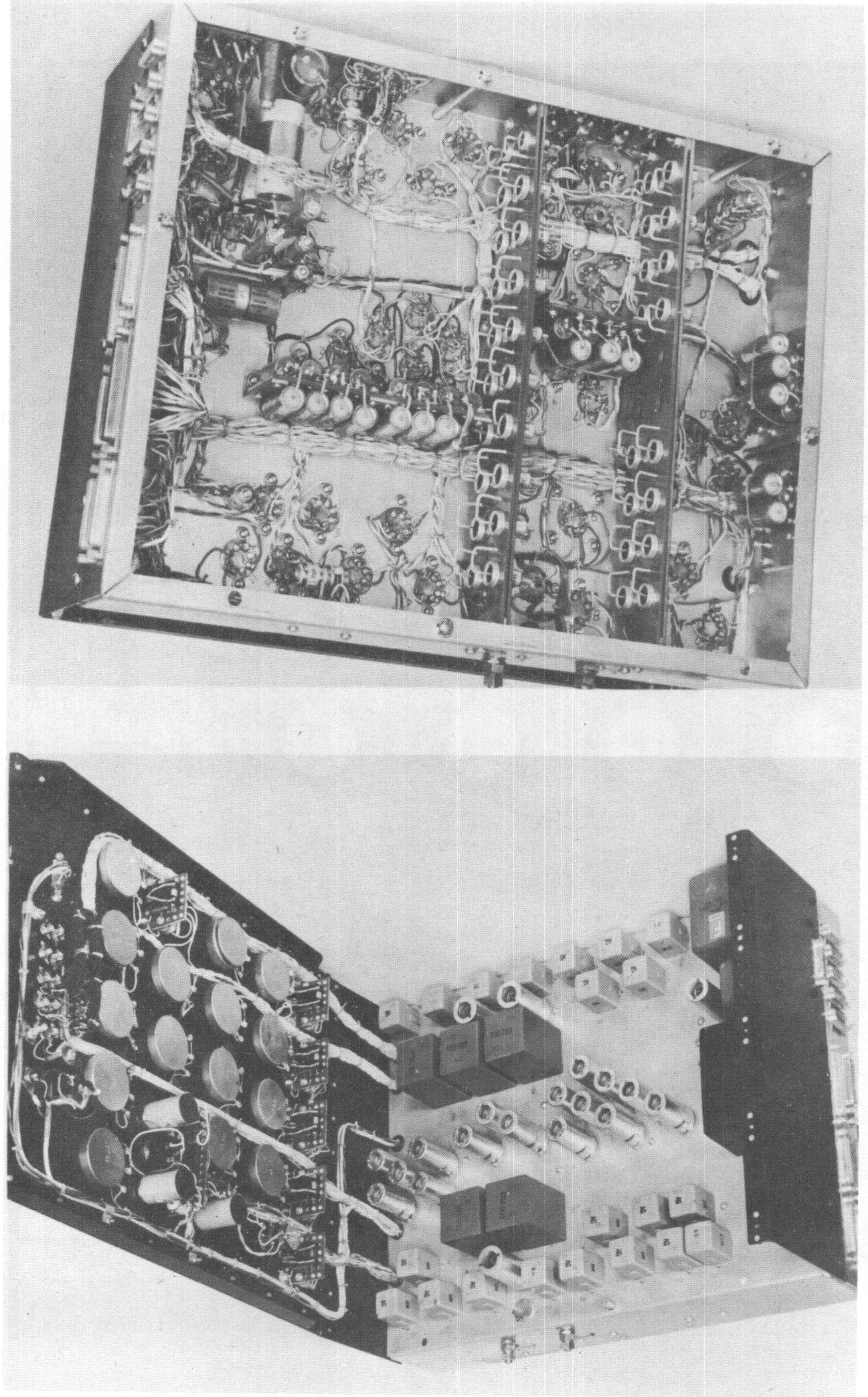

Figure 18 RECORDING MASTER UNIT - REAR THREE-QUARTER VIEW WITH HINGED FRONT PANEL RAISED AND BOTTOM VIEW

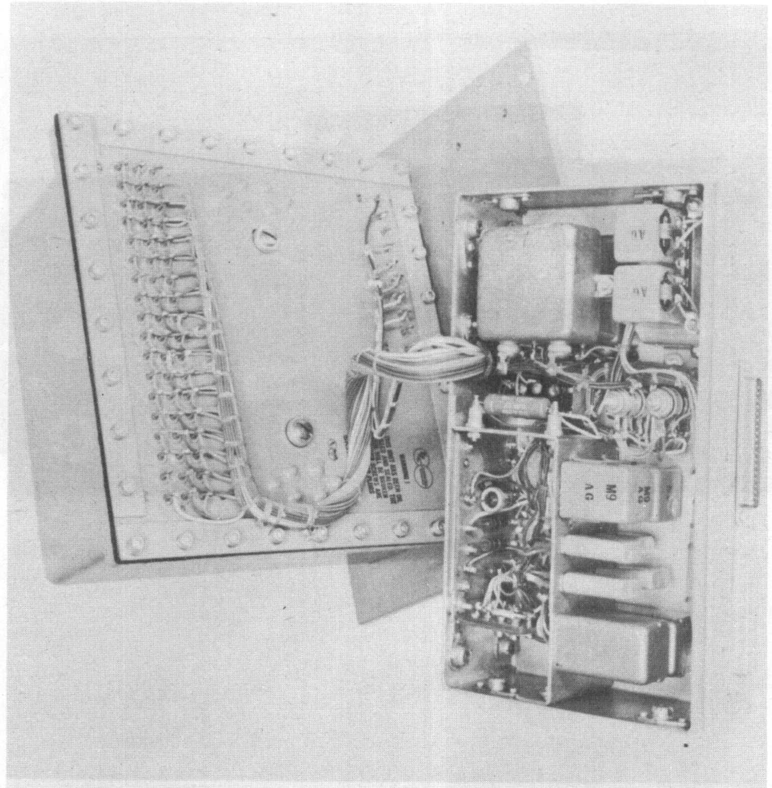

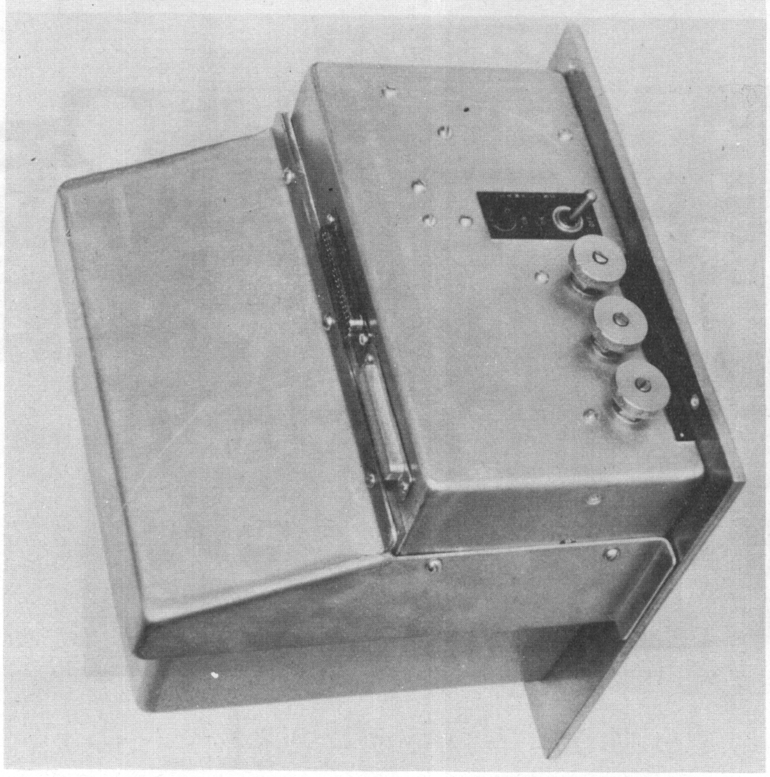

Figure 19 SAMPLING SWITCH UNIT - INTERIOR AND EXTERIOR VIEWS

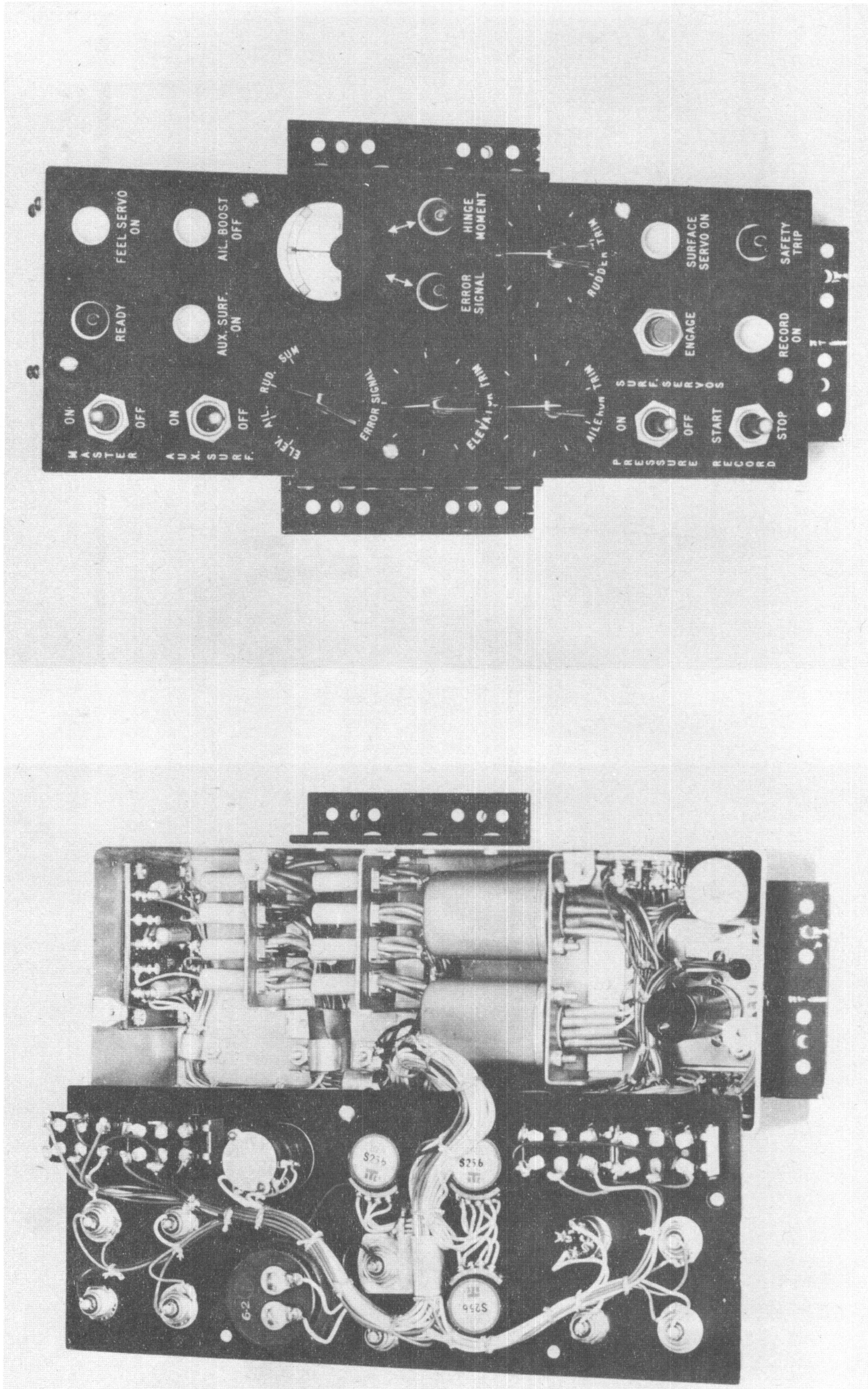

Figure 20 PILOT'S MASTER CONTROL PANEL - FRONT VIEW AND INTERIOR VIEW

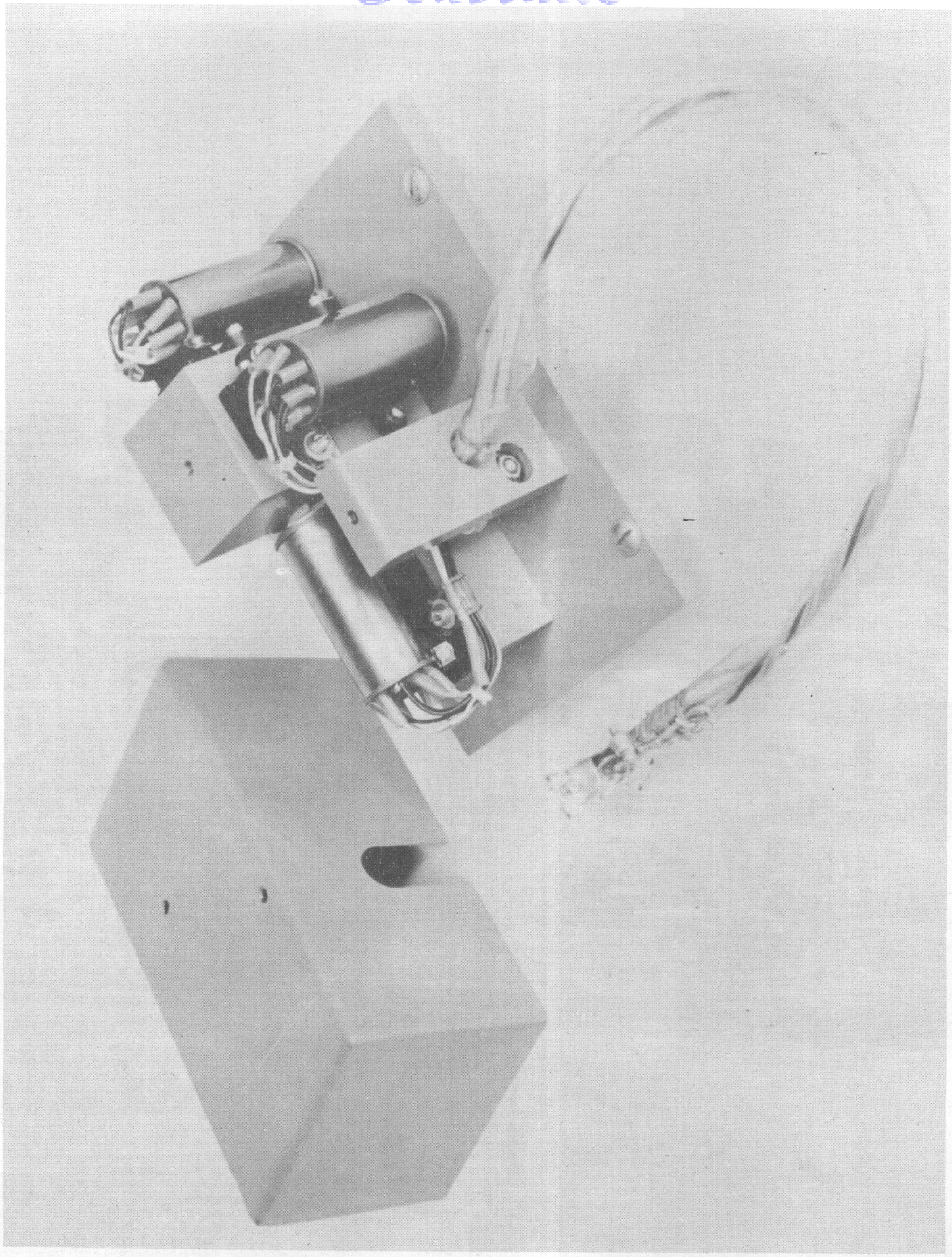

Figure 21 RATE GYRO MOUNTING UNIT

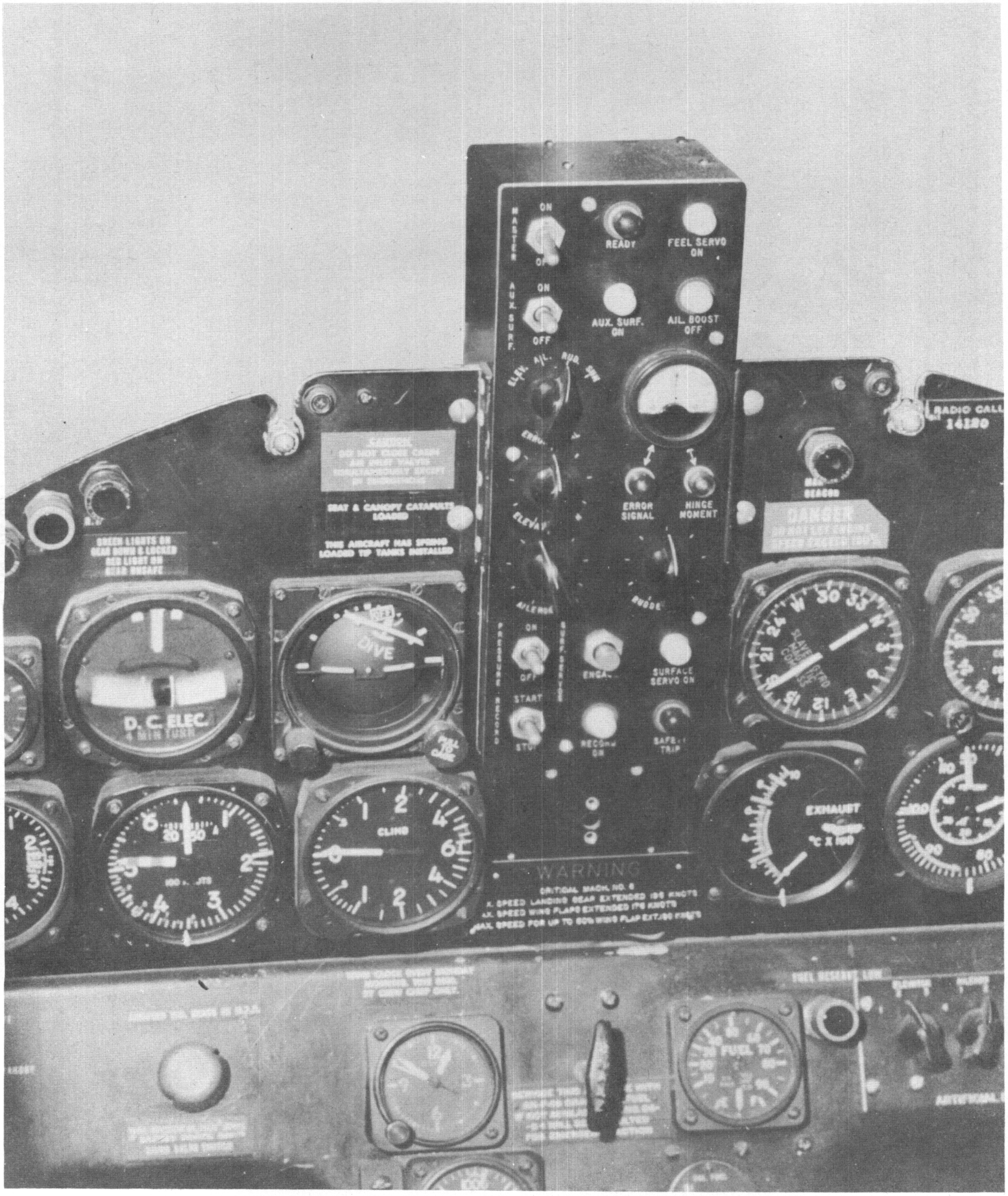

Figure 22 PILOT'S MASTER CONTROL PANEL INSTALLATION IN REAR COCKPIT

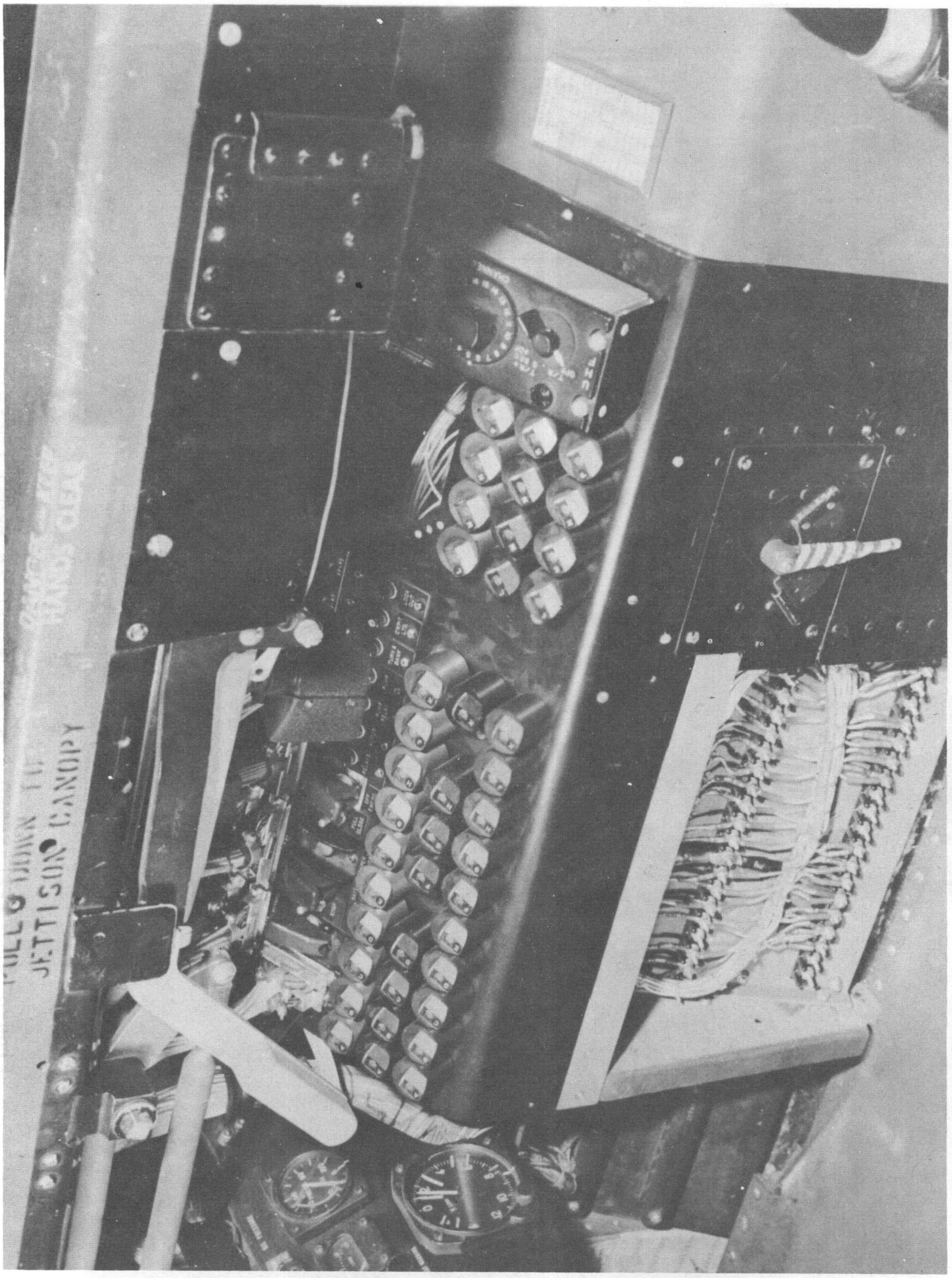

Figure 23 PILOT'S GAIN CONTROL PANEL ON RIGHT CONSOLE OF REAR COCKPIT

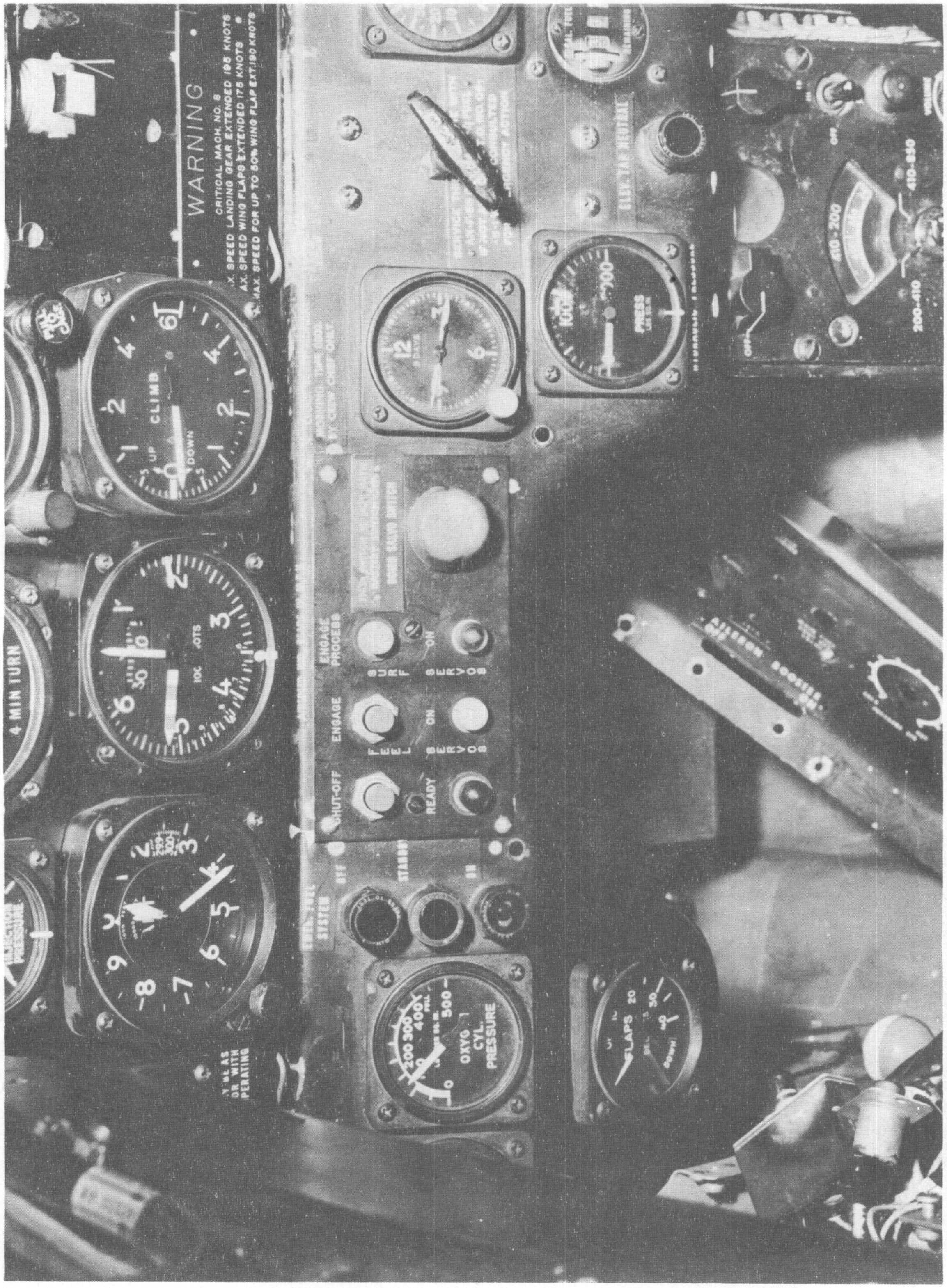

Figure 24 FEEL SERVO CONTROL PANEL IN FRONT COCKPIT

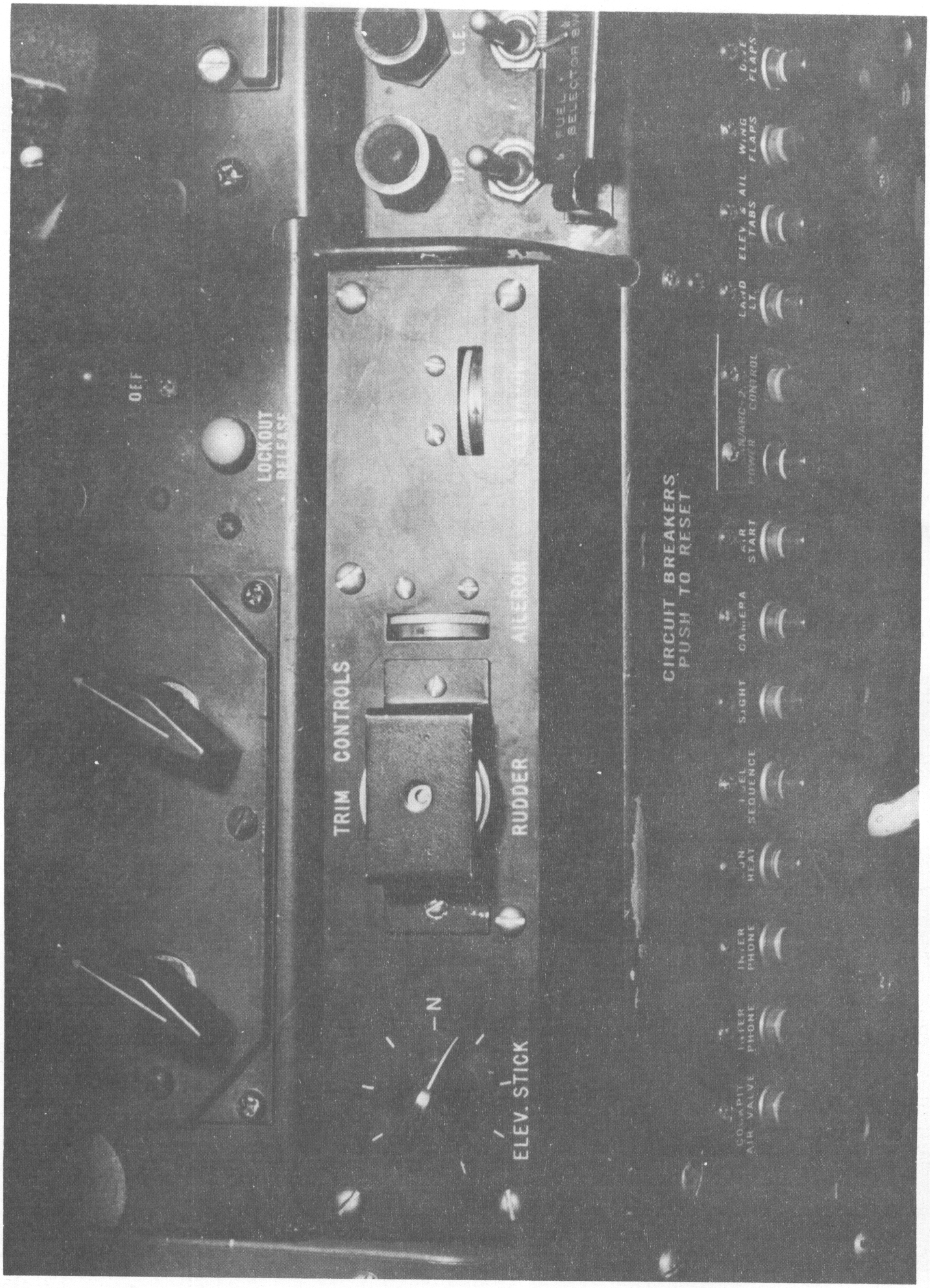

Figure 25 TRIM CONTROL PANEL ON LEFT CONSOLE OF FRONT COCKPIT

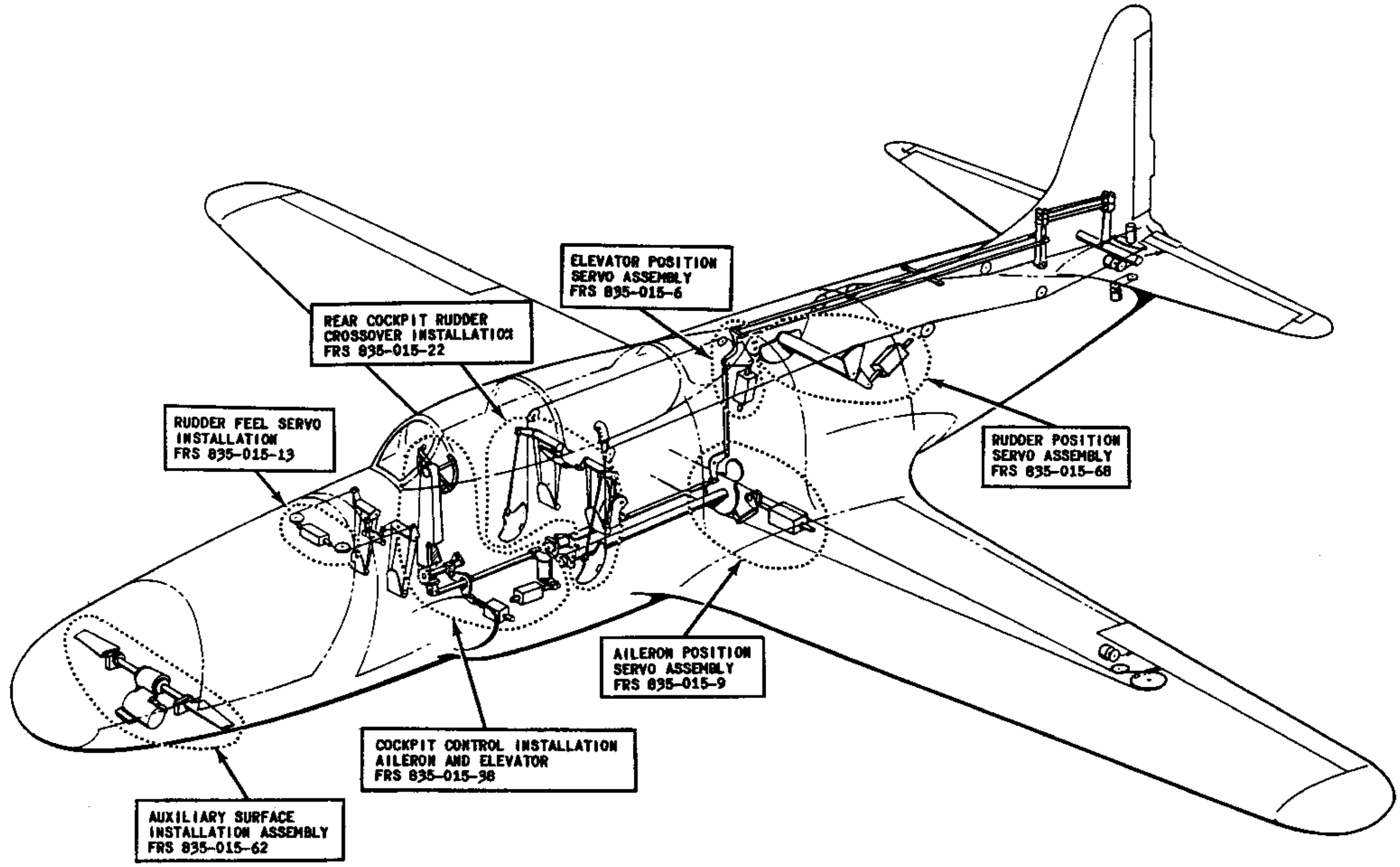

Figure 26 T-33A MODIFIED CONTROL SYSTEM

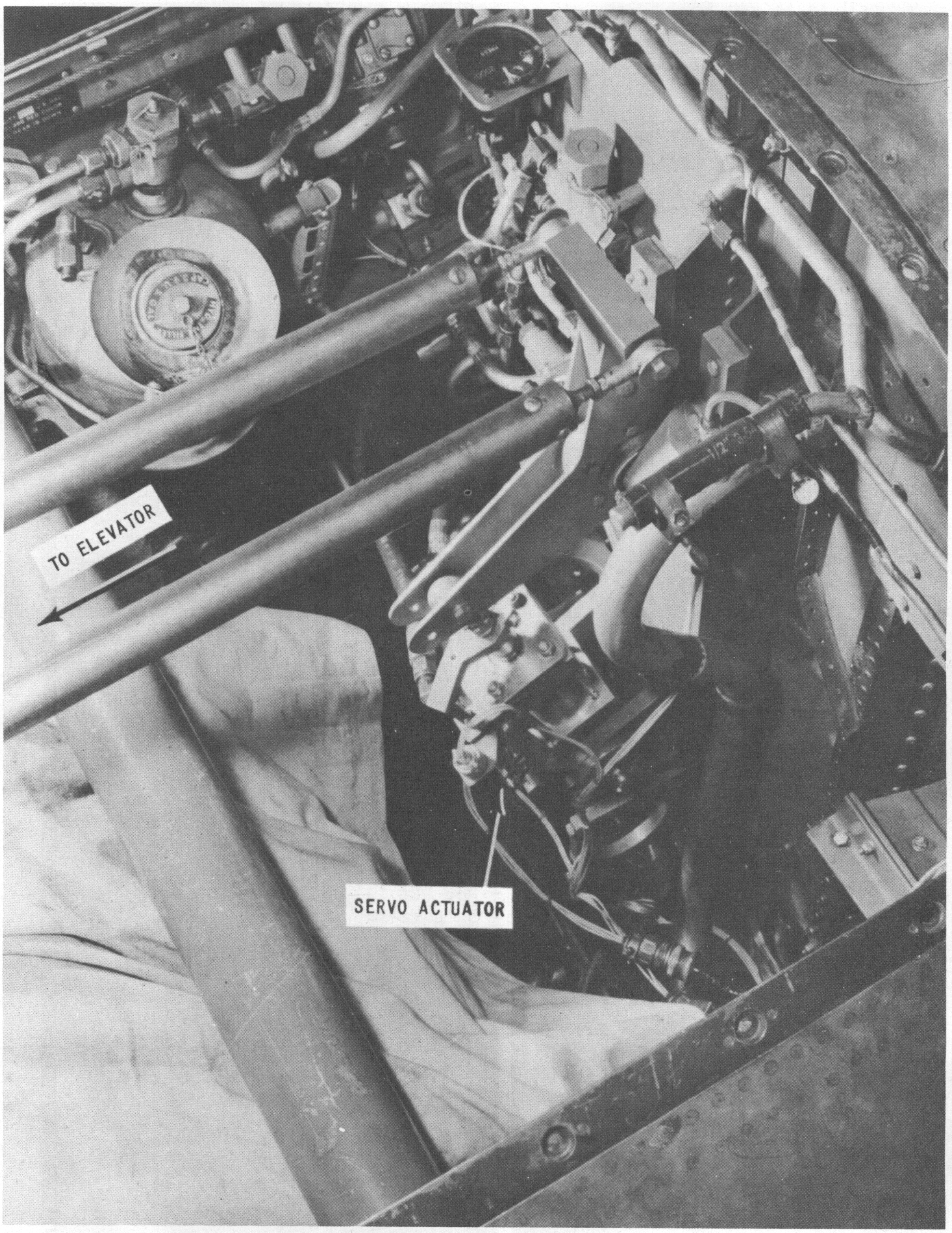

Figure 27 ELEVATOR POSITION SERVO

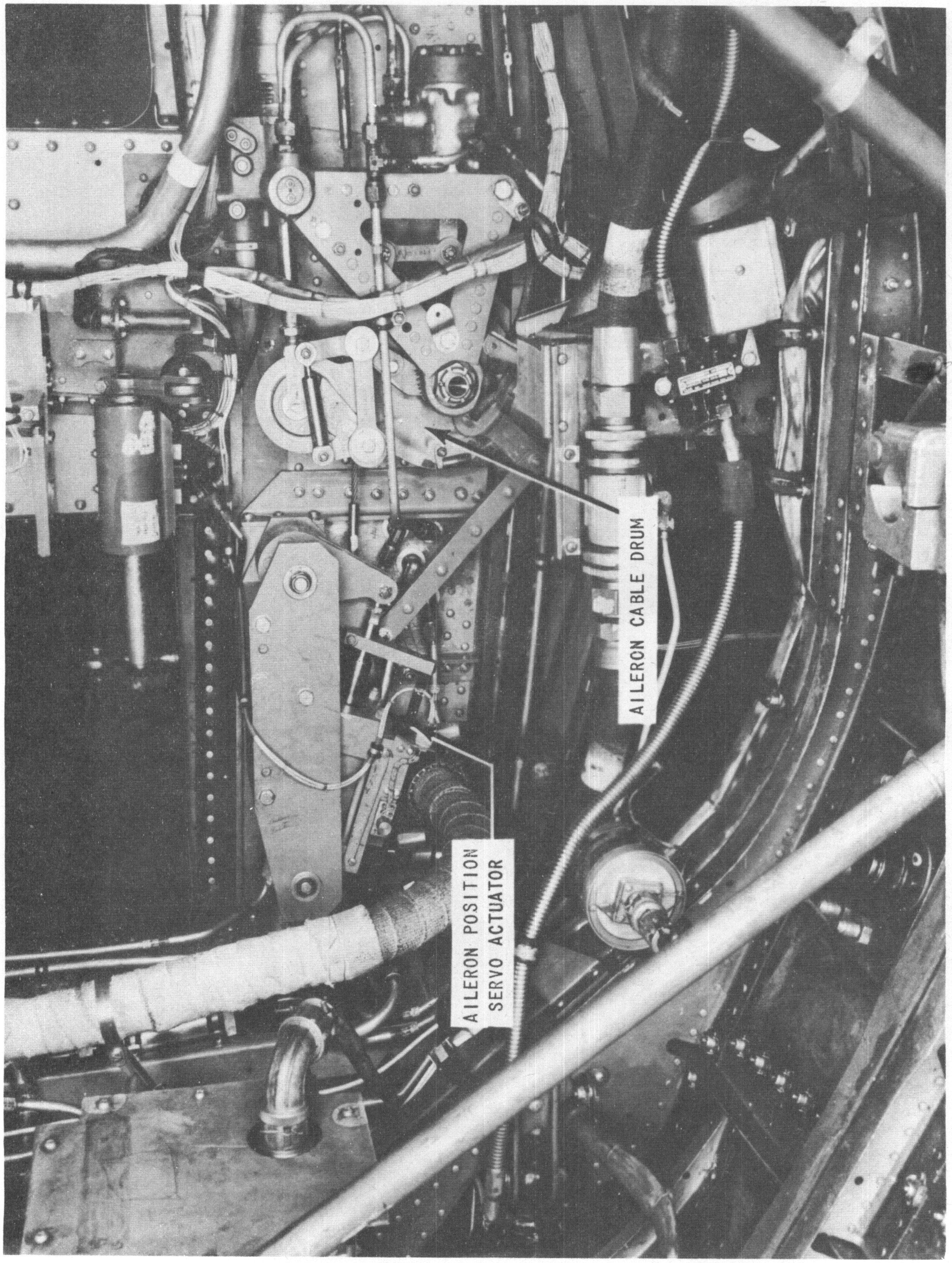

Figure 28 AILERON POSITION SERVO

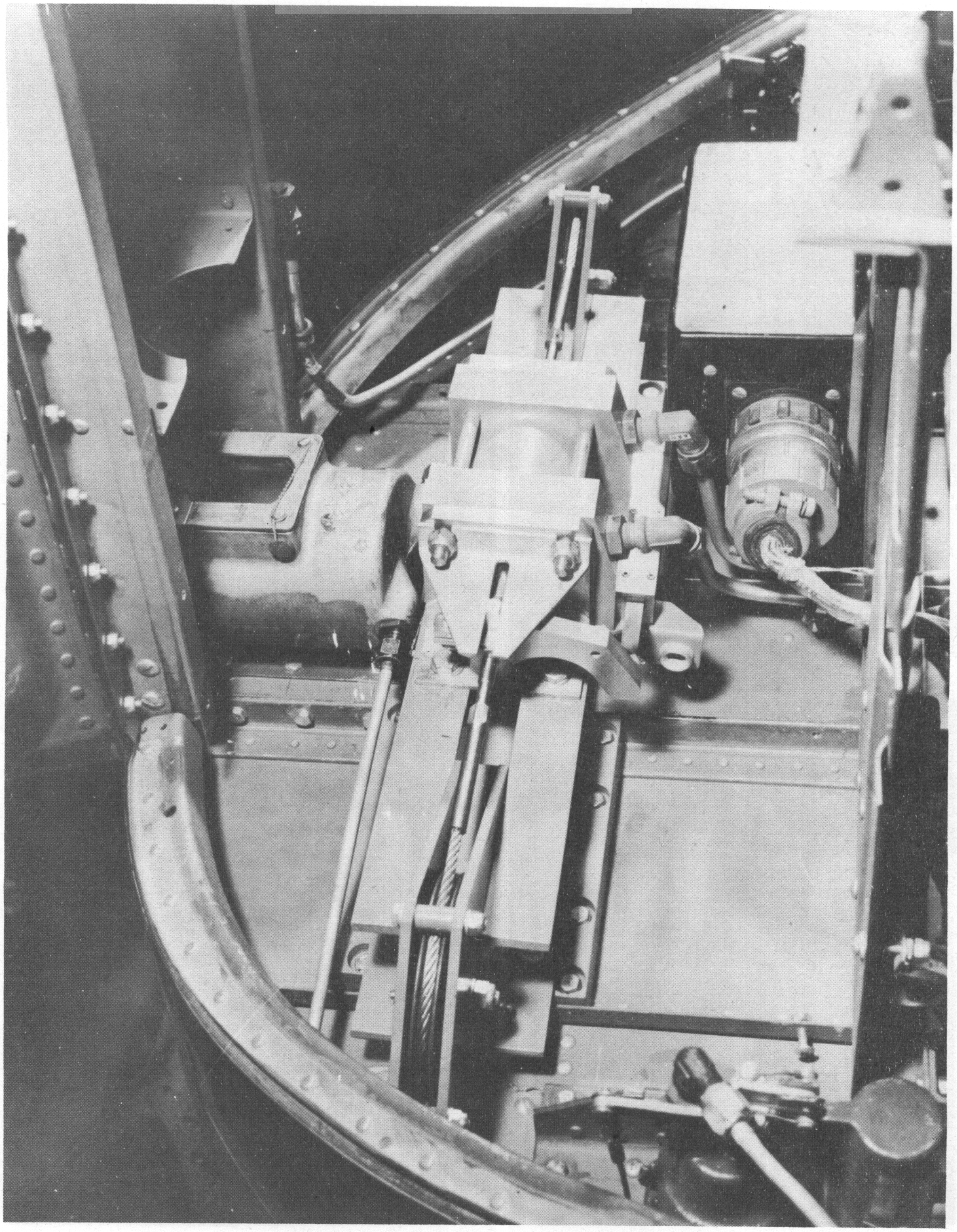

Figure 29 RUDDER FEEL SERVO

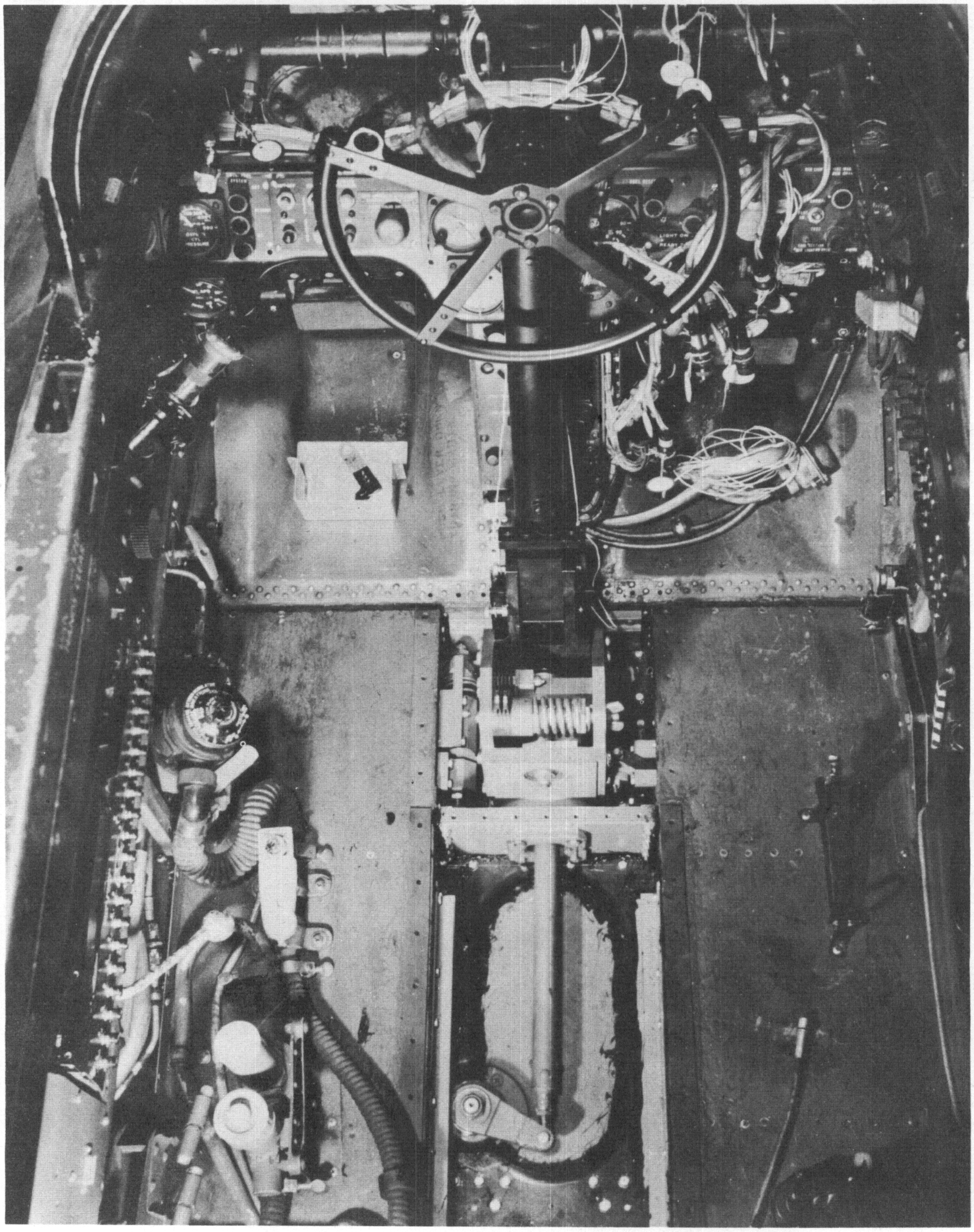

Figure 30 COCKPIT WHEEL CONTROL

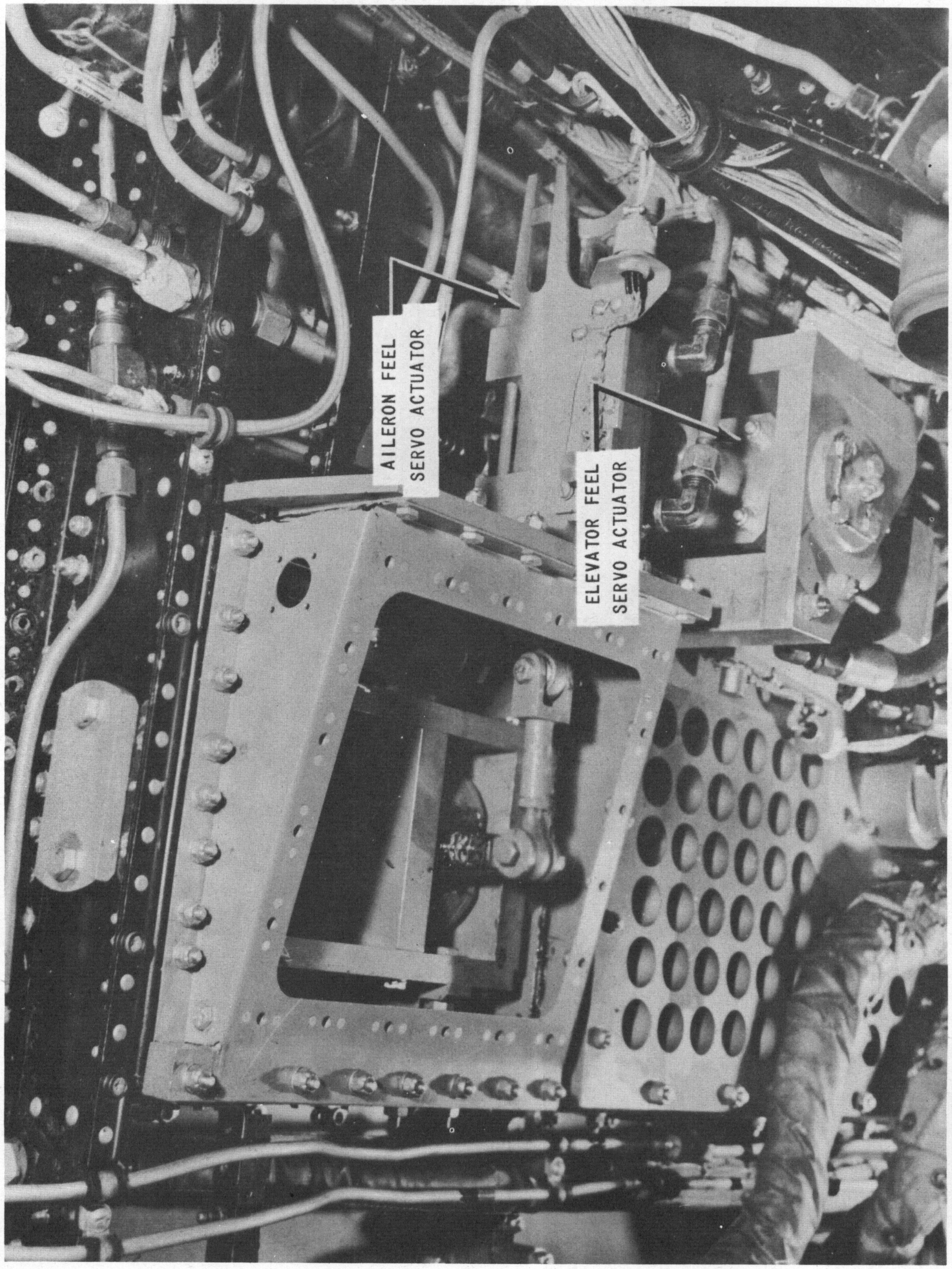

Figure 31 AILERON AND ELEVATOR FEEL SERVOS

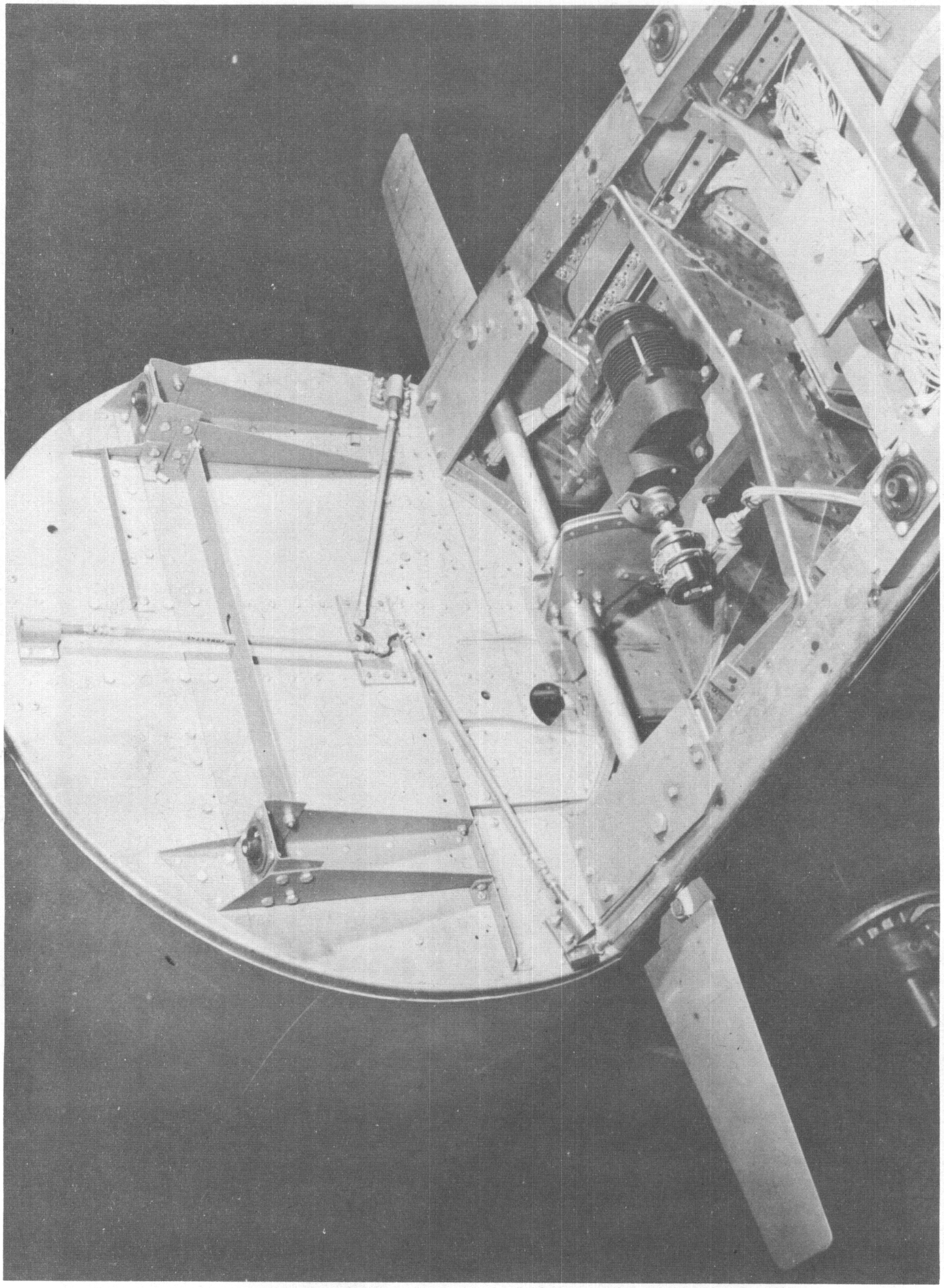

Figure 32 AUXILIARY SURFACE AND SERVO

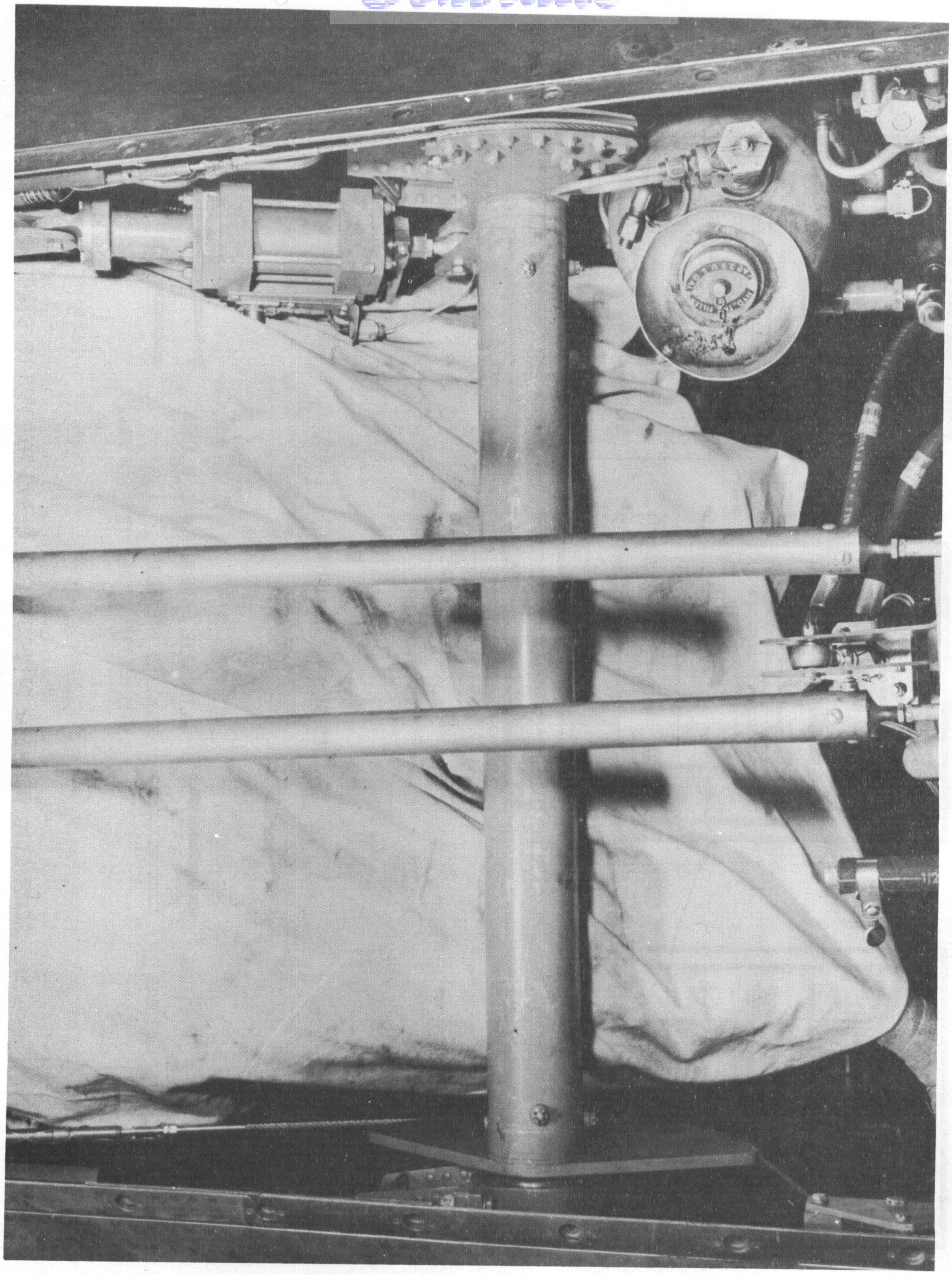

Figure 33 RUDDER POSITION SERVO

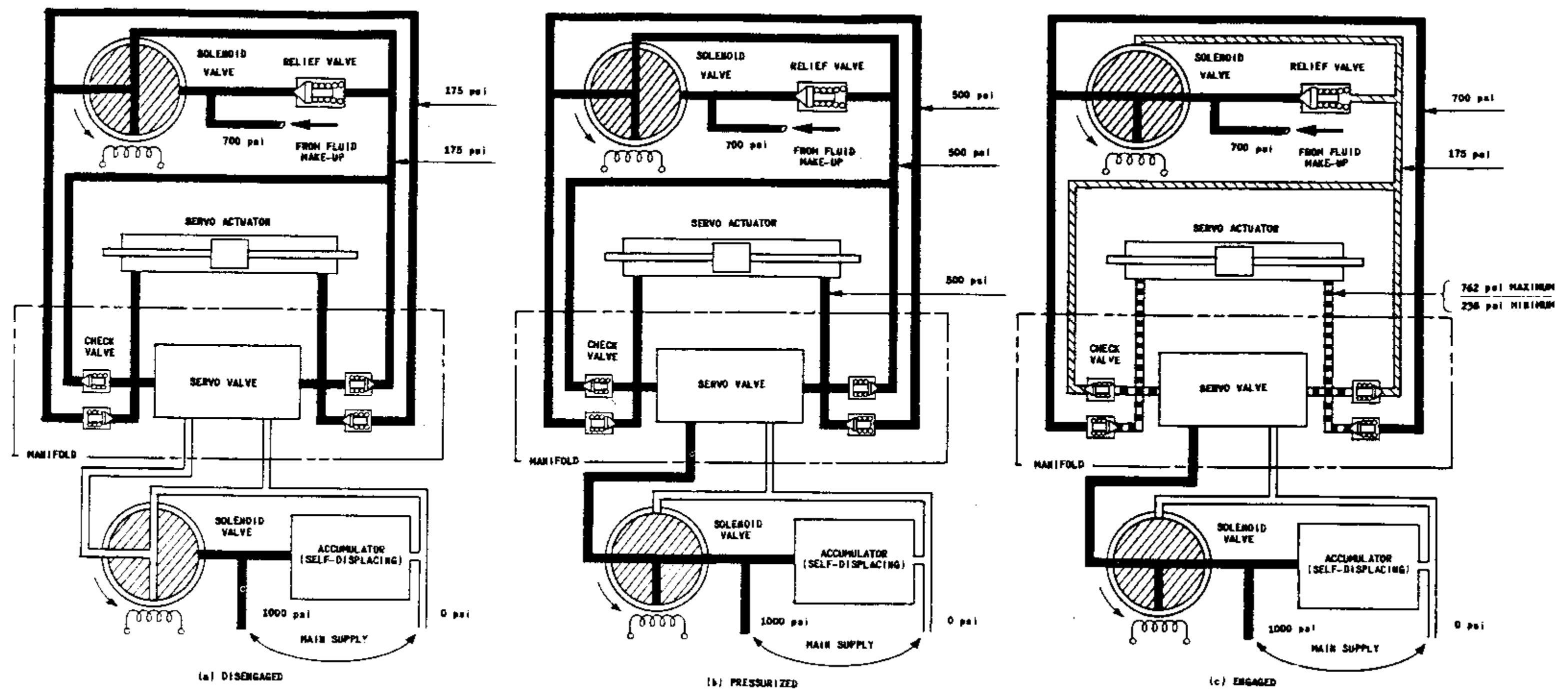

(VALUES SHOWN ARE NOMINAL)

KEY

PRESSURE

RETURN

ALTERNATE PRESSURE AND RETURN

LIMITED PRESSURE
(RELIEF VALVE SETTING 525 psi)

Figure 34 SCHEMATIC DRAWING OF POSITION SERVO HYDRAULIC CIRCUIT

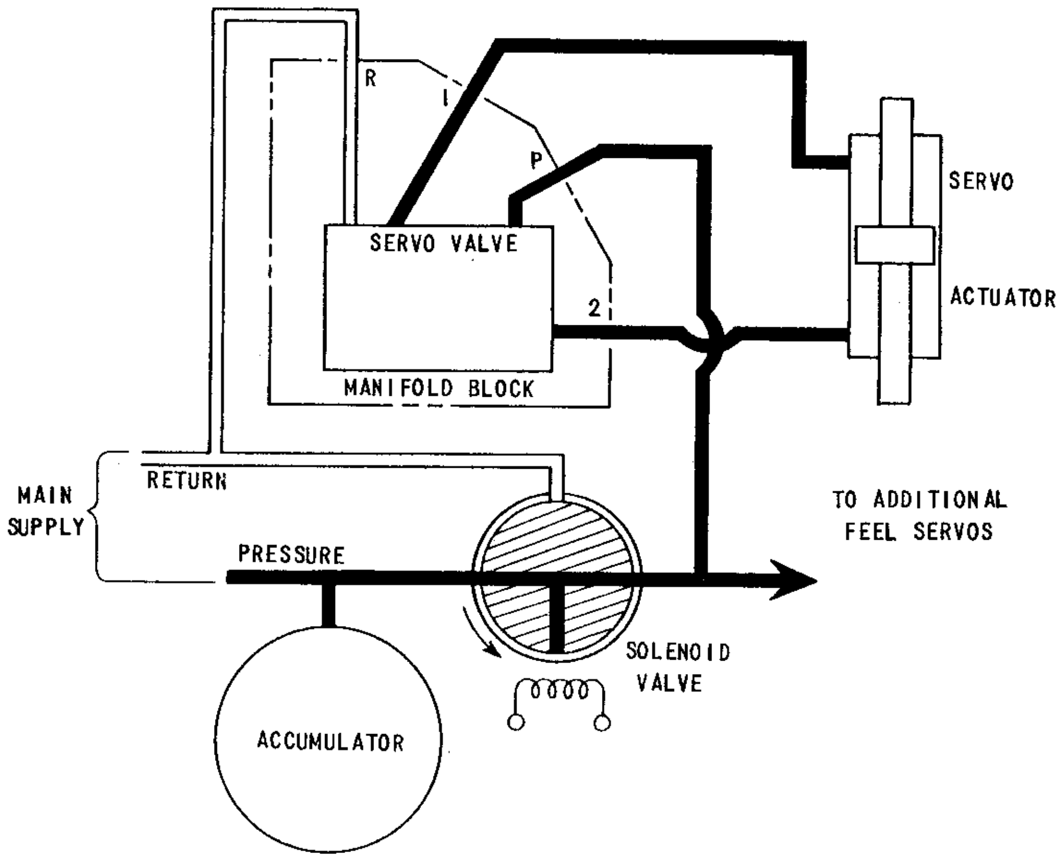

Figure 35 SCHEMATIC DRAWING OF FEEL SERVO HYDRAULIC CIRCUIT

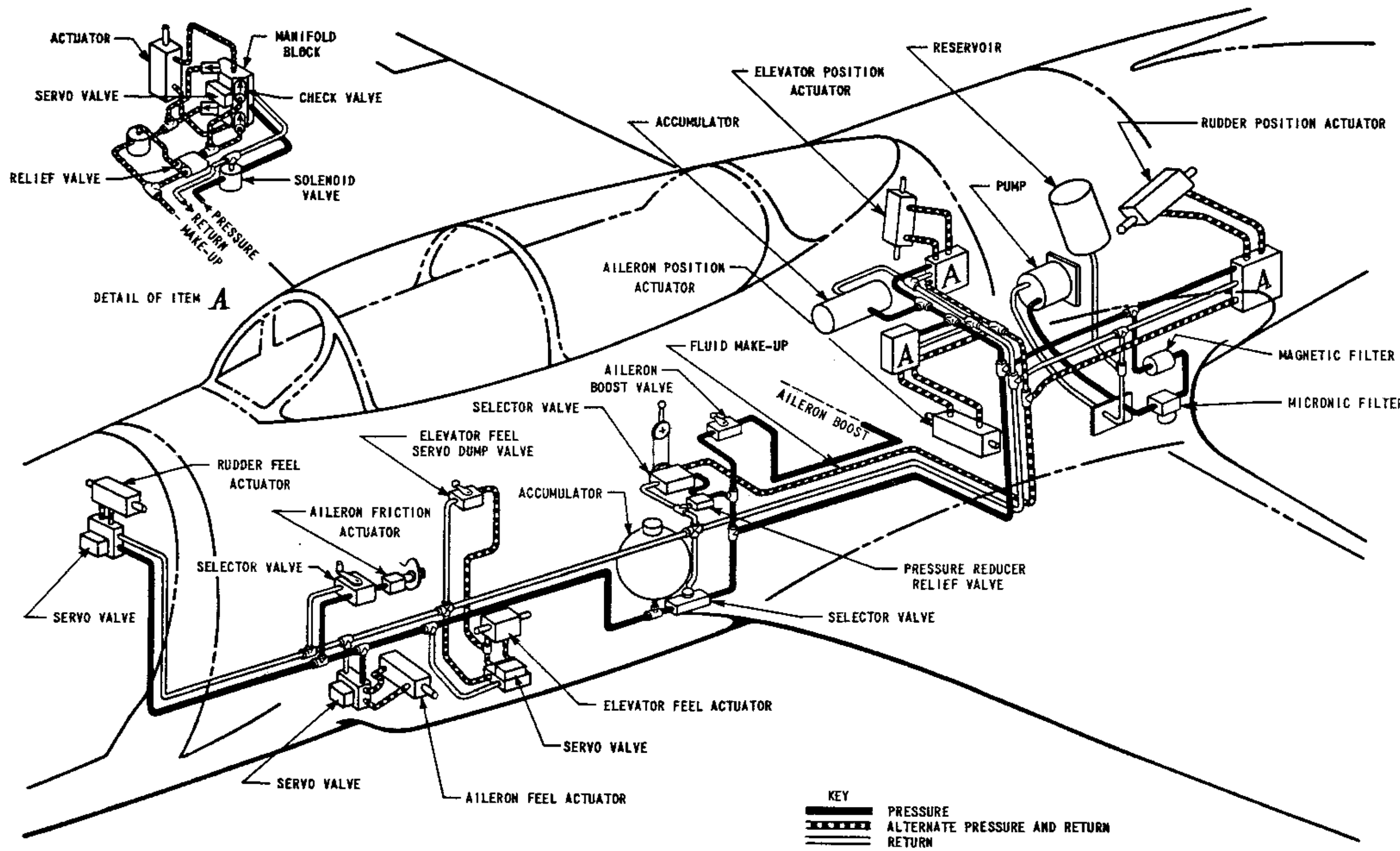

Figure 36 SCHEMATIC DRAWING - T-33 SERVO HYDRAULIC SYSTEM

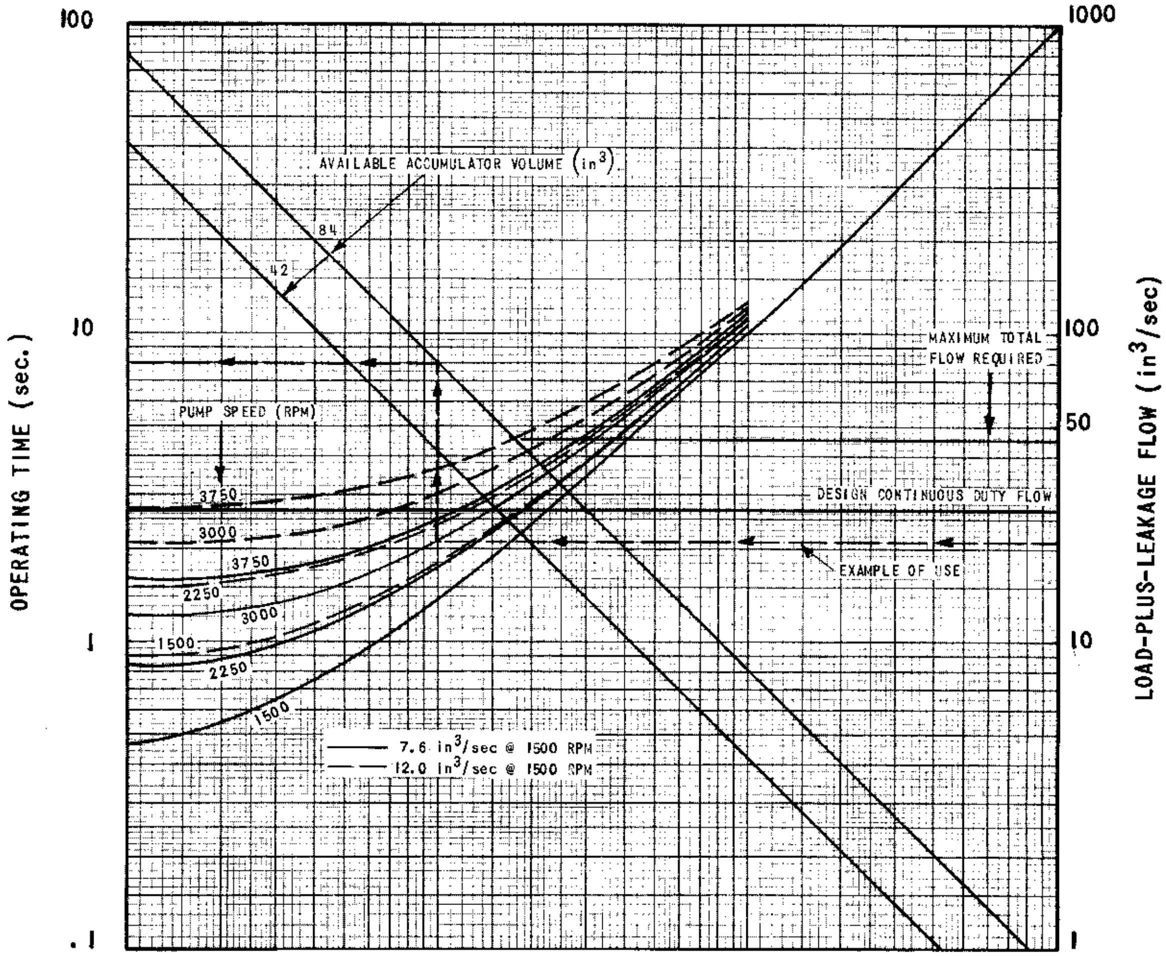

Figure 37 HYDRAULIC SYSTEM FLOW OPERATING CHARACTERISTICS

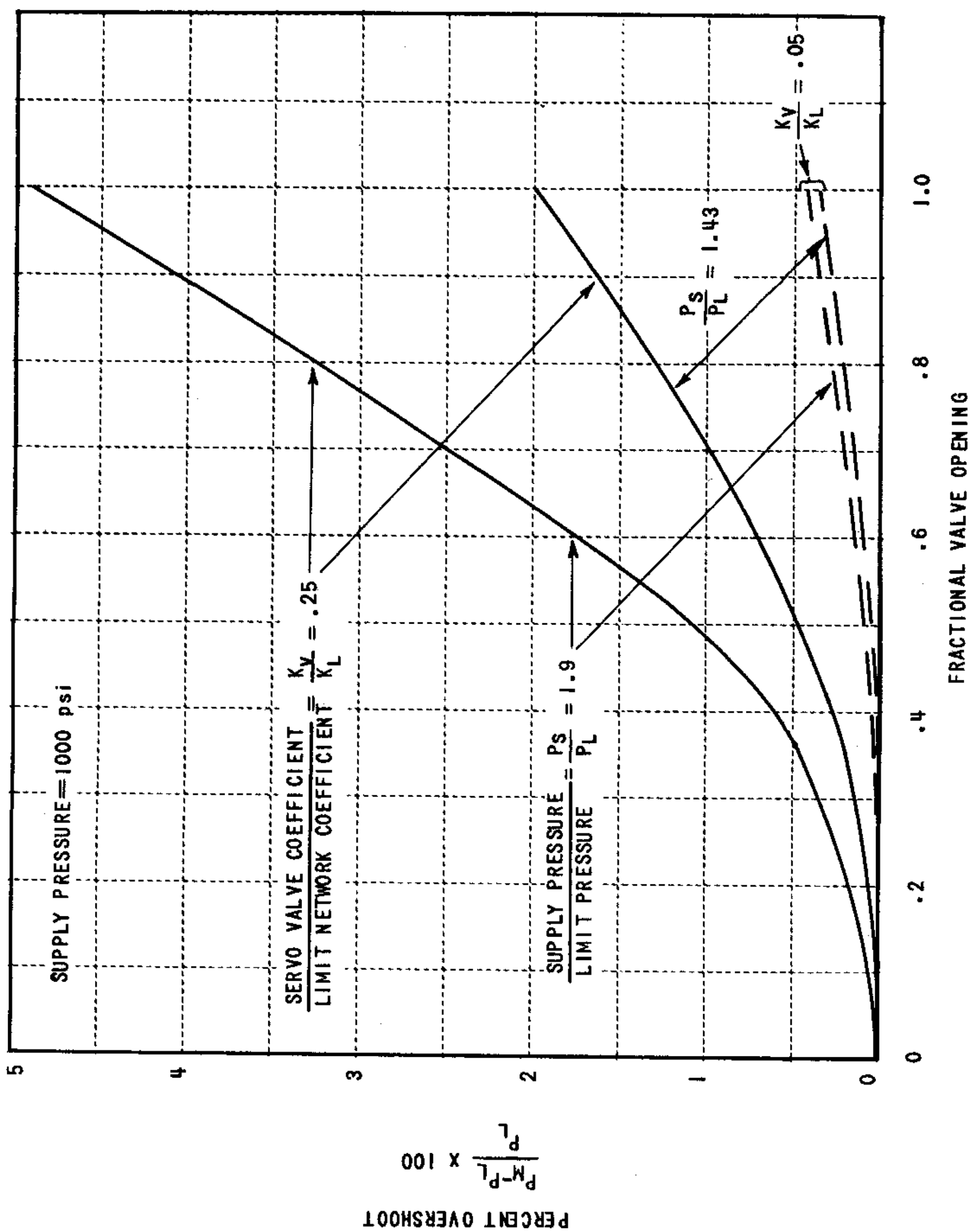

Figure 38 STATIC PERFORMANCE OF PRESSURE LIMITING CIRCUIT

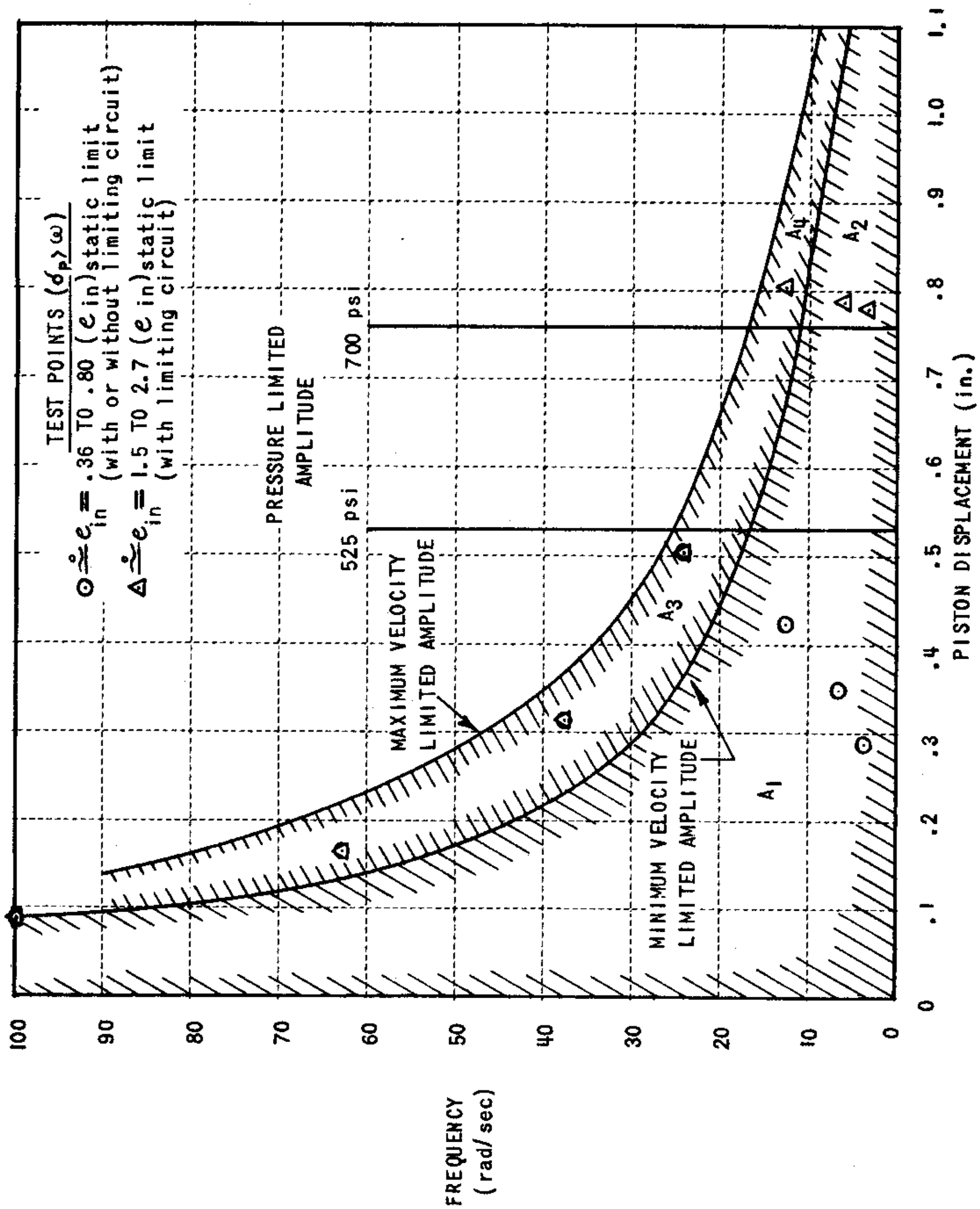

Figure 39 POSITION SERVO FREQUENCY RESPONSE TEST REGIONS

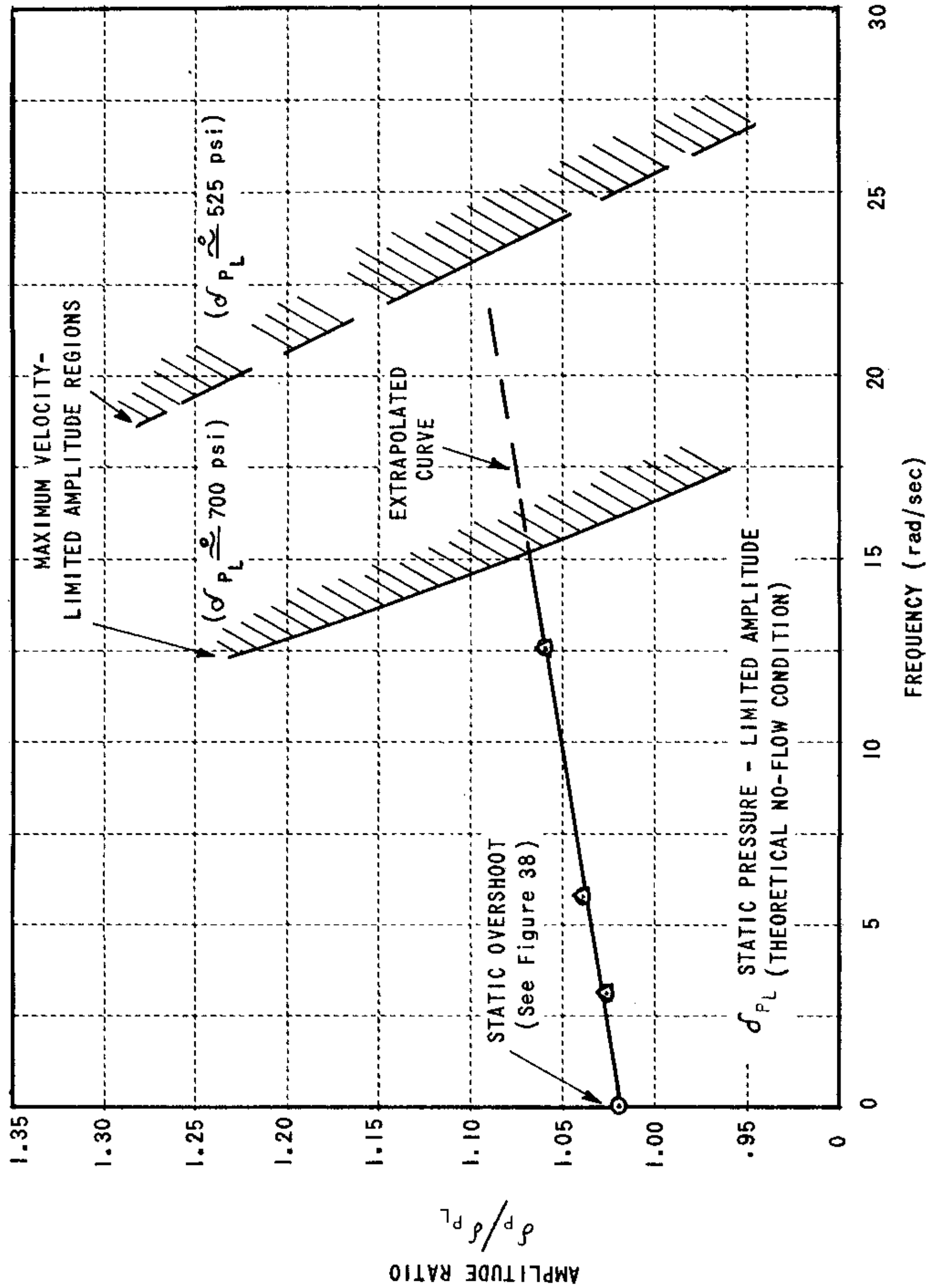

Figure 40 DYNAMIC PRESSURE - LIMITED POSITION OVERSHOOT

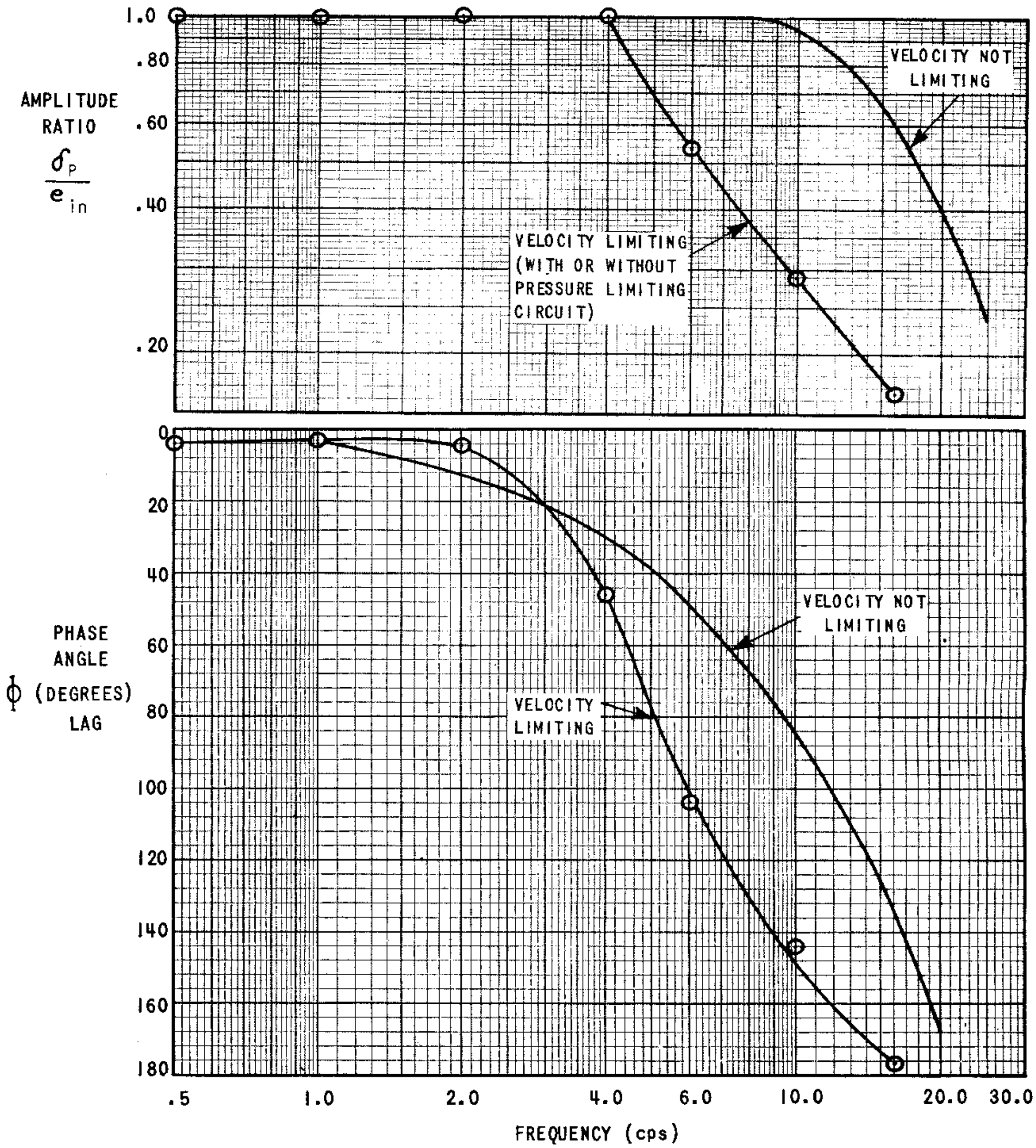

Figure 41 FREQUENCY RESPONSE OF POSITION SERVO

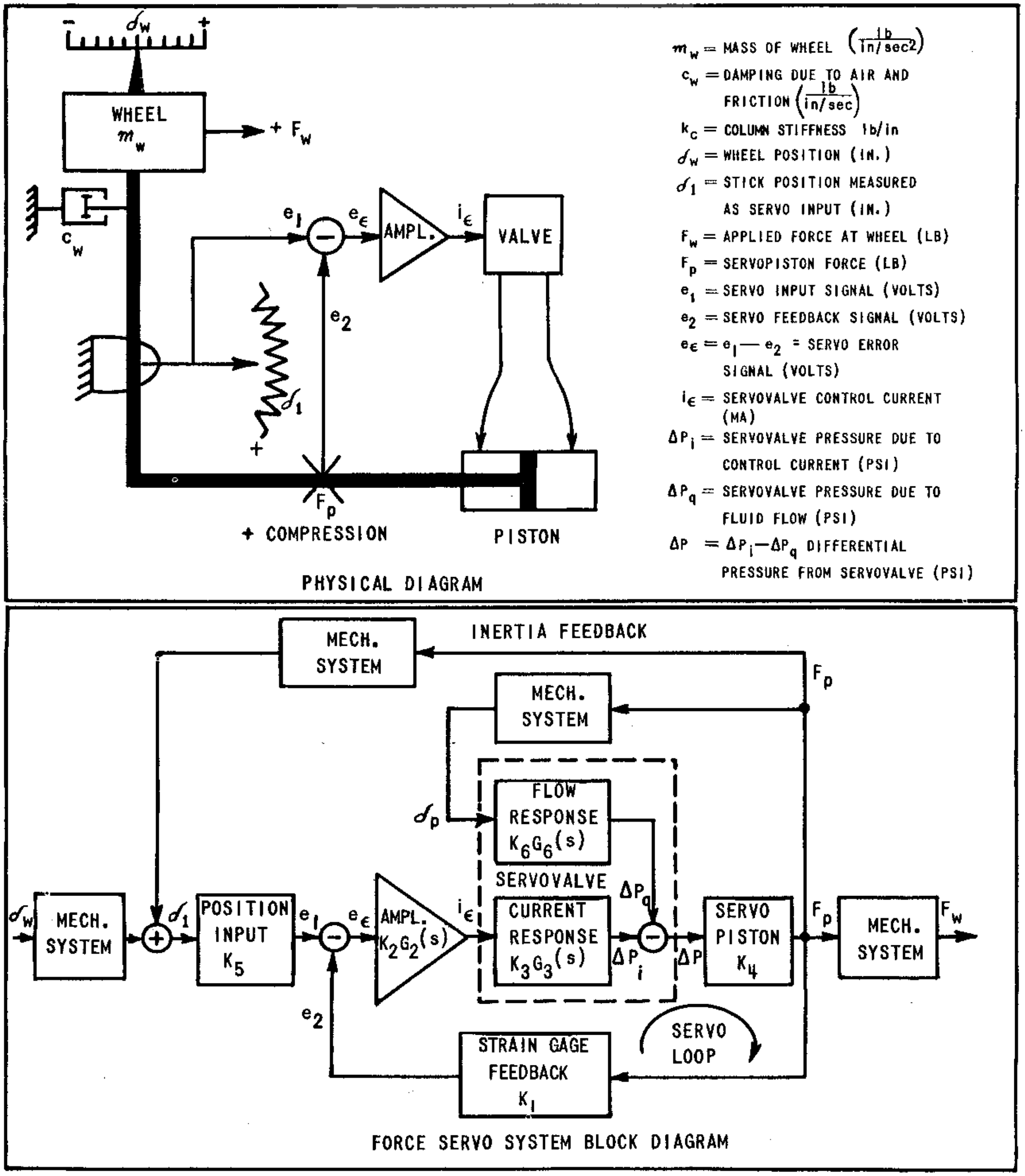

Figure 42 FEEL SERVO WITH PRESSURE - CONTROL SERVOVALVE

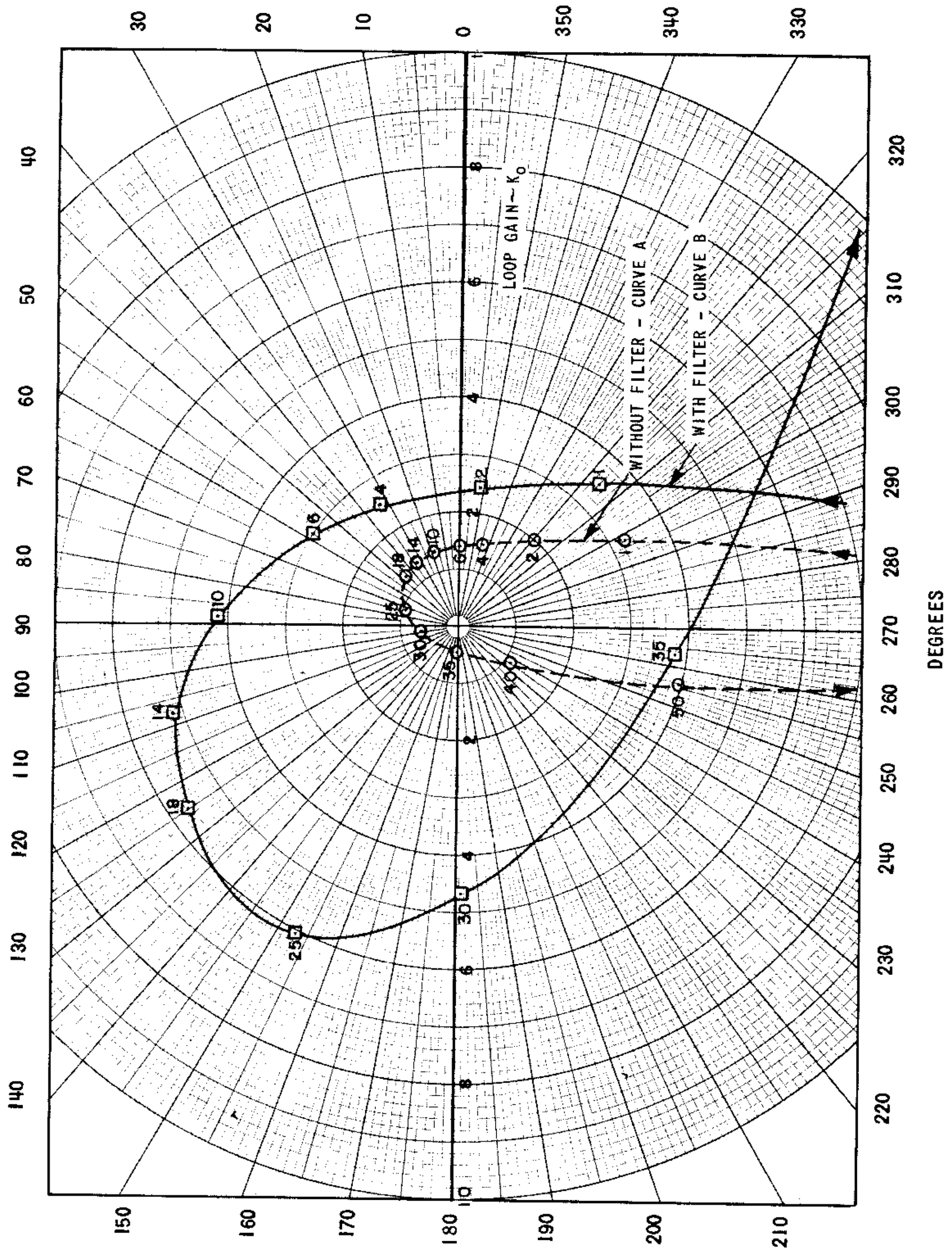

Figure 43 INVERSE OPEN-LOOP RESPONSE FOR TORQUE SERVOLOOP OF FEEL SERVO WITH AND WITHOUT FEEDBACK FILTER